

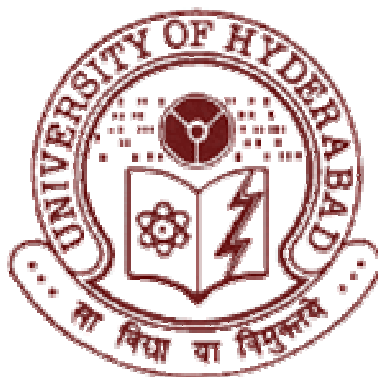
Theoretical Studies on Polyhedral Boranes, Main Group and Transition Metal Compounds

A Thesis

Submitted for the Degree of
DOCTOR OF PHILOSOPHY

By

Biswarup Pathak



School of Chemistry
University of Hyderabad
Hyderabad 500 046
INDIA

July 2007

Dedicated to My Parents

STATEMENT

I do hereby declare that the work embodied in this thesis is the result of investigations carried out by me in the **School of Chemistry, University of Hyderabad, Hyderabad, India and Department of Inorganic and Physical Chemistry, Indian Institute of Science, India**, under the supervisions of **Prof. Eluvathingal D. Jemmis and Prof. M. Durga Prasad**.

In keeping with the general practice of reporting scientific observations, due acknowledgements have been made whenever the work described is based on the findings of other investigators.

Biswarup Pathak

CERTIFICATE

Certified that the work embodied in the thesis entitled “**Theoretical Studies on Polyhedral Boranes, Main Group and Transition Metal Compounds**” has been carried out by **Mr. Biswarup Pathak** under my supervision and the same has not been submitted elsewhere for any degree.

Prof. M. Durga Prasad

Thesis Supervisor

Dean

School of Chemistry

Acknowledgements

I would like to express my deep respect and heartfelt gratitude to my research supervisor Prof. E. D. Jemmis for his invaluable guidance and constant support throughout my research career. He has a dynamic personality, and a unique way to generate simple and nice research problems. The discussions with him were very helpful for me to nurture a deeper understanding of the subject, which I believe will strengthen my future career as a researcher. I will always treasure the care and concern of him towards me. I would like to thank my co-supervisor Prof. M. Durga Prasad for his valuable support. Among my collaborators, I would specially like to thank Prof. N. Hosmane, Department of Chemistry and Biochemistry, Northern Illinois University for his precise and valuable suggestions to our collaborative works which has been a part (chapter 2) of my thesis. I take the opportunity to thank Prof. Henry F. Schaefer III and Prof. R. Bruce King, Center for Computational Quantum Chemistry, University of Georgia for many discussions of (chapter 5) collaborative work. I thank Prof. Uwe Rosenthal, Universität of Rostock and Prof. A. R. Chakravarty, Indian Institute of Science, for the discussions.

Acknowledgement

I express my sincere thank to CSIR, New Delhi for the financial assistance. Computational facilities of the Centre for Modeling Simulation and Design (CMSD), University of Hyderabad, Maui High Performance Computing Center (MHPCC), Hawaii and Supercomputer Education and Research Centre (SERC), Indian Institute of Science are greatly acknowledged.

It was pleasure to work in the warm and cordial atmosphere offered by School of Chemistry, University of Hyderabad, Hyderabad and Department of Inorganic and Physical Chemistry, Indian Institute of Science, Bangalore. I thank the former and present Deans, School of Chemistry and all the faculty members of the School and of Department of Inorganic and Physical Chemistry, Indian Institute of Science for their cooperation.

I would like to thank all the non-teaching staffs at the School of Chemistry and Department of Inorganic and Physical Chemistry for their constant service in each and every matter with a smiling face.

I am enough fortunate to have good labmates. As a person, they have made a great impact on me whenever I think about themselves. I would like to thank my beloved labmates, Ashwini,

Pancharatna, Jayasree, Anoop, Param, Prasad, Usha, Jorly, Susmita, Shameema, Hari and Dibyendu. They are as an excellent group of people as you are ever likely to meet. All in all, we had greater fun together than I could have ever imagined. I thank the project and summer students (Deshigan, Gopan, Shanthi, Claire and Umayal) who worked in our group.

I thank my B.Sc/M.Sc. classmates: Rama, Bama, Mita, Shruthi, Kamaskhi, pratima, Partha, Dipankar, Arnab, Joy, Debasis, Pranab, Shyama, Sankha, Ehesan, subhadip, Soumya, Niladri, Arka, Asmita, Dipti, Sarasij, Indu, Tulika for their timely help and encouragements.

I am thankful to my friends at HCU: Tamalda, Dinuda, Binoyda, Sandy, Rahul, Manab, Suni, Subhas, Abhik, Saikat, Moloy, Archan, Satabdidi, Prasun, Masum, Abhijit, Prashant, Teja, Bhaswati, Aniruddha, Naren, Pradip, Tanmay, Utpal, Bipul, and Balaraman.

I thank my friends at IISc: Priyo, Trina, Snehanshu, Natali, Debbijoy, Abhinanda, Moloy, Debojyoti, Rakhi, Anupama, moumita, Gouri, Ashis, Cris, Sujitda, Sabya, Koushik, Ananya, Pallavidi, Bani, Nupur, Prasanta, Mithun, Shovan, and Pijush. Although I could not mention all my friends name individually, which would

Acknowledgement

have formed a big list, I would like to thank all my friends for their support and encouragement through out my studies.

I would like to thank my family for the patience they have shown during the course of my research. My mother, who has been a great source of inspiration for studies, has also been a solid support throughout my career. She has been extremely patient with me and my studies and has always been by my side whenever I have faced difficult situations. I would like to thank my father for the kind of encouragement and support he has provided me - and their constant blessings for my success. I am deeply indebted to dada, didi and all of my family members. It was impossible to start a journey towards the never-ending destination without their mental support. I may not live up to their expectations, but I hope that my work and establishment will make them happy.

Biswarup Pathak

Table of Contents

Statement	i
Certificate	ii
Acknowledgements	iii

Chapter 1: Introduction to Computational Chemistry and Overview of the Thesis

1.0	Overview of Computational Chemistry	1
1.1	Introduction	1
1.2	Theoretical Methods	3
1.2.1	<i>Ab initio</i> Methods	3
1.2.1.1	The Born-Oppenheimer Approximation	4
1.2.1.2	Variation Theorem	6
1.2.1.3	The LCAO-MO Approximation	6
1.2.1.4	The Hartree-Fock Self Consistent Field Method	8
1.2.1.5	Basis Sets	11
1.2.1.6	Electron Correlation	14
1.2.1.6.1	Configuration Interaction	14
1.2.1.6.2	Møller-Plesset Perturbation Theory...	15
1.2.2	Semiempirical Methods	17
1.2.2.1	Extended Hückel Method	17
1.2.3	Density Functional Theory	19
1.2.3.1	Local Density Approximation	21
1.2.3.1.1	Local Spin Density Approximation	22
1.2.3.2	Generalized Gradient Approximation	22
1.3	Outline of the Thesis	24
1.3.1	Reversal of Stability on Metalation of Pentagonal Bipyramidal ($1\text{-MB}_6\text{H}_7^{2-}$, $1\text{-M-2-CB}_5\text{H}_7^{1-}$ and $1\text{-M-2,4-C}_2\text{B}_4\text{H}_7$) and Icosahedral ($1\text{-MB}_{11}\text{H}_{12}^{2-}$, $1\text{-M-2-CB}_{10}\text{H}_{12}^{1-}$	

	and 1-M-2,4-C ₂ B ₉ H ₁₂) Boranes (M=Al, Ga, In and Tl): Energetics of Condensation and Relationship to Binuclear Metallocenes	25
1.3.2	Condensed 2- and 3-Dimensional Aromatic Systems: A Theoretical Study on the Relative Stabilities of Isomers of CB ₁₉ H ₁₆ ⁺ , B ₂₀ H ₁₅ Cl and B ₂₀ H ₁₄ Cl ₂ and Comparison to B ₁₂ H ₁₀ Cl ₂ ²⁻ , C ₆ H ₄ Cl ₂ , C ₁₀ H ₇ Cl and C ₁₀ H ₆ Cl ₂	27
1.3.3	The Intramolecular Activation of C _β -H Bond by Transition Metal Complexes	29
1.3.4	Bond Length and Bond Multiplicity: σ Bond Prevents Short π Bonds	31
1.4	References	35

Chapter 2: Reversal of Stability on Metalation of Pentagonal Bipyramidal (1-MB₆H₇²⁻, 1-M-2-CB₅H₇¹⁻ and 1-M-2,4-C₂B₄H₇) and Icosahedral (1-MB₁₁H₁₂²⁻, 1-M-2-CB₁₀H₁₂¹⁻ and 1-M-2,4-C₂B₉H₁₂) Boranes (M=Al, Ga, In and Tl): Energetics of Condensation and Relationship to Binuclear Metallocenes

2.0	Abstract	38
2.1	Introduction	39
2.2	Computational Details	44
2.3	Results and Discussion	44
2.3.1	Bonding in the Pentagonal-Bipyramidal Systems	46
2.3.2	Bonding in the Icosahedral Boranes and Comparison to Pentagonal-Bipyramids	50
2.3.3	Condensation through Single-Atom Sharing: Sandwich Structures involving Pentagonal-Bipyramidal and Icosahedral Metallaboranes	55
2.3.4	Binuclear metallocenes	57

2.4	Conclusions.....	62
2.5	References	63

Chapter 3: Condensed 2- and 3-Dimensional Aromatic Systems: A Theoretical Study on the Relative Stabilities of Isomers of $\text{CB}_{19}\text{H}_{16}^+$, $\text{B}_{20}\text{H}_{15}\text{Cl}$ and $\text{B}_{20}\text{H}_{14}\text{Cl}_2$ and Comparison to $\text{B}_{12}\text{H}_{10}\text{Cl}_2^{2-}$, $\text{C}_6\text{H}_4\text{Cl}_2$, $\text{C}_{10}\text{H}_7\text{Cl}$ and $\text{C}_{10}\text{H}_6\text{Cl}_2$

3.0	Abstract	68
3.1	Introduction	69
3.2	Computational Details	70
3.3	Results and Discussion	71
3.3.1	Comparison of $\text{C}_2\text{B}_{10}\text{H}_{12}$ and $\text{CB}_{19}\text{H}_{16}^+$	71
3.3.2	$\text{B}_{12}\text{H}_{11}\text{Cl}^{2-}$, $\text{B}_{12}\text{H}_{10}\text{Cl}_2^{2-}$, $\text{C}_6\text{H}_5\text{Cl}$ and $\text{C}_6\text{H}_4\text{Cl}_2$	75
3.3.3	$\text{B}_{20}\text{H}_{16}$, $\text{B}_{20}\text{H}_{15}\text{Cl}$, $\text{B}_{20}\text{H}_{14}\text{Cl}_2$, C_{10}H_8 , $\text{C}_{10}\text{H}_7\text{Cl}$, and $\text{C}_{10}\text{H}_6\text{Cl}_2$	77
3.4	Conclusions	82
3.5	References	84

Chapter 4: The Intramolecular Activation of $\text{C}_\beta\text{-H}$ Bond by Transition Metal Complexes

4.0	Abstract	88
4.1	Introduction	89
4.2	Computational Details	95
4.3	Results and Discussion	96
4.3.1	Metal-ethyl, Metal-agostic and Metal-ethylene-hydride Complexes	101
4.4	Conclusions	124
4.5	References	126

Chapter 5: Bond Length and Bond Multiplicity: σ Bond Prevents Short π Bonds

5.0	Abstract	137
5.1	Introduction	138
5.2	Computational Details	142
5.3	Results and Discussion	143
5.3.1	Short Bonds in Main Group Compounds	143
5.3.1.1	Five Valance Electron Diatomic Species	145
5.3.1.2	Six Valance Electron Diatomic Species	146
5.3.1.3	Seven Valance Electron Diatomic Species	148
5.3.1.4	Eight Valance Electron Diatomic Species	150
5.3.2	Short Bonds in Transition Metal Complexes	152
5.4	Conclusions	156
5.5	References	158
	List of Publications	162

CHAPTER 1

INTRODUCTION TO COMPUTATIONAL CHEMISTRY AND OVERVIEW OF THE THESIS

[1] Overview of Computational Chemistry

[1.1] Introduction

A series of observations such as the black body radiation, photoelectric effect, atomic and molecular spectra of the 19th century could not be explained by the then well known classical mechanics. Attempt in the early 20th century by several scientists to explain these observations led to the birth of quantum mechanics.

Quantum mechanics mainly based on (i) Wave-particle duality, (ii) Energy quantization, (iii) Uncertainty principle, and (iv) Non-locality concepts.

Quantum mechanics acknowledges the wave-particle duality of matter by supposing that, rather than traveling along a definite path, a particle is distributed through space like a wave. The concept of trajectory in classical mechanics is replaced by a wave function, ψ , in the new mechanics.

In 1926, Schrödinger proposed an equation which can be regarded as a postulate, like Newton's equations of motion for finding the wavefunction of any system. The time independent Schrödinger equation for a particle of mass m moving in one dimension with energy E is

$$-\frac{\hbar^2}{2m_e} \left[\frac{d^2\psi}{dx^2} + \frac{d^2\psi}{dy^2} + \frac{d^2\psi}{dz^2} \right] + V(x, y, z)\psi(x, y, z) = E\psi(x, y, z) \quad (1.1)$$

The factor $V(x)$ is the potential energy of the particle at the point x ; \hbar is the convenient modification of the plank constant ($\hbar = h/2\pi$). In the general case the Schrödinger equation is written as

$$H\Psi = E\psi \quad (1.2)$$

Where H is the Hamiltonian, an energy operator for the system:

$$H = -\frac{\hbar}{2m}\nabla^2 + V \quad (1.3)$$

The time (t) dependent Schrödinger equation is

$$H\Psi = i\hbar \frac{d\psi}{dt} \quad (1.4)$$

Schrödinger equation is one of the starting points for most of the quantum chemical calculations that are done now using computers. It should be emphasized that the equation cannot really be solved analytically for many electron systems; this means we can solve the equation for hydrogen, but not for many electron atoms or molecules. There have been, however, a number of mathematical methods that use approximation techniques to help chemists to solve Schrödinger equation for the structure and properties of atoms and molecules. Reliability of the results depends on the approximations employed in the theoretical formulations. This thesis uses solution of Schrödinger equation at various levels to solve problems of structure and reactivity in chemistry. The methods used in the calculations reported in the thesis are discussed in the following sections of this chapter. The details of the application of electronic structure theory to the selected problems are given in the remaining four chapters.

[1.2] Theoretical Methods

The quantum theories used in computational chemistry can be broadly classified into two groups which are wave function and density based methods. *Ab initio* and semiempirical methods are wave function based approaches whereas density functional method falls in the latter category. These are the three major methods which will be briefly discussed in the following sections.

[1.2.1] *Ab initio* Methods¹⁻²

The quantum mechanical calculation used in computational chemistry involves finding the solution of Schrödinger equation associated with the molecular Hamiltonian. The Schrödinger equation (1.1) cannot be solved exactly for many electron systems. Thus various approximations are used for solving the Schrödinger equation (1.1). The Hamiltonian for a molecule with M numbers of nuclei (α, β, \dots) and N number of electrons (i, j, \dots) is given by,

$$\hat{H} = -\frac{\hbar^2}{2} \sum_{\alpha} \frac{1}{m_{\alpha}} \nabla_{\alpha}^2 - \frac{\hbar^2}{2m_e} \sum_i \nabla_i^2 - \sum_{\alpha} \sum_i \frac{Z_{\alpha} e^2}{r_{i\alpha}} + \sum_{\alpha} \sum_{\beta > \alpha} \frac{Z_{\alpha} Z_{\beta} e^2}{r_{\alpha\beta}} + \sum_j \sum_{i > j} \frac{e^2}{r_{ij}} \quad (1.5)$$

where m , e , Z and r are the mass of the particle, electronic charge, atomic number and distance between the particles respectively. The first and second terms are the nuclear and electronic kinetic energy operators. The third, fourth, and fifth terms represent the potential energy for the nuclear-electron attraction, nuclear-nuclear repulsion and electron-electron repulsion respectively. The following mathematical approximations are used for solving the Schrödinger equation.

Methods that do not include any experimental data other than fundamental constants (electronic mass, charge, Planck's constant etc.) are called *ab initio* (*ab initio* is from the Latin: "from the first principles") methods. The *ab initio* method solves the Schrödinger equation for a molecule and its properties. *Ab initio* methods provide highly accurate quantitative prediction for varying range of systems. They were quite expensive computationally, but with the advent of hardware and softwares of ever increasing sophistication they could be performed for fairly large molecules in reasonably short time.

[1.2.1.1] The Born-Oppenheimer Approximation³

The nuclei in a molecule, may be treated as stationary with respect to the motion of the electrons as the masses of the nuclei (m_α) are much greater than the mass of the electron (m_e). So, the Hamiltonian of the nuclei and electron become separable and the total wavefunction can be written as a product of the electronic and nuclear wavefunctions. The full Hamiltonian [$\hat{H}(r, R)$] for the molecule is

$$\hat{H}(r, R) = \hat{T}_N + \hat{T}_e + \hat{V}_{ee}(r) + \hat{V}_{eN}(r, R) + \hat{V}_{NN}(R) \quad (1.6)$$

where r , and R the electronic and nuclear coordinates. The first two terms are the kinetic energy operators for the nuclei and the electrons, respectively, and the last three terms are the potential energy operators for the Coulombic interactions: electron-electron, electron-nuclear, and nuclear-nuclear. Thus for the purpose of finding the electronic energy, we consider the nuclear position fixed. The operator

\hat{T}_N (1.6) is then neglected and the potential \hat{V}_{NN} is considered as a constant. Thus the

Hamiltonian (1.6) can be simplified as $\hat{H}_{el} = \hat{T}_e + \hat{V}_{ee} + \hat{V}_{eN}$:

$$\hat{H}_{el} \Psi_{el} = E_{el} \Psi_{el} \quad (1.7)$$

$$\text{Where} \quad \hat{H}_{el} = -\frac{\hbar^2}{2m_e} \sum_i \nabla_i^2 + \sum_j \sum_{i>j}^N \frac{e^2}{r_{ij}} - \sum_\alpha \sum_i^N \frac{Z_\alpha e^2}{r_{i\alpha}} \quad (1.8)$$

Since, the electron-nuclear potential energy (\hat{V}_{eN}) depends on the fixed position of the nuclei; the wavefunction for the electronic state i depends explicitly on the electronic coordinate (r) and parametrically on the internuclear distance R .

$$(\hat{H}_{el} + \hat{V}_{NN}) \Psi_{el} = (E_{el} + V_{NN}) \Psi_{el} = U \Psi_{el} \quad (1.9)$$

$$\text{Where} \quad \hat{V}_{NN} = \sum_\alpha \sum_{\beta>\alpha}^M \frac{Z_\alpha Z_\beta e^2}{R_{\alpha\beta}} \quad (1.10)$$

The energy, U in (1.9) is the electronic energy including internuclear repulsion (V_{NN}). The internuclear distances $R_{\alpha\beta}$ in equation 1.10 are not variables, but are fixed at some constant values. Thus, the electronic wave functions and energies depend parametrically on the nuclear configuration. The energy U (1.9) is the potential function $V_i(R)$ for the nuclear motion in electronic state i :

$$V_i(R) = E_i(R) + V_{NN} \quad (1.11)$$

The most important consequence of this approximation is the potential energy surface concept, which provides a conceptual as well as a computational base for molecular physics and chemistry. The idea of separation of nuclear and electron motion was suggested by Born and Oppenheimer; hence this is called Born-Oppenheimer approximation.

[1.2.1.2] Variation Theorem

Despite the Born-Oppenheimer approximation, it is not possible to solve the Schrödinger equation. If a good approximation is available for the wave function, the variation theorem can be used to improve this. In this approach, one uses an approximate normalized wave function Ψ which obeys the appropriate boundary conditions. The variation theorem states that the energy expectation value calculated (E_Ψ) using this trial function (Ψ) can not be lower than the true ground-state energy E_0 :

$$E_\Psi = \frac{\int \Psi^* \hat{H} \Psi d\tau}{\int \Psi^* \Psi d\tau} \geq E_0 \quad (1.12)$$

The ground state energy is obtained by minimizing E_Ψ with respect to parameters present in the trial function. The variation principle says that the ground state energy can be calculated (E_0) by tuning the trial function along with their arbitrary parameters. The energy also will depend upon these variational parameters.

[1.2.1.3] The LCAO-MO Approximation

To solve the Schrödinger equation of a molecule having several atoms, one has to consider a trial function Ψ . The Linear Combination of Atomic Orbital Molecular Orbital (LCAO-MO) is found to be one of the best trial functions for electronic structure calculations. If $\phi_1, \phi_2, \phi_3, \dots, \phi_n$ are the atomic orbitals then

$$\Psi = \sum_{i=1}^n c_i \phi_i \quad (1.13)$$

Where, c_i is the coefficient of i^{th} atomic orbital.

The calculated energy (E_Ψ) using this trial function should be

$$E_\Psi = \frac{\int (\sum_i^n c_i \phi_i)^* \hat{H} (\sum_i^n c_i \phi_i) d\tau}{\int (\sum_i^n c_i \phi_i)^* (\sum_i^n c_i \phi_i) d\tau} \geq E_0 \quad (1.14)$$

The minimization of the energy using the variation theorem leads to n linear homogeneous equations known as Secular equations. For non trivial solution (i.e. solutions other than $c_i=0$) the corresponding Secular Determinant will be equal to zero:

$$H_{ij} - ES_{ij} = \begin{vmatrix} H_{11} - ES_{11} & H_{12} - ES_{12} & \dots & H_{1n} - ES_{1n} \\ H_{21} - ES_{21} & H_{22} - ES_{22} & \dots & H_{2n} - ES_{2n} \\ \dots & \dots & \dots & \dots \\ H_{n1} - ES_{n1} & H_{n2} - ES_{n2} & \dots & H_{nn} - ES_{nn} \end{vmatrix} = 0 \quad (1.15)$$

$$\text{Where,} \quad H_{ii} = \int \phi_i^* \hat{H} \phi_i d\tau \quad (1.16)$$

$$H_{ij} = \int \phi_i^* \hat{H} \phi_j d\tau \quad (1.17)$$

$$S_{ij} = \int \phi_i^* \phi_j d\tau \quad (1.18)$$

The integrals H_{ii} and H_{ij} are called coulomb integrals where as S_{ij} is the overlap integral. Solving the n^{th} order determinant will give n roots i.e., a set of n energy values, $E_1, E_2, E_3, \dots, E_n$ and a set of n wave functions, $\Psi_1, \Psi_2, \dots, \Psi_n$.

Antisymmetric nature of complete wave function Ψ leads to the following Slater Determinantal form of the wave function,

$$\Psi = \begin{vmatrix} \Psi_1(1) & \Psi_2(1) & \dots & \Psi_n(1) \\ \Psi_1(2) & \Psi_2(2) & \dots & \Psi_n(2) \\ \dots & \dots & \dots & \dots \\ \Psi_1(n) & \Psi_2(n) & \dots & \Psi_n(n) \end{vmatrix} = 0 \quad (1.19)$$

where, $\Psi_n(i)$ is the spin orbital of i^{th} particle.

[1.2.1.4] The Hartree-Fock Self Consistent Field Method⁴

Hartree-Fock methods is based on variational principle according to which the energy obtained using an antisymmetric trial wave function is always greater than the exact energy. The main problem arises from the fact that any atom or molecule with more than one electron could not be solved exactly, because of the electron-electron repulsion terms. The Hamiltonian for N electrons system (equation 1.20), under Born-Oppenheimer approximation assuming the nuclei (M) and electrons to be point masses is

$$\hat{H}_{el} = -\frac{\hbar^2}{2m_e} \sum_i^N \nabla_i^2 - \sum_{\alpha}^M \sum_i^N \frac{Z_{\alpha} e^2}{r_{i\alpha}} + \sum_j^N \sum_{i>j}^N \frac{e^2}{r_{ij}} \quad (1.20)$$

The electron-electron repulsion terms make the Schrödinger equation non-separable. Hartree's method calculates the effective repulsion on a single electron by the rest of the electron cloud which makes Hamiltonian separable. Hartree's method writes a plausible approximate polyelectronic wavefunctions for an atom as the product of one-electron wavefunction. The Ψ_0 can be written as the product of hydrogen like one electron orbital as follows,

$$\Psi_0 = \Psi_0(1)\Psi_0(2)\Psi_0(3)\cdots\Psi_0(n) = \prod_i^n \Psi_0(i) \quad (1.21)$$

$$\text{Where } \Psi_0(i) = f_i(r_i, \varphi_i, \theta_i) \quad (1.22)$$

This function is called Hartree product. Here Ψ_0 is a function of the coordinates of all the electrons in the atom, $\Psi_0(i)$ is a function of the coordinates of the i^{th} electron. The initial guess $\Psi_0(i)$, is the zeroth approximation to the true total wavefunction Ψ . The function f has radial and angular part as given below,

$$f = R_{nl}(r)Y_l^m(\varphi, \theta) \quad (1.23)$$

Where r, φ, θ are spherical polar coordinates; R_{nl} is radial part and Y_l^m is spherical harmonics of the electronic wave function.

Although the approximate wave function (equation 1.21) is qualitatively advantageous but certainly it lacks the quantitative accuracy. The accuracy of the wave function can be improved by considering effective quantum numbers for each orbitals, which takes care of the screening effect of electrons. Further improvement of the wave function can be done using variational theorem. The trial function for the variation theorem is

$$\phi = g_1(r_1, \varphi_1, \theta_1)g_2(r_2, \varphi_2, \theta_2)\dots g_n(r_n, \varphi_n, \theta_n) \quad (1.24)$$

where $g_i = h_i(r_i)Y_{l_i}^{m_i}(\varphi_i, \theta_i)$, which minimizes the variational integral,

The procedure for calculating the g_i is called Hartree Self Consistent Field (SCF) method. In this method, the wave function lacks the antisymmetric nature. The antisymmetric nature of the wave function has been included by Fock, defining the Slater determinant. Thus, the SCF calculation which gives antisymmetrized spin orbitals is called Hartree-Fock method. The differential equation for the Hartree-Fock orbitals is

$$\hat{F}\mu_i = \varepsilon_i \mu_i \quad i = 1, 2, \dots, n \quad (1.25)$$

where F is Hartree-Fock operator, μ_i is i^{th} spin-orbital and ε_i is the spin orbital energy. The Hartree Fock operator (\hat{F}) is defined as

$$\hat{F} = -\frac{1}{2}\nabla_i^2 - \sum_i^N \frac{Z_\alpha}{r_{i\alpha}} + \sum_i^{N/2} \sum_j^{N/2} 2J_{ij} - K_{ij} \quad (1.26)$$

$$= \hat{H}^{\text{core}} + \sum_i^{N/2} \sum_j^{N/2} 2J_{ij} - K_{ij} \quad (1.27)$$

The one electron core Hamiltonian,

$$\hat{H}^{\text{core}} = \int \phi_i \left(-\frac{1}{2} \nabla_i^2 - \sum_{\alpha}^N \frac{Z_{\alpha}}{r_{i\alpha}} \right) \phi_i^* d\tau \quad (1.28)$$

$$J_{ij} = \int \phi_i(1) \phi_j(2) \left(\frac{1}{r_{12}} \right) \phi_i^*(1) \phi_j^*(2) d\tau \quad (1.29)$$

$$K_{ij} = \int \phi_i(1) \phi_j(2) \left(\frac{1}{r_{12}} \right) \phi_i^*(2) \phi_j^*(1) d\tau \quad (1.30)$$

J_{ij} and K_{ij} are called Coulomb and Exchange integrals respectively. The Coulomb integral corresponds to the potential energy of the interaction between a given electron and the rest of the electron cloud. The Exchange integral will take care of the antisymmetric nature of the wavefunction with respect to the electron exchange.

In Hartree-Fock theory, the inter-electronic interactions are taken into account using an average potential resulting single Slater determinant solution. Exact wave functions, however, cannot generally be expressed as single determinants. The single-determinant approximation does not consider Coulomb correlation, leading to a total electronic energy different from the exact solution of the non-relativistic Schrödinger equation. Therefore the Hartree-Fock limit is always above the exact energy. The difference between non-relativistic and Hartree Fock energy is called the *correlation energy*.

The correlation energy (E_{corr}) is given by,

$$E_{\text{corr}} = E_{\text{nonrel}} - E_{\text{HF}} \quad (1.31)$$

E_{nonrel} is the exact non-relativistic energy and E_{HF} is HF energy.

[1.2.1.5] Basis Sets

In the *ab initio* method, basis set is an approximation like several other approximations used for solving Schrödinger equation. A basis set is a set of functions which is used to describe the state of the molecular system. Usually these functions are atomic orbitals, which are expanded as a linear combination to create the molecular orbitals. When molecular calculations are performed, it is common to use a basis composed of a finite number of atomic orbitals, centered at each atomic nucleus within the molecule. For many electron system the orbitals can be replaced by Slater type orbitals (STO).⁵ The functional form of Slater Type Orbitals (STOs) is

$$\chi_{p,n,l,m}(r, \theta, \phi) = NY_{l,m}(\theta, \phi)r^{n-1}e^{-\zeta r} \quad (1.32)$$

Where $Y_{l,m}$ is the spherical harmonic function, and N is the normalization constant. It resembles the hydrogen like orbitals which is obvious from the exponential dependence on the distance between the nucleus and the electron.

Even though STOs can well describe the state of many electrons system, the evaluation of integrals in terms of STO is computationally demanding. The Slater-type orbitals could in turn be approximated as linear combinations of Gaussian orbitals⁶ which are easier to calculate the overlap and other integrals with Gaussian basis functions and this led to huge computational savings.

The Cartesian Gaussian Type Orbital (GTO) has the form:

$$\chi_{p,l_x,l_y,l_z}(x, y, z) = Nx^{l_x}y^{l_y}z^{l_z}e^{-\zeta r^2} \quad (1.33)$$

where l_x , l_y and l_z are integers and ζ is the orbital exponent. Though the use of GTOs makes the computation easier but they are functionally different from the

atomic orbital wave functions. In particular, the Gaussian function lacks a cusp at the nucleus and hence the region near the nucleus is described rather poorly.

So, the basis sets can be expressed linear combination of Gaussian-type orbitals (GTOs). The smallest of these are called *minimal* basis sets and they are typically composed of the minimum number of basis functions required to represent the state of the system. The STO-3G basis set is a minimal basis set, which uses 3GTOs (primitive Gaussian) to form the basis set. Depending upon the molecular system and properties, the basis set can be functionally modified. During the molecular bonding, it is the valance electrons which mainly take part in the bonding. So, we have to represent the valance orbitals by more than one basis functions. This is called Split-Valance basis sets. The Split-Valance basis sets are typically M-NOg where M, N and O are integers. The presence of two numbers after the hyphens implies that this basis set is a *split-valence double-zeta* basis set. A double zeta (DZ) basis set contains two STOs that differ in the orbital exponent for each AO. Similarly, triple zeta (TZ) basis set has the form M-NOPg which uses three STOs for the construction of basis set. The integers before and after hyphen (-) represents the number of primitive Gaussian function used to represent core and valance orbitals respectively. For example, the basis set 6-31G uses 6 primitive Gaussian function for representing core orbitals. The two digits after hyphen indicates that each valance orbitals are spitted into two basis function. The first one composed of a linear combination of 3 primitive Gaussian functions, the other composed of a linear combination of only 1 primitive Gaussian functions.

The shape of the orbital becomes more real when we add polarization functions to the basis set. This is done by the addition of orbitals with higher angular momentum than what is necessary to describe the ground state of an atom. For example, polarized basis set add f-function to transition metal atoms, d-function to C atoms and p-functions to H atoms. Basis set like 6-31G(d) means d-functions are added to the heavy atoms of the standard 6-31G basis sets.

Another type of basis set, known as diffuse basis set. It allows orbitals to occupy large region of space. These Gaussian basis functions describe the molecules containing lone pair, anions or systems with low ionization potential where electrons are relatively farther from the nucleus. They are indicated as a '+' sign. For example 6-31 + G(d) basis set indicates that diffuse functions are added to the heavy atoms. The computational cost increases gradually while computing the molecules involving heavier atoms (third and higher rows of the periodic table) in comparison to first and second row atoms. This is because of increasing number of two electron integrals and the relativistic effects. This could be overcome by the use of pseudo potentials or effective core potential. Since, the valance electrons are mainly responsible for the chemical bonding so the core orbitals electrons could be treated as an average potential. The state of valence electrons can be described by proper basis functions. A commonly used pseudo potential is the Effective Core Potential (ECP)⁷ and is of the general form,

$$\text{ECP}(r) = \sum_i^k C_i r^{n_i} e^{(-\alpha_i r^2)} \quad (1.34)$$

where, k is the number of terms in the expansion, C_i is a coefficient characteristic of each term, r is the distance from the nucleus, n_i and α_i is an exponent for i^{th} term.

The use of ECP is found to be computationally very efficient, especially for transition metals, because it reduces the number of basis functions significantly. ECP also makes room for the incorporation of relativistic effects.

[1.2.1.6] Electron Correlation

The Hartree-Fock method is not capable of giving the correct solution to the Schrödinger equation even if a very large and flexible basis set is selected.⁸ The very best Hartree-Fock wave function, obtained with just such a large and flexible basis set, is called the "Hartree-Fock limit". The problem is that electrons are not paired up in the way that the Hartree-Fock method supposes. It suggests that the two electrons have the same probability of being in the same region of space as being in separate symmetry equivalent regions of space. For example, in H₂ it would give the same probability of both electrons being near one atom as one being near one atom and the other near the second atom. This is clearly wrong. The Hartree-Fock method also only evaluates the repulsion energy as an average over the whole molecular orbital. There are three common methods which included electron correlation viz. Configuration Interaction,⁹ Møller-Plesset Perturbation theory,¹⁰ and Coupled Cluster Theory.¹¹ These calculations are in principle HF calculations where the correlation term is corrected.

[1.2.1.6.1] Configuration Interaction

Configuration interaction (CI) is a post Hartree-Fock linear variational method for solving the nonrelativistic Schrödinger equation. *Configuration* simply describes the linear combination of Slater determinants used for the wave function. *Interaction* means the mixing (interaction) of different electronic configurations (states). In

contrast to the Hartree-Fock method, in order to account for electron correlation, CI uses a variational wave function that is a linear combination of configuration state functions (CSFs) built from spin orbitals (denoted by the superscript SO),

$$\Psi = \sum_{I=0} c_I \Phi_I^{SO} = c_0 \Phi_0^{SO} + c_1 \Phi_1^{SO} + \dots \quad (1.35)$$

where Ψ is usually the electronic ground state of the system. If the expansion includes all possible CSFs of the appropriate symmetry, then this is a full configuration interaction procedure which exactly solves the electronic Schrödinger equation within the space spanned by the one-particle basis set. The configuration function in a CI calculations are classified as singly excited (CIS), doubly excited, triply excited, ..., according to whether 1, 2, 3, ... electrons are excited from occupied to unoccupied orbitals. CIS calculation is the most common way to get excited state energies. In the case of single and double excitation (CISD) calculations, it yields a ground state energy that has been corrected for correlation. However, full CI calculations needs high computational power even for small molecule.

[1.2.1.6.2] Møller-Plesset Perturbation Theory

Møller-Plesset Perturbation Theory is a post HF ab initio method. It improves the HF method by adding electron correlation effects using perturbation theorem. Here, the sum of the one electron HF operator as the unperturbed Hamiltonian (\hat{H}_0).

$$\hat{H}_0 = \sum_m^n F(m) \quad (1.36)$$

The unperturbed Hamiltonian operator \hat{H}_0 is extended by adding a small perturbation H' .

$$\hat{H} = \hat{H}_0 + \lambda H' \quad (1.37)$$

$\lambda H'$ is the perturbation where λ is a dimensionless parameter.

From Rayleigh-Schrödinger perturbation theory we have,

$$\psi_\lambda = \psi^{(0)} + \lambda \psi^{(1)} + \lambda^2 \psi^{(2)} + \dots \quad (1.38)$$

$$E_\lambda = E^{(0)} + \lambda E^{(1)} + \lambda^2 E^{(2)} + \dots \quad (1.39)$$

Substituting (1.37), (1.38), and (1.39) in the Schrödinger equation, we obtain

$$(\hat{H}_0 + \lambda H')(\psi^{(0)} + \lambda \psi^{(1)} + \lambda^2 \psi^{(2)} + \dots) = (E^{(0)} + \lambda E^{(1)} + \lambda^2 E^{(2)} + \dots)(\psi^{(0)} + \lambda \psi^{(1)} + \lambda^2 \psi^{(2)} + \dots) \quad (1.40)$$

Gathering terms having similar power, we get equation

$$\hat{H}_0 \psi_0 = E_0 \psi_0 \quad (1.41)$$

$$(H' - E^{(1)})\psi^{(0)} + (H_0 - E^{(0)})\psi^{(1)} = 0 \quad (1.42)$$

Solving this equation we get first order correction to the energy $E^{(1)}$ and wave function $\psi^{(1)}$.

$$E_1 = \langle \psi^{(0)} | H' | \psi^{(1)} \rangle \quad (1.43)$$

$$\psi^{(1)} = \sum_{j \neq i} \frac{\langle \psi_j | H' | \psi_i \rangle}{E_i - E_j} \psi_j \quad (1.44)$$

The energy correction in MP theory can be taken as various orders like 1st order (HF), 2nd order (MP2), 3rd order (MP3) and so on when the series (1.38) and (1.39) are cut after first, second, third order and so forth.

[1.2.2] Semi-empirical Methods^{1,2}

Semi-empirical methods are simplified version of Hatree-Fock (HF) theory using empirically parameters derived from experimental data in place of integrals in order to improve the performance. Different semi-empirical methods differ in the details of the approximation and in particular in the values of the parameters.

These methods can be classified into two categories: those using a Hamiltonian that is the sum of all one electron terms, and the others that includes two-electron terms in addition to one electron terms. Methods like Hückel and Extended Hückel (EH) fall under the former category, where as MNDO,¹² AM1,¹³ PM3¹⁴ etc. fall under the latter category. The simplest among these methods, the Hückel Molecular Orbital (HMO) theory,¹⁵ developed in 1930's. The HMO theory uses fundamental basis set of valance electrons in addition to the undefined one electron energy operator.

Methods which include two electron integrals are based on the HF approach where as those involving one electron integrals are of different type is discussed in the following sections.

[1.2.2.1] Extended Hückel Method¹⁶

The Extended Hückel (EH) Theory explicitly includes all the overlap integrals between the atomic orbitals and systemic guesses for the elements of the Hamiltonian matrix. The Hamiltonian includes all the valence electrons which are the sum of all one electron Hamiltonians. The nuclei and electron-electron interactions are ignored in this method.

$$\hat{H}_{val} = \sum_i^n H_{eff}(i) \quad (1.45)$$

The basis set used is the Slater type orbitals and MOs are approximated as linear combinations of the valence atomic orbitals:

$$\phi_i = \sum_r^n C_{ri} f_r \quad (1.46)$$

$$\hat{H}_{eff}(i)\phi_i = \varepsilon_i \phi_i \quad (1.47)$$

Here, the total energy is taken as the sum of the one electron energies

$$E_{val} = \sum_i^n \varepsilon_i \quad (1.48)$$

The secular determinant is obtained after applying the variation theorem on the trial function from which the MO coefficients can be determined:

$$|H_{rs}^{eff} - \varepsilon_i S_{rs}| = 0 \quad (1.49)$$

$$\sum_s^n (H_{rs}^{eff} - \varepsilon_i S_{rs}) = 0 \quad r=1, 2, \dots \quad (1.50)$$

EH theory includes overlap integrals (S_{rs})

$$\text{for } r=s, H_{rs}^{eff} = H_{rr}^{eff} = \langle f_r | H_{eff} | f_r \rangle \quad (1.51)$$

$$\text{when } r \neq s, H_{rs}^{eff} = \frac{1}{2} k (H_{rs}^{eff} + H_{rr}^{eff}) S_{rs} \quad (1.52)$$

where, k is a numerical constant. H_{rs}^{eff} and H_{rr}^{eff} are usually negative, as a result, H_{rs}^{eff} in equation (1.50) is also negative. The difference of EH with simple Hückel theory is that, H_{rs}^{eff} is non-zero for all pairs of orbitals unless S_{rs} vanishes for symmetry reasons.

The total energy (Equation 1.48) is the sum of the orbital energies. In EH method, the results are fairly accurate even though the electron-electron and nuclear-nuclear

repulsions are not included. It fails to give accurate results for the polar compounds. Even though the results are not quantitative, it provides good qualitative results in understanding many chemical problems. Walsh diagram and fragment molecular orbital (FMO) analysis can be done qualitatively using EH calculations.

There are several other semiempirical methods like CNDO,^{1,2} INDO,^{1,2} NDDO,^{1,2} MINDO,¹⁷ etc, which includes overlap and electron-electron repulsion integrals to some extent.

[1.2.3] Density Functional Theory¹⁸

The premise behind Density Functional Theory (DFT) is that the chemical properties of a molecule can be determined from the electron density instead of a wave function. The original DFT theorem (Hohenberg-Kohn theorems)^{18c,e} applied only to finding the ground-state electronic energy of a molecule. A practical application of this theory was developed by Kohn and Sham who formulated a method similar in structure to the Hartree-Fock method. In this formulation, the electron density is expressed as a linear combination of basis functions similar in mathematical form to HF orbitals. A determinant is then formed from these functions, called Kohn-Sham orbitals. It is the electron density from this determinant of orbitals that is used to compute the energy.

The first Hohenberg-Kohn (HK) theorem says that any ground state property of a molecule is a functional of the ground state electron density function, e.g. for the energy

$$E_0 = E_0[\rho_0] \quad (1.53)$$

where, the zero (0) subscript indicates ground state. So, the Hamiltonian in this case is

$$\hat{H} = -\frac{1}{2} \sum_i^N \nabla_i^2 + \sum_i^N v(\vec{r}_i) + \sum_j^N \sum_{i>j}^N \frac{1}{r_{ij}} \quad (1.54)$$

where, $v(\vec{r}_i)$ is the potential energy of interaction between electron and nuclei, called as external potential and expressed as

$$v(\vec{r}_i) = - \sum_{\alpha}^N \frac{Z_{\alpha}}{r_{i\alpha}} \quad (1.55)$$

The number of electrons, (n) can be determined from $\rho_0(r)$ as

$$\int \rho_t(r) dr = n \quad (1.56)$$

$$E_v[p_t] \geq E_0[p_0] \quad (1.57)$$

The second Hohenberg-Kohn theorem says (equation 1.55 and 1.56) that any trial electron density function $[\rho_t(r)]$ will give an energy higher than (or equal to, if it were exactly the true electronic density function) the true ground state. Since, $E_0 = E_0[\rho_0]$ where ρ_0 is true ground state electron density, the true ground state electron density minimizes the energy functional, $E_v[\rho_t(r)]$.

The first Kohn-Sham (KS) theorem^{18f} describes that it worth looking for way to calculate molecular properties from the electron density. The energy calculated from this theory is not an accurate as it involves an unknown approximated functional. The accuracy of this method depends on the quality of the unknown functional called exchange-correlation functional, $E_{xc}[\rho_0]$.

$$E_{xc}[\rho_0] = \Delta \bar{T}[\rho_0] + \Delta \bar{V}_{ee}[\rho_0] \quad (1.58)$$

The $\Delta\bar{T}$ term represents the kinetic correlation energy of the electrons and the $\Delta\bar{V}_{ee}$ term the potential correlation energy and the exchange energy. The functional derivatives of E_{xc} is the exchange-correlation potential

$$V_{xc}(r) = \frac{\delta E_{xc}[\rho_0(r)]}{\delta \rho_0(r)} \quad (1.59)$$

Inclusion of variational principle in Hohenberg-Kohn first theorem, we get the second theorem of Hohenberg-Kohn

$$E_{v(r)}[\rho(r)] = T[\rho(r)] + V_{ee}[\rho(r)] + \int \rho_0(r)v(r)dr \geq E_{v(r)}[\rho_0(r)] \quad (1.60)$$

Considering the effect of external potential V_s , the energy become

$$E_s[\rho(r)] = \int \Psi_s[\rho(r)](T + V_s)\Psi[\rho(r)]d\tau + T_s[\rho(r)] + \int \Psi_s[\rho(r)]V_s\Psi[\rho(r)]d\tau \geq E_{v(r)}[\rho_0(r)] \quad (1.61)$$

[1.2.3.1] Local Density Approximation

The key to the success of DFT lies in the approximations made for exchange correlation functional. The local Density Approximation (LDA) is one of the simplest approximations for getting a good exchange correlation functional. It is applied to a uniform (homogenous) electron gas (or one in which the electron density $\rho_0(r)$ varies only very slowly with position). When ρ_0 varies with position extremely slowly, then $E_0[\rho_0]$ can be expressed as,

$$E_{xc}^{LDA}[\rho_0] = \int \rho_0(r)\varepsilon_{xc}^{LDA}[\rho_0]d\tau \quad (1.62)$$

$\varepsilon_{xc}[\rho_0]$ is the exchange and correlation energy per electron in a homogenous electron gas with ρ_0 electron density. The functional derivative of $E_{xc}^{LDA}[\rho_0]$ gives

$$V_{xc}^{LDA} = \frac{\delta E_{xc}^{LDA}[\rho_0]}{\delta \rho} = \varepsilon_{xc}^{LDA}[\rho_0(r)] + \rho_0(r) \frac{\partial \varepsilon_{xc}^{LDA}(\rho)}{\partial \rho} \quad (1.63)$$

Here, ε_{xc} is the sum of exchange and correlation energy

$$\varepsilon_{xc}^{LDA}(\rho_0) = \varepsilon_x^{LDA}(\rho_0) + \varepsilon_c^{LDA}(\rho_0) \quad (1.64)$$

Similarly,

$$E_{xc}^{LDA} = E_x^{LDA} + E_c^{LDA} \quad (1.65)$$

[1.2.3.1.1] Local Spin-Density Approximation

In this Approximation the electrons of α and β spin in the uniform electron gas are assigned different KS orbitals ψ_α^{KS} and ψ_β^{KS} where as in the LDA approximation the electrons of α and β spin paired with each other and occupy same spatial KS orbital. This unrestricted LDA method is called the local spin density approximation, LSDA, and has the advantages that it can handle systems with one or more unpaired electrons. For species, in which the all the electrons are paired, the LSDA is equivalent to LDA.

[1.2.3.2] Generalized Gradient Approximation

This is found to be one of the best approximations for the exchange correlation functional. In this approximation, they consider, the electron density of an atom or molecules varies significantly from positions to positions. Nowadays, most DFT calculations use exchange-correlation energy functional E_{xc} that not only involve the LSDA, but also utilize both the electron density and its gradient. These functional are called gradient-corrected or said to use the generalized-gradient approximations (GGA). The considered exchange correlation function is

$$E_{xc}^{GGA}[\rho_0^\alpha, \rho_0^\beta] = \int f(\rho_0^\alpha(r), \rho_0^\beta(r), \nabla \rho_0^\alpha(r), \nabla \rho_0^\beta(r)) d\tau \quad (1.66)$$

where, f is a function of spin densities of electrons and their gradients. The exchange correlation energy can be written as

$$E_{xc}^{GGA} = E_x^{GGA} + E_c^{GGA} \quad (1.67)$$

The most commonly used gradient-corrected-correlation-energy functionals are the Lee-Yang-Parr (LYP)¹⁹ functional, Perdew-Burke-Ernzerhof (PBE)²⁰ exchange and correlation functional, Vosko-Wilk-Nusani functional (VWN),²¹ Becke 88²² correlation functional. One of the most frequently used density functional theory is hybrid density functional (HF-DFT) method. It uses the exchange and correlation functionals as a linear combination of HF, local and gradient corrected functionals. One of the most regularly used hybrid HF-DFT method is B3LYP.

The computations carried out for the work embedded in the chapters 2, 3, 4 and 5 are done at hybrid HF-DFT method, B3LYP, based on Becke's three-parameter functional including Hartree-Fock exchange contribution with a non-local correction for the exchange potential proposed by Becke together with the non-local correction for the correlation energy suggested by Lee *et al.*

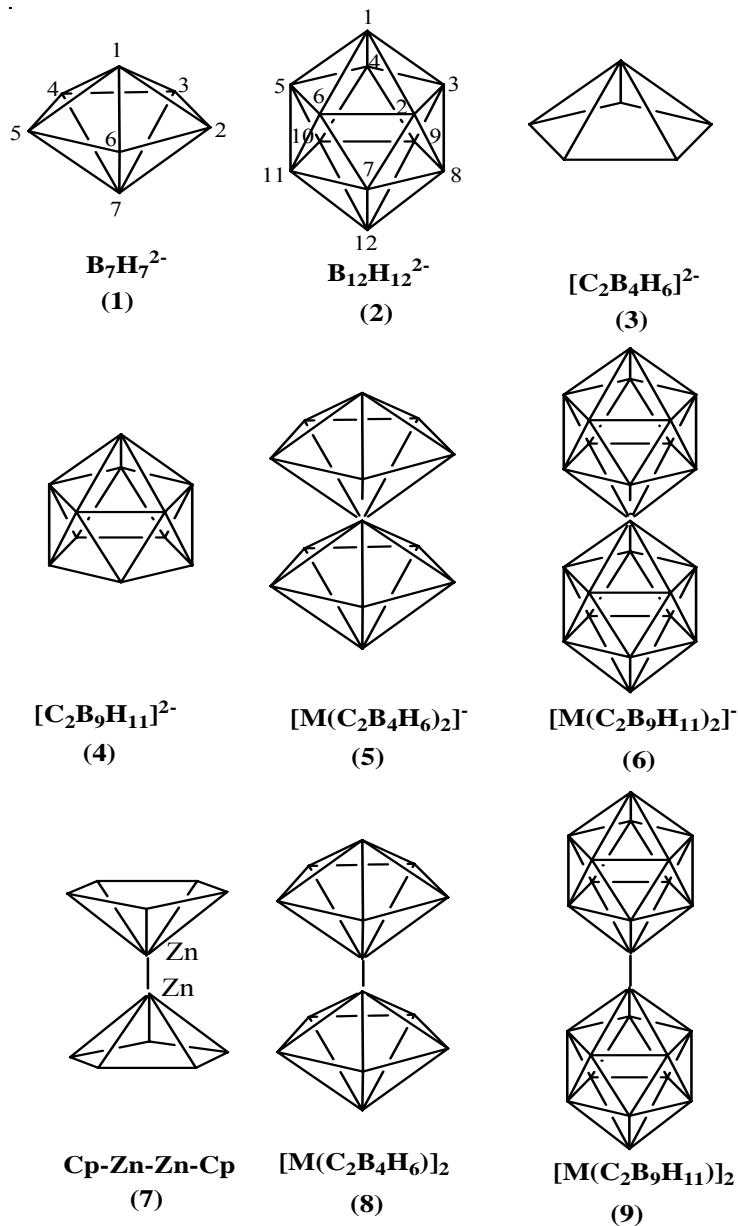
[1.3] Outline of the Thesis

The remaining four chapters are discussed briefly. Second chapter discusses the structure, bonding and relative stabilities of the group 13 incorporated icosahedral and pentagonal-bipyramidal boranes. Further their condensation through single atom sharing and binuclear metallocenes is presented. The condensed single atom sharing polyhedral boranes discussed in the second chapter is extended to the four atom sharing condensed system in the third chapter. Here, we explain the structure and bonding of the condensed four atom sharing ($B_{20}H_{16}$) of the two icosahedral ($B_{12}H_{12}^{2-}$) units and comparisons are made vis-à-vis with the edge sharing ($C_{10}H_8$) of the two benzene units. The electronic requirements of these condensed structures are well understood by *mno* Rule. The metallaboranes studied in the second chapter and benzene, naphthalene as a part of the third chapter lead us to study the C-H bond activation process in presence of transition metal complexes in the fourth chapter. In the fifth chapter we explain the unusual shortness of the bond length in several main group and transition metal compounds on the basis of their π -alone bonding.

[1.3.1] Chapter 2: Reversal of Stability on Metalation of Pentagonal Bipyramidal ($1\text{-MB}_6\text{H}_7^{2-}$, $1\text{-M-2-CB}_5\text{H}_7^{1-}$ and $1\text{-M-2,4-C}_2\text{B}_4\text{H}_7$) and Icosahedral ($1\text{-MB}_{11}\text{H}_{12}^{2-}$, $1\text{-M-2-CB}_{10}\text{H}_{12}^{1-}$ and $1\text{-M-2,4-C}_2\text{B}_9\text{H}_{12}$) Boranes (M=Al, Ga, In and Tl): Energetics of Condensation and Relationship to Binuclear Metallocenes

The pentagonal-bipyramid (**1**) and the icosahedron (**2**) are the two related polyhedra that dominate the chemistry of polyhedral boranes. The icosahedral boranes are usually considered to be the most stable among the polyhedral boranes. The pentagonal-bipyramidal *closo*-borane $\text{B}_7\text{H}_7^{2-}$ (**1**), in contrast, is highly reactive. However this difference in reactivity appears to be altered with the substitution of one of the vertices by a heavier group 13 metal.

We show here that the usual assumption of the extra stability of icosahedral boranes (**2**) over pentagonal-bipyramidal boranes (**1**) is reversed by substitution of a boron vertex by a group 13 metal. This preference is a result of the geometrical requirements for optimum overlap between the five membered face of the ligand and the metal fragment as they all obey the *mno* Rule. Isodesmic equations calculated at the B3LYP/LANL2DZ level indicate that the extra stability of $1\text{-M-2,4-C}_2\text{B}_4\text{H}_7$ (**1**) varies from 14.44 kcal/mol (M = Al) to 15.30 kcal/mol (M = Tl). Similarly, $\text{M}(2,4\text{-C}_2\text{B}_4\text{H}_6)_2^{1-}$ (**5**) is more stable than $\text{M}(2,4\text{-C}_2\text{B}_9\text{H}_{11})_2^{1-}$ (**6**) by 9.26 kcal/mol (M = Al) and by 6.75 kcal/mol (M = Tl). The preference for $(\text{MC}_2\text{B}_4\text{H}_6)_2$ (**8**) over $(\text{MC}_2\text{B}_9\text{H}_{11})_2$ (**9**) at the same level is 30.54 kcal/mol (M = Al), 33.16 kcal/mol (M = Ga) and 37.77 kcal/mol (M = In). The metal-metal bonding here is



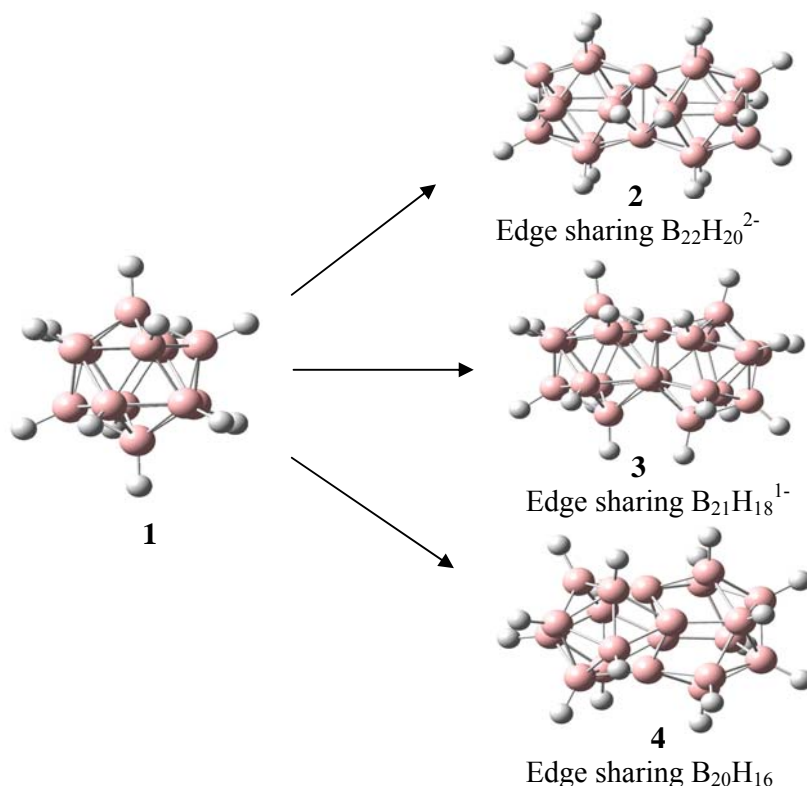
comparable to those in CpZn-Zn-Cp (7) and H_2M-MH_2 ($M = Al, Ga, \text{ and } In$). The trend that group 13 metals prefer pentagonal-bipyramidal skeleton, rather than an icosahedron, is well explained by the orientation of the π -orbitals of the ring in both cases. In $B_7H_7^{2-}$, the π MOs of the B_5H_5 ring will span too large an area to have optimum overlap with the MOs of the two BH fragments. A B_4H_4 ring or caps with

more diffuse orbitals would have been better suited for such interaction. Thus, the B-H bonds of the B_5H_5 ring would bend out of the B_5 plane, rehybridizing the orbitals so that the larger lobe is directed toward the group with more diffuse orbitals. The overlap of fragment MOs in $B_{11}H_{11}^{2-}$ requires rehybridization for better overlap with the metal atom. This leads to the distortion of *exo*-polyhedral B-H bonds farther away from the metal so that there is a better orbital match. The overlap between ring π -orbitals and the cap orbitals is improved by the out-of-plane bending of ring hydrogens. The five-membered ring of a pentagonal-bipyramid makes better overlap with the diffuse orbital of metals more effectively than that of an icosahedron. Five-membered faces of the $C_2B_4H_6$ ring can be more easily brought together to form a sandwich because the B-H and the C-H bonds of the five-membered rings are bent away from the central metal atom. This explains the relative stability of the single-atom sharing complexes involving $C_2B_4H_6$ over their icosahedral analogues.

[1.3.2] Chapter 3: Condensed 2- and 3-Dimensional Aromatic Systems: A Theoretical Study on the Relative Stabilities of Isomers of $CB_{19}H_{16}^+$, $B_{20}H_{15}Cl$ and $B_{20}H_{14}Cl_2$ and Comparison to $B_{12}H_{10}Cl_2^{2-}$, $C_6H_4Cl_2$, $C_{10}H_7Cl$ and $C_{10}H_6Cl_2$

Benzene and $B_{12}H_{12}^{2-}$ are important prototypes of two- and three-dimensional aromatic compounds in the carbon and boron families. Condensation of two benzenes sharing an edge gives naphthalene, which has a well-developed chemistry of its own. The properties

of benzene and naphthalene are contrasted frequently in the early days of aromaticity. The variation of aromaticity and reactivity has been especially noted. In contrast, the chemistry of condensed polyhedral borane is only being developed. Among the possible condensation products of $B_{12}H_{12}^{2-}$ (**1**), such as the edge sharing $B_{22}H_{20}^{2-}$ (**2**), face sharing $B_{21}H_{18}^{-}$ (**3**) and four-atom sharing $B_{20}H_{16}$ (**4**) (Scheme 1),



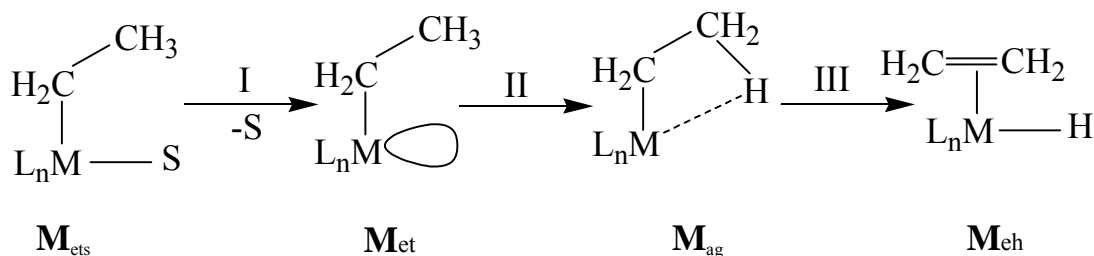
the latter is synthesized and characterized. Though $B_{20}H_{16}$ is one of the borane equivalent of naphthalene, there is limited information available on $B_{20}H_{16}$. A major part of the development in the chemistry of polyhedral boranes came from the study of carboranes. While borane cations are not common, we compare here the isomers of $C_2B_{10}H_{12}$ and $CB_{19}H_{16}^{+}$. We find that such cross comparisons between two and three dimensional structures are useful for understanding their chemistry.

We also study here the structure and stability of the chloroderivatives of $B_{12}H_{12}^{2-}$ and of the condensed product $B_{20}H_{16}$ and compare them to their benzenoid counterparts.

Our DFT studies (B3LYP/6-31G*) on mono- and dichloroderivatives of benzene, naphthalene, $B_{12}H_{12}^{2-}$, four atom sharing condensed systems $B_{20}H_{16}$, and mono-carborane isomers of $B_{20}H_{16}$, are used to compare the variation of relative stability and aromaticity between condensed aromatics. The trends in the variation of the relative energies and aromaticity in these 2- and 3-Dimensional systems are similar. Aromaticity, estimated by NICS values, does not change considerably with condensation or substitution. The minor variation in the relative energies of the isomers of chloro derivatives are explained by the topological charge stabilization rule of Gimarc. The compatibility of cap and ring orbitals decides the relative stability of $CB_{19}H_{16}^+$.

[1.3.3] Chapter 4: The Intra-molecular Activation of C_β -H Bond by Transition Metal Complexes

The activation of inert C-H bonds by a transition metal is of fundamental interest for stoichiometric and catalytic reactions particularly for functionalization of hydrocarbons. The development of catalytic variants of these high barrier reactions allows for efficient syntheses of many types of organic molecules. Binding a transition metal to the C-H bond is the first step in the activation of C-H bonds which leads to the formation of agostic complexes. This is considered to be important especially for α - and β -hydride elimination reactions.



Scheme 1

In this chapter, we attempt to find factors that distinguish the process of C-H bond activation as a function of the transition metal. In addition, we compare agostic complex formation and β -hydride addition reactions catalyzed by transition metal complexes along the groups and across the row of a periodic table. We predict based on their relative stabilities whether a given metal complex will be suitable for a polymerization reactions or β -hydride elimination reactions.

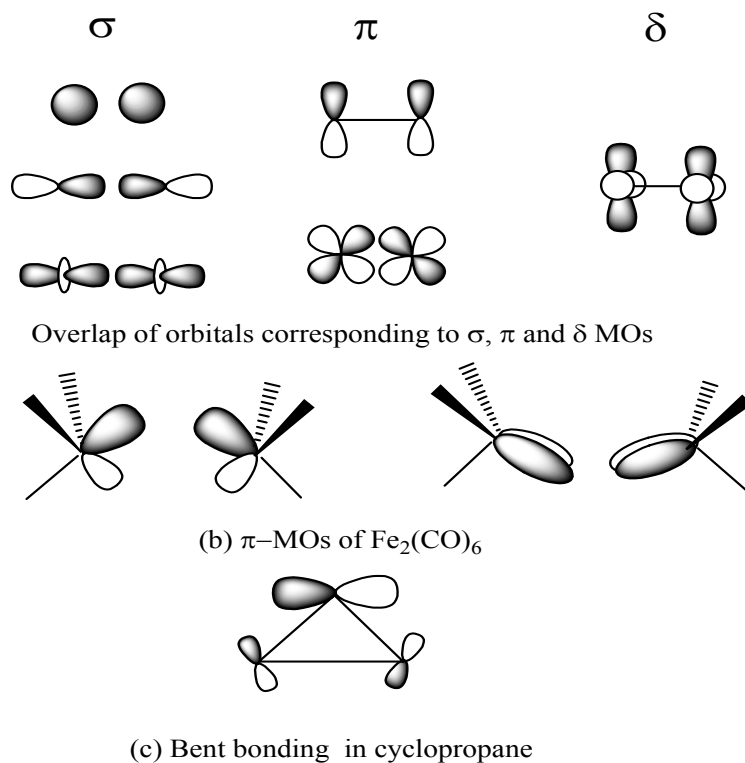
The $\text{C}_\beta\text{-H}$ bond activation process is studied in greater detail using two model set of complexes. The neutral first row complexes are modeled by $\text{Sc}(\text{Cp})_2\text{Et}$, $\text{TiCpEt}(\text{PH}_3)_2$, $\text{VCpEt}(\text{NO})$, $\text{Cr}(\text{PH}_3)_2\text{CpEt}$, $\text{MnEt}(\text{PH}_3)_4$, $\text{FeEt}(\text{PH}_3)_2\text{NO}$, $\text{CoC}_6\text{H}_6\text{Et}$, and $\text{Ni}(\text{Cp})\text{Et}$ and the cationic first row complexes by $[\text{ScCp}(\text{C}_6\text{H}_6)\text{Et}]^+$, $[\text{TiCpEt}(\text{NO})]^+$, $[\text{V}(\text{Cp})\text{Et}(\text{PH}_3)_2]^+$, $[\text{Cr}(\text{Cp})_2\text{Et}]^+$, $[\text{MnEt}(\text{PH}_3)_2\text{NO}]^+$, $[\text{FeEt}(\text{PH}_3)_4]^+$, $[\text{CoCpEt}(\text{PH}_3)]^+$, and $[\text{Ni}(\text{C}_6\text{H}_6)\text{Et}]^+$. The combination of ligands used around the metal centre is from the group Cp, C_6H_6 , $-\text{PH}_3$, and $-\text{NO}$ ligands. Same model complexes are studied for their corresponding group metals. The three possible species involved in the bond activation reaction are Metal-ethyl (M_{et}), Metal-agostic (M_{ag}) and Metal-ethylene-hydride (M_{eh}) (Scheme 1).

It has been noticed that as we move from left to right across the periodic table, the metal atomic energy levels increase but proper combination of ligands prevents the usual trend. As a result the LUMO of the unsaturated metal-ethyl complex comes within the range of interaction for C-H σ -bonding MO and this complex gets stabilized by forming an agostic metal complex. It is possible to fine tune ligands in transition metal complexes so that metal LUMO energy is brought down to interact with the C-H σ -bonding MO. We conclude that any transition metal could be capable of activating the C-H bond if the proper combinations of ligands are provided.

[1.3.4] Chapter 5: Bond Length and Bond Multiplicity: σ Bond Prevents Short π Bonds

The concept of σ -, π - and δ -bonds is ingrained into the thought process of chemists. The cylindrically symmetrical σ -bond is traditionally estimated to be stronger than the π -bond, which in turn is stronger than the δ -bond. The linear overlap of orbitals in the σ -bond is supposed to be more effective than the sideways overlap available in the π - and δ -bonds [Scheme 1a]. Closely related to the discussion of σ -, π - and δ -bonds and their bond strengths is the issue of bond length. The decrease of bond length in going from a single σ -bond to multiple bonds involving σ and π components are exemplified by $\text{H}_3\text{C}-\text{CH}_3$, $\text{H}_2\text{C}=\text{CH}_2$, and $\text{HC}\equiv\text{CH}$ with C-C bond length of 1.538 Å, 1.338 Å and 1.203 Å, respectively. In transition metal chemistry there are the familiar examples of short M-M quadruple bonds constituted from one σ -, two π -, and one δ -bonds as in $\text{Re}_2\text{Cl}_8^{2-}$ of 2.240 Å. Very recently (*Angew. Chem.*

Int. Ed. Volume 46, Page No 1469-72) Roos et. al concludes that the maximum number of covalent chemical bonds between two shared atoms will be six. To find the molecules with the highest bond order, they theoretically studied the transition metal dimers of chromium (Cr_2), molybdenum (Mo_2) and tungsten (W_2) respectively. They predict the maximum number of chemical bonds will be six because the atoms of these transition metals have six outer, or 'valence' orbitals, all of which are available for bonding. The Corresponding short M-M bond distances are 1.66 1.95 and 2.01 Å for Cr_2 , Mo_2 and W_2 respectively. So, the bond length decreases as their bond order increases.



However the variation of orbital overlap as a function of internuclear distance (Figure 1) shows that maximum overlap occurs at shorter distances for π - and δ -bonds. It is therefore logical to anticipate that π -bonds (unsupported by an

underlying σ -bond) could be shorter than σ -bonds. We present here several such examples and conclude that σ -bonds prevent π -bonds from getting to their natural, shorter interatomic distances. Here, we have used DFT theory for analyzing main group and transition metal compounds in greater detail. First row diatomics provide examples where π -orbitals are filled before σ . The diatomic C_2 (1.240 Å, Scheme 2a) has a ground state $^1\Sigma_g^+$ with a double bond,

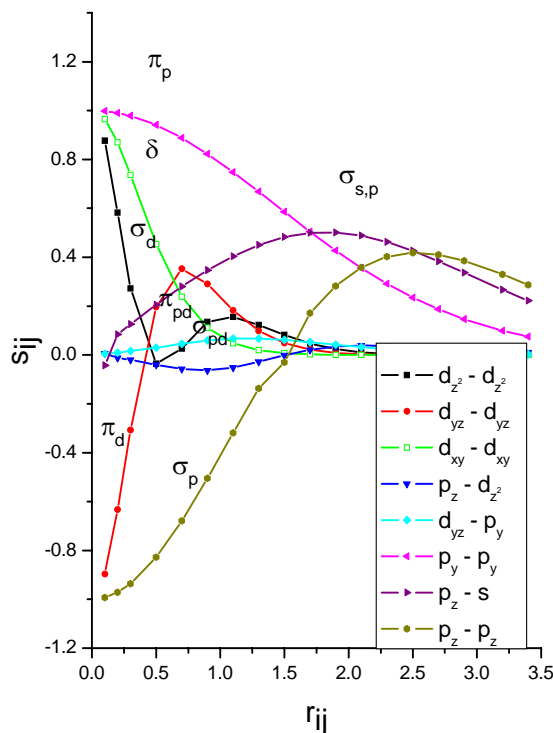


Figure 1: Variation of orbital overlap (s_{ij}) as a function of internuclear distance (r_{ij}) using contracted Gaussian orbitals corresponding to a minimal basis of Fe.

both components of which are π -bonds. A triplet state obtained by shifting [Scheme 2b] one of the electrons from the π -bonding MO of C_2 to the vacant σ -bonding MO should increase the C-C distance ($^3\Pi_u$, 1.313 Å, Scheme 2b). Another triplet state ($^3\Sigma_g^+$) obtained by shifting another electron from π to σ -level elongates the bond to

1.370 Å (Scheme 2c). This led to the conclusion that π^4 ($^1\Sigma^+$) configuration has uniformly shorter R_e than their $\pi^3\sigma^1$ ($^3\Pi$) counterparts by 0.073 Å. Corresponding bond lengths for the $\pi^2\sigma^2$ ($^3\Sigma_g^+$) species are seen to increase by an additional 0.13 Å. Similarly, the diatomic B_2 (Scheme 2d) has a ground state $^3\Sigma_g^-$ ($\sigma_g^2\sigma_u^2\pi_u^2$) with two half π -bonds. The B-B distance (Scheme 2d, 1.590 Å) in B_2 is shorter than any B-B single (~ 1.706 Å) σ -bond.

	$^1\Sigma_g^+$	$^3\Pi_u$	$^3\Sigma_g^+$	$^3\Sigma_g^-$
$3\sigma_g$	—	↑↓	↑↓	—
$1\pi_u$	↑↓ ↑↓	↑↓ ↑	↑ ↑	↑ ↑
$2\sigma_u^*$	↑↓	↑↓	↑↓	↑↓
$2\sigma_g$	↑↓	↑↓	↑↓	↑↓
Bond length	1.240 Å	1.313 Å	1.370 Å	1.590 Å
	(a)	(b)	(c)	(d)

Scheme 2: Experimental bond lengths of C_2 (a) $^1\Sigma_g^+$, (b) $^3\Pi_u$, and of B_2 (d) $^3\Sigma_g^-$. Bond length of C_2 (c) $^3\Sigma_g^+$ is obtained from calculations at B3LYP/6-311+G* method.

We have found similar examples in the transition metal complexes too. Our detailed electronic structure calculation on the transition metal compound, $Fe_2(CO)_6$, explains the unusual shortness of Fe-Fe bond (Fe-Fe=2.002 Å) on the basis of their π -alone bonding. Our detailed study on the second and third row diatomics and transition metal complexes shows that π -bonds left to themselves are shorter than σ -bonds; in many ways σ -bonds prevent π -bonds from adopting their optimal shorter distances.

[1.4] References

1. (a) Levine, I. N. *Quantum Chemistry*, 5th Edition, Prentice Hall, NJ, 2000. (b) McQuarrie, D. A. *Quantum Chemistry*, Oxford University Press, California, 1983. (c) Pilar, F. L. *Elementary Quantum Chemistry*, Mc-Graw Hill Publishing Co., NewYork, 1968. (d) Chandra, A. K. *Introductory Quantum Chemistry*, Tata Mc-Graw Hill Publishing Co., New Delhi, 1988. (e) Szabo, A.; Ostlund, N. S. *Modern Quantum Chemistry*, Mc-Graw Hill Publishing Co., NewYork, **1982**.
2. (a) Hehre, W. J.; Radom, L.; Schleyer, P. v. R.; Pople, J. A. *Ab-initio Molecular Orbital Theory*, John Wiley & Sons, Inc., New York, 1986. (b) Pople, J. A.; Beveridge, D. L. *Approximate Molecular Orbital Theory*, Mc-Graw Hill Publishing Co., NewYork, 1970. (c) Lowe, J. P. *Quantum Chemistry*, Academic Press, New York, 1978. (d) Schaefer III, H. F. *The Electronic Structure of Atoms and Molecules*, Addison-Wesley, Massachusetts, USA, 1972. (e) Foresman, J. B.; Frisch, A. *Exploring Chemistry with Electronic Structure Methods*, Gaussian Inc. Pittsburgh, USA. 2004 (f) Richards, W. G.; Cooper, D. L. *Ab initio Molecular Orbital Calculations for Chemists*, Clarendon Press, Oxford, 1983. (g) Jensen, F. *Introduction to Computational Chemistry*, John Wiley & Sons, New York, 1999.
3. Born, M.; Oppenheimer, J. R. *Ann. Physik* **1927**, 84, 457.
4. (a) Hartree, D. R. *Proc. Cambridge Phil. Soc.* **1928**, 24, 89. (b) Fock, V. Z. *Phys.* **1930**, 61,126.
5. Slater, J. C. *Phys. Rev.* **1930**, 36, 57.
6. Boys, S. F. *Proc. R. Soc. (London)* **1950**, A200, 542.

7. Frenking, G.; Seijo, L.; Bohme, M.; Dapprich, S.; Ehlers, A. W.; Jonas, V.; Neuhaus, A.; Otto, M.; Stegmann, R.; Veldkamp, A.; Vyboishchikov, S. F.; *Reviews in Computational Chemistry*; Lipkowitz, K. B., Boyd, D. B., Eds.; VCH: New York, 1996, 8, 63.
8. McWeeny, R. *Int. J. Quant. Chem.* **1967**, 15, 351.
9. (a) Hurley, A. C. *Electron Correlation in Small Molecules* Academic Press, London, 1977. (b) Wilson, S. *Electron Correlation in Molecules* Clarendon Press, Oxford, 1984. (c) Raghavachari, K.; Anderson, J. B. *J. Phys. Chem.* **1996**, 100, 12960.
10. Moller, C.; Plesset, M. S. *Phys. Rev.* **1934**, 46, 618.
11. Hoffmann, M. R.; Schaefer, H. F. *Adv. Quantum Chem.* **1986**, 18, 207.
12. Dewar, M. J. S.; Thiel, W. *J. Am. Chem. Soc.* **1977**, 99, 4899.
13. Dewar, M. J. S.; Zoebisch, E. G.; Healy, E. F.; Stewart, J. J. P. *J. Am. Chem. Soc.* **1985**, 107, 3902.
14. (a) Stewart, J. J. P. *J. Comp. Chem.* **1989**, 10, 209. (b) Stewart, J. J. P. *J. Comp. Chem.* **1989**, 10, 221.
15. Hückel, E. *Z. Phys.* **1931**, 70, 204.
16. Hoffmann, R.; Lipscomb, W. N. *J. Chem. Phys.* **1962**, 36, 2179. (b) Hoffmann, R. *J. Chem. Phys.* **1963**, 39, 1397; **1964**, 40, 2474; 2480; 2745. (c) Hoffmann, R. *Angew. Chem., Int. Ed. Engl.* **1982**, 21, 711.
17. Bingham, R. C.; Dewar, M. J. S.; Lo, D. H. *J. Am. Chem. Soc.* **1975**, 97, 1285; 1294; 1302; 1307.
18. (a) Parr, R. G.; Yang, W. *Density Functional Theory of Atoms and Molecules*, Oxford University Press, Oxford, 1989. (b) Dreisler, R. M.; Gross, E. K. V.

- Density Functional Theory: An Approach to the Quantum Many-body Problem*, Springer-Verlag, Berlin, 1990. (c) Hohenberg, P. C.; Kohn, W.; Sham, L. J. *Advances in Quantum Chemistry*, Vol. 21, Academic Press, 1990. (d) Kohn, W.; Becke, A. D.; Parr, R. G. *J. Phys. Chem.* **1996**, *100*, 12974. (e) Hohenberg, P. C.; Kohn, W. *Phys. Rev.* **1964**, *136*, B864. (f) Kohn, W.; Sham, L. J. *Phys. Rev.* **1965**, *A140*, 1133. (g) Geerlings, P.; De Proft, F.; Langenaeker, W. *Chem. Rev.* **2003**, *103*, 1793.
19. Lee, C.; Yang, W.; Parr, R. G. *Phys. Rev. B* **1988**, *37*, 785.
20. Perdew, J. P.; Burke, K.; Ernzerhof, M. *Phys. Rev. Lett.* **1996**, *77*, 3865.
21. Vosko, S. H.; Wilk, L.; Nusair, M. *Can. J. Phys.* **1980**, *58*, 1200.
22. (a) Becke, A. D. *J. Chem. Phys.* **1993**, *98*, 1372. (b) Becke, A. D. *J. Chem. Phys.* **1993**, *98*, 5648.

CHAPTER 2

REVERSAL OF STABILITY ON METALATION OF PENTAGONAL BIPYRAMIDAL (1-MB₆H₇²⁻, 1-M-2-CB₅H₇¹⁻ AND 1-M-2,4-C₂B₄H₇) AND ICOSAHEDRAL (1-MB₁₁H₁₂²⁻, 1-M-2-CB₁₀H₁₂¹⁻ AND 1-M-2,4-C₂B₉H₁₂) BORANES (M=Al, Ga, In AND Tl):
ENERGETICS OF CONDENSATION AND RELATIONSHIP TO BINUCLEAR
METALLOCENES

[2.0] Abstract

The usual assumption of the extra stability of icosahedral boranes (**2**) over pentagonal-bipyramidal boranes (**1**) is reversed by substitution of a vertex by a group 13 metal. This preference is a result of the geometrical requirements for optimum overlap between the five membered face of the ligand and the metal fragment. Isodesmic equations calculated at the B3LYP/LANL2DZ level indicate that the extra stability of 1-M-2,4-C₂B₄H₇ varies from 14.44 kcal/mol (M = Al) to 15.30 kcal/mol (M = Tl). Similarly, M(2,4-C₂B₄H₆)₂¹⁻ is more stable than M(2,4-C₂B₉H₁₁)₂¹⁻ by 9.26 kcal/mol (M = Al) and by 6.75 kcal/mol (M = Tl). The preference for (MC₂B₄H₆)₂ over (MC₂B₉H₁₁)₂ at the same level is 30.54 kcal/mol (M = Al), 33.16 kcal/mol (M = Ga) and 37.77 kcal/mol (M = In). The metal-metal bonding here is comparable to those in CpZn-ZnCp and H₂M-MH₂ (M= Al, Ga, and In).

[2.1] Introduction

The pentagonal-bipyramid (**1**) and the icosahedron (**2**) are the two related polyhedra that dominate the chemistry of polyhedral boranes. The icosahedral boranes are usually considered to be the most stable among the polyhedral boranes. The pentagonal-bipyramidal *closo*-borane $B_7H_7^{2-}$ (**1**), in contrast, is highly reactive.¹ However this difference in reactivity appears to be altered with the substitution of one of the vertices by a heavier group 13 metal. During the last three decades several molecules isoelectronic with $B_nH_n^{2-}$ ($n=7, 12$), containing one or two heteroatoms other than carbon in the cage, have been prepared.¹⁻⁶ These include metallocarboranes involving heavier elements of the boron group. Early examples of the group 13 *closo*-metallocarboranes, especially in the smaller cage, such as the galla- and inda-carboranes [*closo*-1-CH₃-1,2,3-MC₂B₄H₆ (M=Ga and In)] were synthesized by Grimes and coworkers.^{3b} These complexes have varying distortions from the pentagonal-bipyramidal geometry, but the metal occupies the apical position above the open pentagonal face of the carborane. The most common distortion of the metal in 1-M-2,4-C₂B_{n-3}H_n ($n=7, 12$) is along the pseudo-mirror plane of the molecule, toward the unique boron atom. Several similar structures, 1a-n, are characterized over the years with one Al, Ga or In in place of boron and these are tabulated here (Table 1).

In contrast there is less information available on the icosahedral structures with group 13 metals, although the first structure of a group 13 metallocarborane in the icosahedral system (**2**), [1-R-1,2,3-AlC₂B₉H₁₁ (R=CH₃, C₂H₅)], was reported by Hawthorne and coworkers in 1970.⁴ Structures 2a-g (Table 1) form the characterized members of this

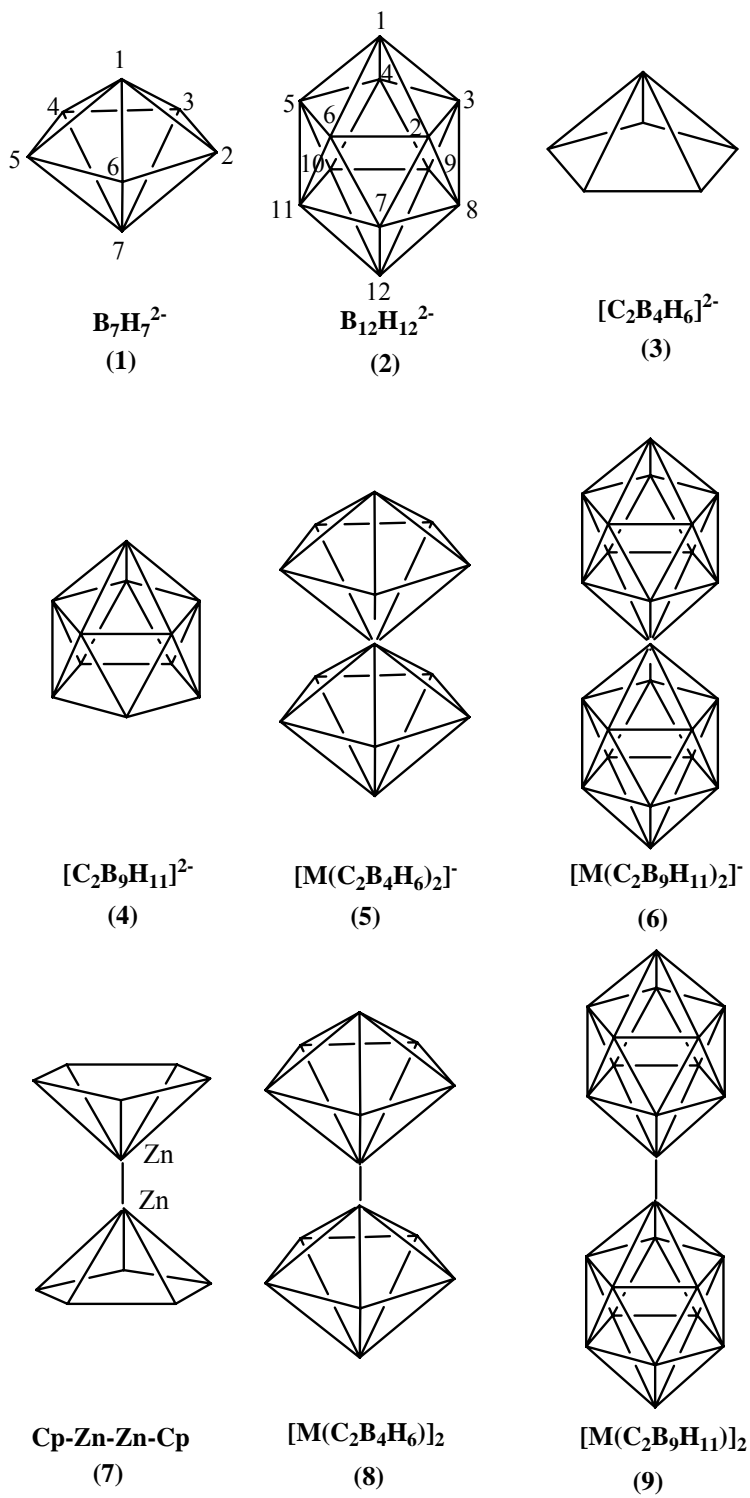
family. Metallaborane structures with pentagonal-bipyramidal skeleton are more common than those with the icosahedral skeleton. While this may be the result of a greater synthetic effort towards the pentagonal-bipyramidal skeletons, is there in addition a thermodynamic preference? We have reasons to expect so and this is, in part, the motivation to undertake the present study.

Table 1: Experimentally characterized structures of Pentagonal-bipyramidal and Icosahedral metallaboranes and carboranes (from Cambridge Structural Database^{3a}) with one of the vertices substituted by heavier group 13 elements.

Molecular formula	Ref.	Molecular formula	Ref.
1. M(R)-C₂B₄H₆		c) Al(Me)-2,3-C ₂ B ₉ H ₁₁	3g
a) Ga(CH ₃)-2,3-C ₂ B ₄ H ₆	3b	d) Al(C ₂ H ₅)-2,3-C ₂ B ₉ H ₁₁	3i
b) Ga(CMe ₃)-2,3-(CSiMe ₃) ₂ B ₄ H ₄	3c	e) Al(Me) ₂ -2,3-C ₂ B ₉ H ₁₁	3i
(c) Ga(CMe ₃)-2,4-(CSiMe ₃) ₂ B ₄ H ₄	3d	f) Al(Et)(PEt ₃) ₂ -2,3-C ₂ B ₉ H ₁₁	3j
d) Ga(C ₁₀ N ₂ H ₈)(tBu)-2,3-(CSiMe ₃) ₂ B ₄ H ₄ . 2C ₆ H ₆	3d	g) Tl-2,3-C ₂ B ₉ H ₁₁ . PPh ₃	3k
e) Ga(C ₁₀ N ₂ H ₈)(tBu)-2,4-(CSiMe ₃) ₂ B ₄ H ₄ . 2C ₆ H ₆	3d	5. M(C₂B₄H₆)₂	
f) Ga(C ₈ N ₄ H ₆)(tBu)-2,4-(CSiMe ₃) ₂ B ₄ H ₄	3d	a) Ga[(2,3-CSiMe ₃) ₂ B ₄ H ₄] ₂ ⁻	3e
g) Ga(Cl)(CH ₂ NMe ₂) ₂ -2,3-(CSiMe ₃) ₂ B ₄ H ₄ . C ₆ H ₆	3e	[Na(TMEDA) ₂] ⁺	
h) Ga(Cl)(CH ₂ NMe ₂) ₂ -2,4-(CSiMe ₃) ₂ B ₄ H ₄ . C ₆ H ₆	3e	b) Ga[(2,4-CSiMe ₃) ₂ B ₄ H ₄] ₂ ⁻	3e
i) In(CH ₃)-2,3-C ₂ B ₄ H ₆	3b	[Na(TMEDA) ₂] ⁺	
j) In(CHMe ₂)-2,3-(CSiMe ₃)B ₄ H ₄	3f	6. M(C₂B₉H₁₁)₂	
k) In(CHMe ₂)-2,4-(CSiMe ₃)B ₄ H ₄	3c	a) Ga[2,3-C ₂ B ₉ H ₁₁] ₂ ¹⁻ ·Tl ⁺	3j,3l
l) In(C ₁₀ N ₂ H ₈)(CHMe ₂)-2,3-(CSiMe ₃) ₂ B ₄ H ₄	3c	b) Al[2,3-C ₂ B ₉ H ₁₁] ₂ ¹⁻	3j
m) In(C ₁₀ N ₂ H ₈)(CHMe ₂)-2,4-(CSiMe ₃) ₂ B ₄ H ₄	3c	8. C₂B₄H₆-M-M-C₂B₄H₆	
n) In(C ₈ N ₄ H ₆)(CHMe ₂)-2,3-(CSiMe ₃) ₂ B ₄ H ₄	3d	a) [Ga-(2,4-(CSiMe ₃) ₂ B ₄ H ₆) ₂	12
2. M(R)-C₂B₉H₁₁			
a) Ga(C ₂ H ₅)-2,3-C ₂ B ₁₀ H ₁₁	3g	[1-C(Ph)B ₆ H ₆] ¹⁻ [N(Et) ₄] ¹⁺	3m
b) [Al(Me)B ₁₁ H ₁₁] ²⁻ . [AsPh ₃] ₂	3h	[1-CB ₅ (I)H ₄] ¹⁻ [P(Ph) ₄] ¹⁺	3n

The term dicarbollide was introduced by Hawthorne to describe the *nido*-C₂B₉H₁₁²⁻ anion, indicating the bowl-like shape. The *nido*-C₂B₄H₆²⁻ (**3**) and -C₂B₉H₁₁²⁻ (**4**)

carborane ligands have been compared to Cp^- so that metallocene like structures $\text{C}_2\text{B}_4\text{H}_6\text{MC}_2\text{B}_4\text{H}_6^{1-}$ (**5**) and $\text{C}_2\text{B}_9\text{H}_{11}\text{MC}_2\text{B}_9\text{H}_{11}^{1-}$ (**6**) are expected to be stable. Several derivatives of **5** and **6** are known and Table 1 provides well characterized examples which can be considered as condensed products from structure **1** and **2**, respectively. While the well known Wade's $n+1$ skeleton electron pair rule is applicable to **1** and **2**, it is outside of its realm for **5** and **6**.⁷ Electron-counting rule that applies equally well for metallocenes, metallacarboranes and condensed polyhedral boranes has been introduced by us.⁸ According to this rule, commonly known as *Jemmis* Rule, where m is the number of polyhedra, n is the number of vertices and o is the number of single-vertex-sharing condensation structures with $m+n+o$ skeletal electrons are extra stable. Thus for structure **5**, we have $m=2$, $n=13$ and $o=1$ so that 16 electron pairs are required for skeleton bonding. The number of electron pairs in **5a** (Table 1), for example, is 15.5 (8 from 8 BH groups, 6 from 4 CH groups and 1.5 from the Ga) so that the complex has a negative charge. Similarly, the *Jemmis* Rule stipulates 26 electron pairs for **6**. A negative charge is required to meet the target as found experimentally. Here also we would like to see any inherent preference, if any, for this.



Scheme 1

Another connection between metallaboranes and metallocenes is brought to attention by the recent synthesis of $\text{Me}_5\text{C}_5\text{-Zn-Zn-C}_5\text{Me}_5$ (**7**), which are commonly called binuclear metallocenes.⁹ This is indeed a new development in metallocene chemistry of the main group, but main group metallacarboranes have a similar precedent. In general, compounds having bonds between two Ga atoms or other heavier group 13 elements are rare. There are a few classical inorganic compounds with Ga-Ga bond such as Ga_2Br_3 , $[\text{GaC}(\text{SiMe}_3)_3]_4$ and Ga_2R_4 [$\text{R}=(\text{Me}_3\text{Si})_2\text{CH}$, 2,4,6- $^i\text{Pr}_3\text{C}_6\text{H}_2$, and 2,4,6- $(\text{CF}_3)_3\text{C}_6\text{H}_2$] known for some time.¹⁰ In 1995, Hosmane and coworkers synthesized a novel class of compounds (**8**) where Ga-Ga bond is stabilized by two 2,4-dicarba-nido-hexaborate(2-) carborane ligands.¹¹ This is an equivalent of CpZn-ZnCp (**7**). We compare the metal-ligand and metal-metal bonding in the binuclear metallocenes and binuclear metallacarboranes. There are no equivalent metal-metal bonded icosahedral structures. We search here for reasons, if any, that prevent the formation of such species.

The group 13 metallacarboranes serve as useful reagents for the introduction of carborane cage moieties.¹² The high reactivity of the aluminacarborane coupled with their excellent solubility in organic solvents have led to their potential usefulness as transmetalation reagents. The insoluble thallacarboranes¹³ are highly valued as synthetic reagents. The present study on the structure and bonding compliments the experimental study of carboranes in relation to nano carborarods and bundles.¹⁴ Our focus is on the differential effect of a group 13 element as a cap on the icosahedral and pentagonal-bipyramidal cage systems.

[2.2] Computational Details

All the polyhedral structures of molecular formula $\text{HM-B}_n\text{H}_{n-1}^{2-}$, $\text{HM-2CB}_{n-2}\text{H}_{n-1}^{1-}$, $\text{HM-2,4-C}_2\text{B}_{n-3}\text{H}_{n-1}$, $\text{2,4-C}_2\text{B}_{n-3}\text{H}_{n-1}\text{-M-2,4-C}_2\text{B}_{n-3}\text{H}_{n-1}$, and $\text{2,4-C}_2\text{B}_{n-3}\text{H}_{n-1}\text{-M-M-2,4-C}_2\text{B}_{n-3}\text{H}_{n-1}$ [where $n=7, 12$ and $\text{M}=\text{B}, \text{Al}, \text{Ga}, \text{In}$ and Tl] are optimized at B3LYP method using LANL2DZ basis set.^{15a} This uses well-known three parameters functional of Becke's including Hatree-Fock exchange contribution with non local corrections for exchange potential together with non local correction for the correlation energy suggested by Lee, Young and Parr.^{15b-c} In addition, we have used 6-31G* basis set for compounds having aluminum and gallium. All calculations were carried out using the Gaussian 03 program package.¹⁶ Total energies and the Cartesian coordinates of the structures studied are given in the supplementary information. Energetic comparisons are made after Basis set superposition error wherever possible.

[2.3] Results and Discussion

We begin the analysis by describing the structural features of metallaborane dianions, monoanionic metallacarboranes and neutral metallacarboranes based on pentagonal-bipyramidal (**1**) and icosahedral (**2**) skeletons. Among the monocarbaboranes, only structures with carbon at 2-position are considered. The dicarbaborane structures considered have the carbon atoms in the 2,4- positions (Figure 1). The details of the structure and bonding of the icosahedral and pentagonal-bipyramidal structures are given in sections A and B. Isodesmic equations (1-4) are used to estimate the relative preferences for these two structures. A relationship is then brought out between the

geometric parameters and the preference of the polyhedra for a particular metal using fragment molecular orbitals. This approach is extended to the condensed structures based on **5** and **6** in section 2.3.3. The preference of specific polyhedra for the M-M bonded structures is discussed at the end.

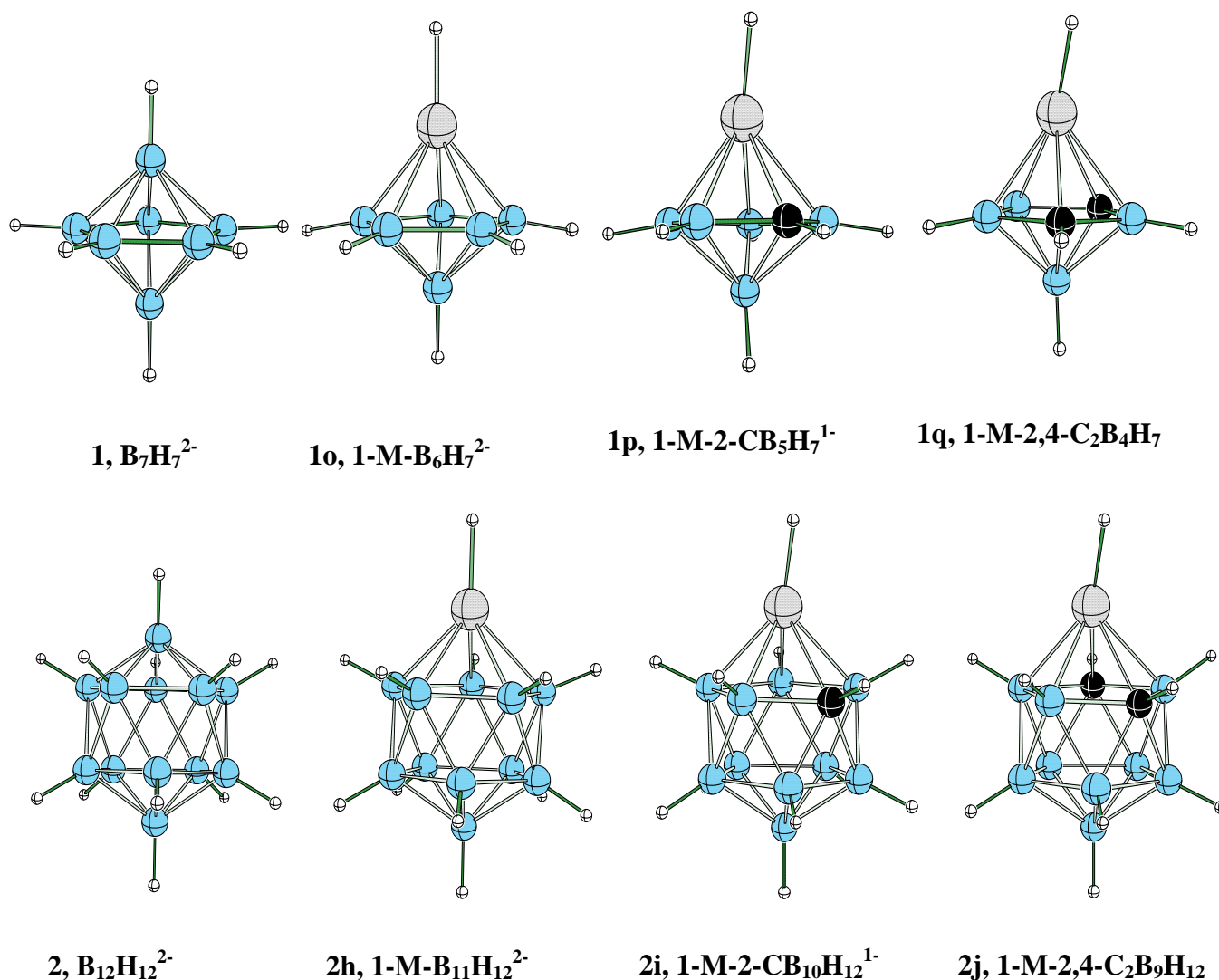


Figure 1: Structures of pentagonal-bipyramidal and icosahedral metallaboranes and metallocarboranes indicating the numbering scheme.

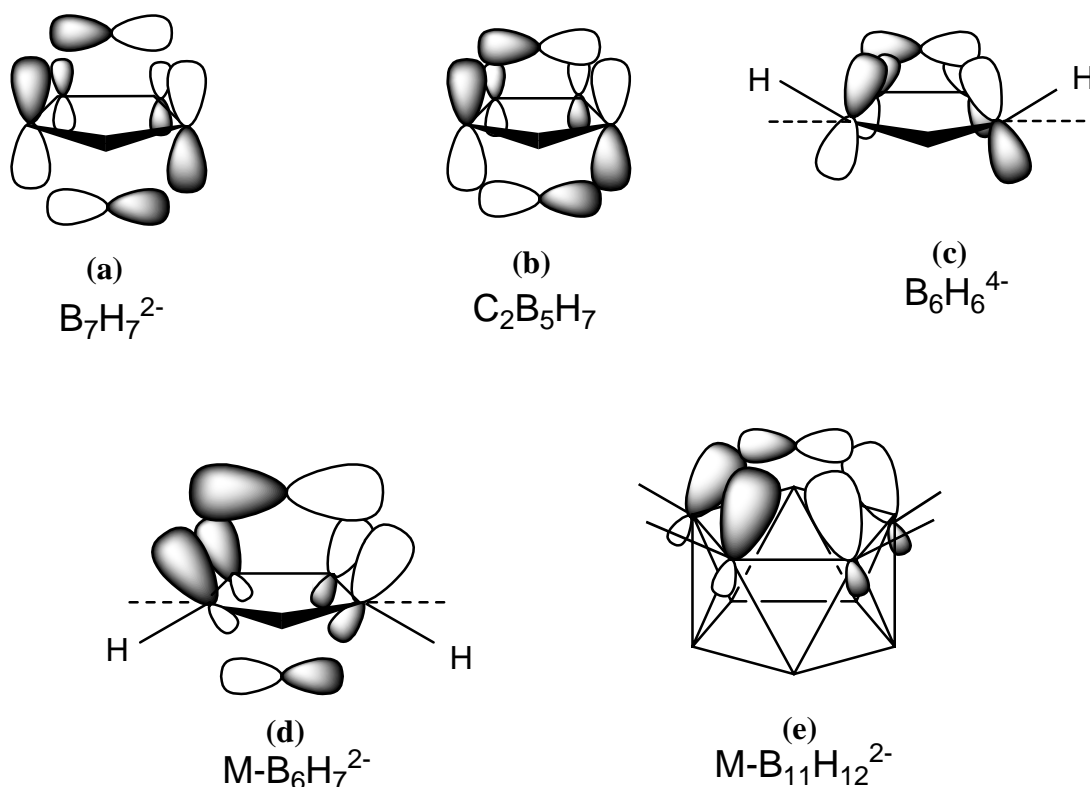
[2.3.1] Bonding in the pentagonal-bipyramidal systems

The electron requirements of the polyhedral structure is well-defined by the Wade's Rules.⁸ The variations in the structure of $B_7H_7^{2-}$ (D_{5h}) when a BH group is substituted by an AlH group are noteworthy. The ring hydrogens of the 5-membered ring, which is in the B5 plane in $B_7H_7^{2-}$, bend away from Al-H in $AlB_6H_7^{2-}$ by 9.3 deg (Table 2). The extended overlap approach (Scheme 2). The π MOs of the B_5H_5 ring span too large an area to have optimum overlap with the MOs of the two BH fragments (Scheme 2).

Table 2: The out-of-plane bending [$180 - \angle X1BH$, where X1 is the centroid of the five membered ring; The X1-M-H bonds bend away from the capping atom considered as (-)ve sign] values of the *exo*-polyhedral bonds in the pentagonal-bipyramidal boranes and carboranes (Figure 1) at B3LYP/LANL2DZ. Geometrical parameters of the corresponding experimentally characterized structures are in parentheses and the superscript on the parentheses correspond experimental structures listed in the Table 1.

Structures	Angles in degrees	M=BH	AlH	GaH	InH	TlH
1-M- $B_6H_6^{2-}$	X1-M-H	0.00	-0.02	-0.03	-0.05	-0.31
	X1-B ₁₋₆ -H	0.00	-9.34	-8.51	-10.45	-10.64
1-M-2-CB ₅ H ₆ ¹⁻	X1-M-H	-8.32 (-9.80) ^{1b}	-12.87	-15.43	-18.65	-32.58
	X1-C2-H	-0.01 (-1.83)	-10.74	-10.07	-12.51	-13.87
	X1-B3/6-H	-5.74 (-8.22)	-9.75	-9.32	-10.84	-12.00
	X1-B ₄₋₅ -H	-0.35 (-3.04)	-7.66	-7.00	-8.37	-8.70
1-M-2,4-C ₂ B ₄ H ₆	X1-M-H	-6.66	-12.43	-15.41	-20.38	-43.78
	X1-C2/4-H	-1.09	-10.01	-9.32 (-8.56) ^{1h}	-11.22 (9.75) ^{1k}	-12.14
	X1-B3-H	-1.10	-5.92	-5.99 (-8.43)	-7.27 (-11.85)	-8.12
	X1-B5/6-H	-5.61	-8.49	-7.01 (-8.79)	-8.67 (-8.99)	-6.62

A B_4H_4 ring or of B-H bending depends on the metal and decreases to 8.5 in Ga. However, it increases to 10.5 and to 10.6 with In and Tl, respectively. The corresponding B-B bond lengths (Table 3) of the five membered rings are 1.68, 1.74, 1.74, 1.75 and 1.76 Å for BH, AlH, GaH, InH and TlH, respectively, indicate an enlargement of the five-membered ring. Considerable ring expansions (Table 3) and



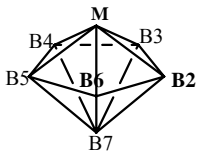
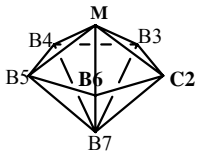
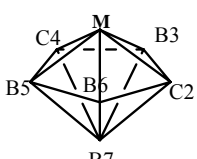
Scheme 2

bending of ring hydrogens (Table 2) were observed for their carborane analogues too. These out-of-plane bending can be understood using a fragment MO caps with more diffuse orbitals would have been an ideal situation. However, the $C_2B_3H_5$ ring is smaller by virtue of shorter B-C bonds. This helps to have better overlaps with the ring and cap orbitals, thus explaining the better stability of $C_2B_3H_7$

over $B_7H_7^{2-}$ (Scheme 2b). When one of the apical B-H groups in $B_7H_7^{2-}$ is substituted by the M-H group such as Al-H, an advantageous situation arises for both the B-H and the M-H groups (Figure 1). The B-H bonds of the B_5H_5 ring bend out of the B_5 plane and rehybridize the orbitals so that the larger lobe is directed toward the group with more diffuse orbitals (Scheme 2d). The process of rehybridization increases the B-B bond lengths of the B_5 ring, bringing the apical B-H group closer to the centroid of the B_5 ring. This also helps to have larger orbital span for the B_5 fragment toward the M-H cap. The out-of-plane bending of the ring B-H toward the unique B-H increases with increasing diffuse nature of the orbitals of the M-H groups; the largest bending is calculated for Tl-H. The advantage of the out-of-plane bending for the interaction between B-H cap and B_5H_5 ring is indicated by the decrease of the ringBH-capBH distance of 1.87, 1.84, 1.84, 1.83 and 1.81 Å for BH, AlH, GaH, InH and TlH, respectively (Table 3). The general considerations of structure and bonding do not change in going to the monoanionic carborane 1-M-2- $CB_5H_7^{1-}$ and the neutral 1-M-2,4- $C_2B_4H_7$ derivatives (Figure 1). Major differences come from the distortions arising from the lower symmetry of the five-membered ring resulting from the carbon atoms. The calculations refer to molecules where all exohedral substituents are replaced by hydrogens (Table 2, 3). The geometrical parameters of the corresponding experimental structures are also indicated in parentheses. Experimental structures are available for the neutral derivatives with Ga (1h in Table 1) and In (1k in Table 1) as the metals. The geometrical parameters of these experimentally characterized structures are compared

with the model structures. The calculated ring B-B, B-C and C-C bond distances fall within ± 0.06 Å of the experimental values (Table 3).

Table 3: Important interatomic distances of pentagonal-bipyramidal boranes and carboranes (Figure 1) at B3LYP/LANL2DZ level of theory (where X1 is the centroid of the five membered ring). Geometrical parameters of the corresponding experimentally characterized structures are in parentheses and the superscript on the parenthesis correspond experimental structures listed in the Table 1.

Structures	Distance (Å)	M=BH	AlH	GaH	InH	TlH
	Ring B-B	1.68	1.74	1.74	1.75	1.76
	M- B ₂₋₆	1.87	2.22	2.22	2.39	2.51
	B7-B ₂₋₆	1.87	1.84	1.84	1.83	1.81
	M-X1	1.20	1.66	1.66	1.87	2.02
	B7-X1	1.20	1.09	1.09	1.06	1.03
	C2-B3/6	1.57 (1.56) ^b	1.60	1.59	1.59	1.58
	B3/5-B4/6	1.67 (1.65)	1.72	1.72	1.73	1.72
	B4-B5	1.70 (1.66)	1.76	1.76	1.79	1.82
	M-C2	1.79 (1.74)	2.18	2.22	2.41	2.75
	M-B3/6	1.87 (1.82)	2.23	2.25	2.42	2.66
	M-B4/B5	1.83 (1.80)	2.18	2.17	2.33	2.41
	M-X1	1.21 (1.16)	1.68	1.69	1.90	2.14
	B7-X1	1.21 (1.16)	1.11	1.11	1.09	1.07
	C2/4-B3	1.56	1.58	1.58 (1.52) ^{lh}	1.58 (1.57) ^{lk}	1.57
	C2/4-B5/6	1.59	1.62	1.62 (1.56)	1.62 (1.60)	1.58
	B5-B6	1.68	1.72	1.73 (1.76)	1.74 (1.71)	1.85
	M-C2/4	1.76	2.16	2.18 (2.88)	2.38 (2.44)	2.75
	M-B3	1.90	2.28	2.31 (3.08)	2.50 (2.52)	2.92
	M-B5/B6	1.83	2.20	2.18 (2.25)	2.33 (2.32)	2.44
	M-X1	1.21	1.71	1.72 (2.27)	1.94 (1.99)	2.28
	B7-X1	1.208	1.132	1.132 (1.083)	1.119 (1.060)	1.123

The in-plane bending of the *exo*-polyhedral bonds vary somewhat more (Table 2) from the experimental values, probably because of the bulkier substituents present in the experimental structures. The slip-distortion of the -MR groups located above the C₂B₃ face of the carborane toward the boron side of the face has been noted earlier for Ga and In derivatives and a molecular orbital explanation provided.^{3a,17} Here the ring-cap bonding is fine-tuned by the re-orientation of orbitals by shifting the substituent of the metal toward the carbon side of the five-membered ring. Detailed MO studies to explain these structural distortions is available in the literature.¹⁷

[2.3.2] Bonding in the Icosahedral Boranes and Comparison to Pentagonal-bipyramids

Icosahedral [M(R)C₂B₉H₁₁)] species is isoelectronic with *closo*-1,*n*-C₂B₁₀H₁₂ (*n*=2, 7, 12), *closo*-1-CB₁₁H₁₂¹⁻ and *closo*-B₁₂H₁₂²⁻. The extra stability of the icosahedral *closo*-B₁₂H₁₂²⁻ is attributed to its high symmetry and the consequent orientation of the exohedral bonds it provides. This orientation is very close to that is required for ideal bonding in a pentagonal-pyramidal borane. For example, the exohedral B-H bonds of the five membered ring in B₆H₆⁴⁻ or B₆H₁₀ are bent toward the apical B-H group by about 25° (Scheme 2c). The pentagonal-pyramid, which can be obtained by halving the icosahedron, provides an angle of 26.6° by the icosahedral symmetry. This coincidence of the requirement of a pentagonal-pyramidal borane and the symmetry dictated angle available for the icosahedron leads to the unusual stability for icosahedral B₁₂H₁₂²⁻. The fragment orbitals of the B₁₁H₁₁²⁻ are oriented toward the missing vertex. Substitutions of

two boron atoms of $B_{12}H_{12}^{2-}$ by two carbon atoms do not change this considerably. However, metal atoms with highly diffuse orbitals affect the stability. These metals have more diffuse orbitals that require a larger orbital span of the B_5 ring. We have studied the variation in geometry in going from $B_{12}H_{12}^{2-}$ to $M-B_{11}H_{12}^{2-}$, $1-M-2-CB_{11}H_{12}^{1-}$ and $1-M-2,4-C_2B_9H_{12}$ (where $M = Al, Ga, In$ and Tl) (Table 4 & 5). There is substantial ring expansion as the size of M increases. The overlap of fragment MOs requires rehybridization to regain better overlap (Scheme 2e vs. 2d). This leads to the distortion of *exo*-polyhedral B-H bonds farther away from the metal so that there is better orbital match. By symmetry the angle that B-H makes with the B_5 plane is calculated as 26.6° in $B_{12}H_{12}^{2-}$ (Figure 1). It changes to 29.9° (average of 28.8 , 31.7 and 29.2) in $2,4-C_2B_{10}H_{12}$. This is changed to 24.7 (average of 21.6 , 28.5 and 24.1) in $1-Al-2,4-C_2B_9H_{12}$. The average B-H in-plane bending of their carborane derivatives decreases (going away from the metal) when we go down the group 13 elements from Al to Tl (Table 4 & 5). The symmetry of the top B_5H_5 plane is decreased while substituting one or two boron atoms by carbons. This is the main reason for not following the same trends for all in-plane bending of *exo*-polyhedral H-bonds in their carborane derivatives. These distortions, however, decreases the overall stability of the system. Thus the initial orientation of the fragment orbitals of B_6H_6 away from the vacant vertex and of $B_{11}H_{11}$ toward the vacant vertex predisposes the former for capping groups with more diffuse orbitals and the latter to caps with less diffuse orbitals (Scheme 2e). This should lead to a reversal of relative stabilities in relation to the parent

systems for the metallaboranes. The calculated structural parameters agree with the experimental data for most of the structures, given in parenthesis in Tables 3 and 4.

Table 4: The in-plane-bending ($180-\angle X1BH$, where X1 is the centroid of the five membered ring) values of the *exo*-polyhedral bonds of the icosahedral boranes and carboranes (Figure 1) at B3LYP/LANL2DZ level of theory. Geometrical parameters of the corresponding experimentally characterized structures are in parentheses and the superscript on the parenthesis is the corresponding experimental structure listed in the Table 1.

Structures	Angle in degree	M=AlH	GaH	InH	TiH
1-M-B ₁₁ H ₁₁ ²⁻	X1-M-H	0.00 (1.60) ^{2b}	0.00	0.00	0.00
	X1-B ₂₋₆ -H	20.81 (25.46)	20.87	19.31	18.89
	X2-B ₇₋₁₁ -H	27.70 (25.40)	27.71	27.94	27.96
1-M-2-CB ₁₀ H ₁₁ ¹⁻	X1-M-H	12.85	15.05	19.36	33.28
	X1-C2-H	22.73	23.46	22.89	24.84
	X1-B3/6-H	24.69	24.39	22.91	23.32
	X1-B4/5-H	20.92	20.64	18.77	17.45
	X2-B7-8-H	23.54	21.80	21.75	21.49
	X2-B9-11-H	27.10	27.50	27.64	26.80
1-M-2,4-C ₂ B ₉ H ₁₁	X1-M-H	11.54	14.34	21.16	45.81
	X1-C2/4-H	21.62	22.11	21.65	25.77
	X1-B3-H	28.46	28.18	27.91	31.63
	X1-B5/6-H	24.13	23.38	20.84	16.71
	X2-B7-10-H	21.51	21.75	21.30	20.51
	X2-B11-H	26.82	27.05	27.22	27.23

Table 5: Important interatomic distances of icosahedral boranes and carboranes (Figure 1) at B3LYP/LANL2DZ level of theory (where X1 is the centroid of the five membered ring). Geometrical parameters of the corresponding experimentally characterized structures are in parentheses and the superscript on the parenthesis correspond experimental structures listed in the Table 1.

Structures	Distances	M=BH	M=AlH	M=GaH	M=InH	M=Tl H
1-MB ₁₁ H ₁₁ ²⁻	Ring B-B	1.82	1.88 (1.84) ^{2b}	1.889	1.90	1.92
	M- B ₂₋₆	1.82	2.18 (2.14)	2.18	2.34	2.47
	M-X1	0.95	1.48 (1.46)	1.47	1.69	1.85
	B12-X2	0.95	0.95 (0.93)	0.95	0.94	0.94
	X1-X2	1.54	1.52 (1.50)	1.52	1.51	1.51
1-M-2-CB ₁₀ H ₁₁ ¹⁻	C2-B3/B6	1.74	1.75	1.75	1.73	1.69
	B3/5-B4/6	1.80	1.84	1.85	1.86	1.85
	B4-B5	1.82	1.89	1.91	1.94	2.04
	M-C2	1.74	2.17	2.20	2.42	2.74
	M-B3/6	1.81	2.18	2.19	2.37	2.60
	M-B4/5	1.80	2.16	2.15	2.30	2.40
	M-X1	0.96	1.53	1.53	1.77	2.03
	B12-X2	0.95	0.95	0.95	0.95	0.94
	X1-X2	1.53	1.51	1.51	1.51	1.51
1-M-2,4-C ₂ B ₉ H ₁₁	C2/4-B3	1.72	1.70	1.71	1.69	1.65
	C2/4-B6/5	1.75	1.76	1.77	1.76	1.67
	B5-B6	1.80	1.82	1.84	1.85	1.98
	M-C2/C4	1.74	2.16	2.18	2.41	2.93
	M-B3	1.83	2.21	2.23	2.44	2.98
	M-B5/6	1.80	2.15	2.14	2.29	2.47
	M-X1	0.97	1.57	1.58	1.84	2.35
	B12-X2	0.96	0.95	0.95	0.95	0.95
	X1-X2	1.52	1.51	1.51	1.51	1.52

We have used isodesmic equations (equation 1-4) to estimate the relative stabilities of various group 13 metallaboranes and their carborane analogues based on pentagonal-pyramid and icosahedron (Table 6).

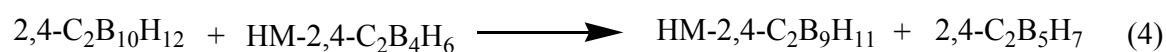
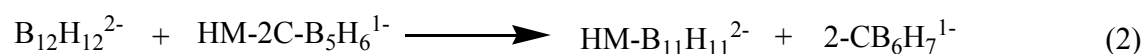


Table 6: Reaction Energies (ΔH , kcal/mol) of these reactions (Equations 1-4) calculated at B3LYP/LANL2DZ level of theory.

Equations	M=Al	Ga	In	Tl
1	27.20	27.04	34.78	41.40
2	22.52	22.78	30.54	40.78
3	24.95	24.50	35.03	49.05
4	14.44	15.87	18.01	15.3

The endothermicity of these reactions are a reflection of the extra stability of pentagonal-bipyramidal geometry when group 13 metals form a part of the skeleton and thus supports our analysis. The energies of reactions for Al and Ga derivatives are similar, in tune with their nearly equal atomic radii. The decrease in the endothermicity for the carborane is due to the decreased size of the C_2B_3 ring, making the difference between the effective orbital span of the two five-membered rings in **3** and **4** less than

that in the parent boranes. The relatively larger number of metallaboranes based on the pentagonal-bipyramid is not an accident after all.

[2.3.3] Condensation through Single-Atom Sharing: Sandwich Structures involving Pentagonal-Bipyramidal (5) and Icosahedral (6) Metallaboranes

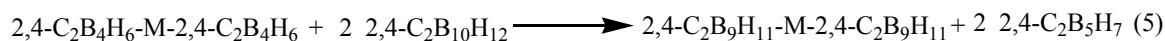
There are only two well-characterized examples where two pentagonal-bipyramidal metallocarboranes (**5a-b**, Table 1) are condensed to form a sandwich structure, both from the Hosmane group. The Hawthorne group contributed the three condensed structures involving icosahedron with Al and Ga. (6a-c, Table 1).^{3j-k} The structures of the series [commo-1,1'-M(1,2,4-GaC₂B_{n-3}H₁₁)₂] (where n=7, 12) at the B3LYP/LANL2DZ level indicate several interesting trends. The structural variations in formation of these sandwich structures are to be seen in relation to the corresponding changes noted in the metallocenes. The metallocenes involving cyclopentadienyl rings retain the planar or nearly-planar geometry of the C₅H₅ ring. The variation of the hydrogen atoms from the C₅ plane is small. The *nido*-C₂B₄H₆²⁻ and C₂B₉H₁₁²⁻ ligands, equivalent of the Cp⁻, are very different from each other. In C₂B₄H₆²⁻, the ring hydrogens are bent away from the incoming metal ion. In the large *nido*-C₂B₉H₁₁²⁻ ion, the ring hydrogens are oriented toward the incoming metal ion.

Table 7: Comparisons of geometrical parameters are made between half-sandwich and single-atom sharing condensed systems (Scheme 1) and calculated at B3LYP/LANL2DZ level of theory. The data of the corresponding experimentally characterized structures are in parentheses and the superscript on the parentheses corresponds experimental structure listed in the Table 1.

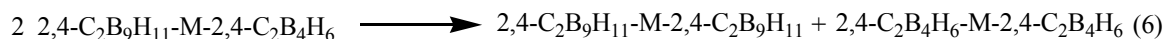
Geometrical Parameters	H-M-C ₂ B ₄ H ₆			M[C ₂ B ₄ H ₆] ₂ ¹⁻		
	Al	Ga	In	Al	Ga	In
X1-C2/4-H	10.01	9.32	11.220	9.75	9.9(12.07) ^{5b}	11.48
X1-B3-H	5.92	5.99	7.275	6.56	7.71(20.10)	8.40
X1-B5/6-H	8.49	7.01	8.673	9.18	9.30(20.09)	9.48
M-X1	1.71	1.72	1.94	1.84	1.93(1.92)	2.13
	HMC ₂ B ₉ H ₁₁			M[C ₂ B ₉ H ₁₁] ₂ ¹⁻		
	Al	Ga	In	Al	Ga	In
X1-C2/4-H	21.62	22.11	21.65	22.80	26.70	24.80
X1-B3-H	28.46	28.18	27.91	27.46	29.23	29.30
X1-B5/6-H	24.13	23.38	20.84	23.16	26.00	23.76
M-X1	1.57	1.58	1.85	1.73	2.28	2.13

It is therefore reasonable to assume that pentagonal-pyramidal anions can be more easily brought together as the B-H and the C-H bonds of the five-membered ring are bent away from the central metal atom. We have used isodesmic equations 5 and 6 to compare the relative stability. The anticipation based on the decreased steric interaction in 5 in comparison to 6 is confirmed by energies of equation 5. Formation of the sandwich complex involving two pentagonal-pyramidal are more favored than those involving two icosahedral fragments by energies ranging from 6 to 13 kcal/mol. Despite

the possible steric interaction, the B-H and C-H out-of-plane bending are not dramatically changed in forming the sandwich complex. Instead, the M-ligand distances are increased as much as 0.2-0.4 Å. It is interesting to note that a mixed complex involving one each of **3** and **4** as ligand is favored over a combination of **5** and **6**.



$\Delta H = 9.26$ (Al), 10.53 (Ga), 12.19 (In) and 6.75 (Tl) kcal/mol, calculated at B3LYP/LANL2DZ level of theory.



$\Delta H = 4.75$ (Al), 4.61 (Ga), 3.57 (In) and 3.11 (Tl) Kcal/mol, calculated at B3LYP/LANL2DZ level of theory.

[2.3.4] Binuclear metallocenes

The recent synthesis of CpZn-ZnCp has brought much attention to the study of binuclear metallocenes.¹⁰ The strength of the M-M bond in this and in many hypothetical binuclear metallocenes has been investigated.¹⁸ The Cp⁻ and the *nido*-carboranes C₂B₄H₆²⁻ (**3**) and C₂B₉H₁₁²⁻ (**4**) are considered as comparable ligands. The synthesis of CpZn-ZnCp complex naturally leads to the question of similar binuclear complexes involving **3** and **4**. In fact **5** and **6** must be considered as experimentally characterized forerunners of binuclear metallocenes. Hosmane et al. synthesized the first binuclear metallacarborane involving gallium, 8a (Table1).¹² We have studied the structure and bonding of a series of binuclear metallaboranes involving pentagonal-bipyramid and icosahedron with metals ranging from Al to Tl but structures involving

Tl atoms are not minima on the potential energy surfaces. The first indications of the strongly bonding nature of the M-M bond in these complexes come from comparisons to the bond lengths in H_2M-MH_2 (D_{2d}). The M-M bond distances in the binuclear metallacarboranes are shorter by about 0.1 Å, indicating the stabilizing influence of these $C_2B_4H_6^{2-}$ and $C_2B_9H_{11}^{2-}$ ligands on the M-M bond. However the experimental Ga-Ga distance in **8a** is considerably shorter than the model at the B3LYP/LANL2DZ level. We have studied the same system using a larger all electron basis set, 6-311++G** at the same level. The Ga-Ga distance of 2.397 Å (Table 10) at this level is close to the experimental value of 2.340 Å. Similarly, we have studied Cp_2Zn_2 complex using the 6-311++G** basis set for comparison and found that Zn-Zn bond distance

Table 8: Geometrical parameters of the binuclear complexes calculated at B3LYP/LANL2DZ level of theory. The data for corresponding experimentally characterized structures are in parentheses and the superscript on the parentheses corresponds experimental structures listed in the Table 1.

Geometrical Parameters	$[MC_2B_4H_6]_2$			$[MC_2B_9H_{11}]_2$		
	Al	Ga	In	Al	Ga	In
X1-M-X2/M	12.41	14.70 (15.6) ^{8a}	20.85	9.19	15.75	22.70
X1-C2/4-H	9.68	9.99 (9.38)	10.97	21.52	22.10	21.70
X1-B3-H	5.93	6.00 (10.8)	7.40	27.70	27.90	26.90
X1-B5/6-H	8.20	8.26 (6.01)	8.41	23.15	23.25	20.88
M-X1/X2	1.72	1.73 (1.68)	1.95	1.58	1.59	1.85
X1-X2	5.90	5.80 (5.55)	6.45	5.64	5.51	6.22
M1-M2	2.52	2.45 (2.34)	2.75	2.52	2.44	2.75

(2.339 Å) is close to the experimental value of 2.305 Å. However, this did not change the energetics as much. The calculated hydrogenation energies of $\text{H}_2\text{M-MH}_2$ (D_{2d}) are -0.83, 2.31 and 9.18 for Al, Ga and In, respectively (equation 7, Table 9). The hydrogenation energy increases (equation 7-10) as we go down the group 13 elements from Al to In. The M-M bond distances in these bi-nuclear complexes are comparable to the distances calculated for the simple dimeric hydrides $\text{H}_2\text{M-MH}_2$. The bond energies are compared between the reactions 7-10 and it has been found that Al-Al bond in binuclear complex **8** is 7.41 kcal/mol stronger (Scheme 1) than in its dimeric hydride complex. It becomes 6.81 kcal/mol stronger in the case of Ga-Ga bond and 6.32 kcal/mol stronger for the In-In bond. These relative hydrogenation energies are the reflections of their extra bonding character in these binuclear complexes. We have calculated hydrogenation energy of Ga_2H_4 (D_{2d}) and $\text{Ga}_2(2,4\text{-C}_2\text{B}_4\text{H}_6)_2$ using 6-311++G** basis set of the same method (Table 8) and the values are -5.52 and -11.70 kcal/mol, respectively, which are comparable with the data calculated at B3LYP/LANL2DZ level of theory. The basis set superposition error (BSSE), associated with the M-M bond energy was calculated directly by the counterpoise method.¹⁹ The values are -0.94 (Al), -0.89 (Ga), and -0.55 (In) kcal/mol for complex **8** and -1.41 (Al), -1.58 (Ga) and -1.34 (In) kcal/mol for complex **9**.

The low exothermicities of these reactions, demonstrating that formation of binuclear metallocenes are more stable with respect to their half-sandwich complexes. Binuclear metallocenes with $\text{C}_2\text{B}_4\text{H}_6^{2-}$ ligands are more stable than the $\text{C}_2\text{B}_9\text{H}_{11}^{2-}$. So the

structures with pentagonal-bipyramids are more favorable than the icosahedrons and it is seen in their corresponding half sandwich complexes too.

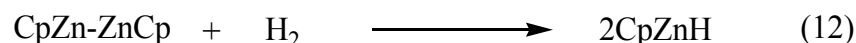
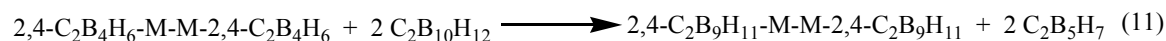
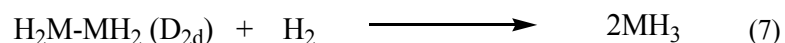


Table 9: Energies (ΔH , kcal/mol) of the reactions (Equations 7-12) calculated at B3LYP/LANL2DZ level of theory (Values are in parenthesis calculated at B3LYP/6-311++G**).

Equations	M=Al	Ga	In
7	-0.83	2.31 (5.52)	9.18
8	6.58	9.12 (11.70)	15.50
9	4.94	7.65	13.74
10	5.94	8.57	14.65
11	30.54	33.16	37.77
12	21.56 (M=Zn)		

Partitioning of electrons in a molecule into contributions to specific bonds is always contentious. Despite this, we have also applied the natural bond orbital (NBO)²⁰ analysis and other methods to study the M-M bonding in these molecules. The Wiberg bond indexes²¹ and Mayer-Mulliken²² bond orders (Table 10) of M-M clearly demonstrate that there is a covalent single metal-metal bond in these complexes. The

metal-metal σ -bonding is stronger in $\text{H}_6\text{C}_2\text{B}_4\text{-M-M-C}_2\text{B}_4\text{H}_6$ than in the corresponding $\text{H}_{11}\text{C}_2\text{B}_9\text{-M-M-C}_2\text{B}_9\text{H}_{11}$ by comparing their relative bond orders (Table 10). The Mulliken overlap populations²² do not do as well; overlap population between Al-Al in $\text{Al}_2(\text{C}_2\text{B}_4\text{H}_6)_2$ and $\text{Al}_2(\text{C}_2\text{B}_9\text{H}_{11})_2$ are -0.2261 and -0.6716, respectively.

Table 10: M-M bond distances and bond orders for group 13 binuclear complexes calculated at B3LYP/LANL2Z level of theory and values are in parentheses calculated at B3LYP/6-311++G**.

Compounds	M-M bond distance (Å)	EH Population	Mulliken Population	Wiberg Bond Index	Mayer-Mulliken bond order
H-C-C-H (10)	1.222	1.892	1.007	2.997	3.067
H-Zn-Zn-H (11)	2.591 (2.445)	0.619	0.354	0.482	0.887
Cp-Zn-Zn-Cp (12)	2.458 (2.339)	0.616	0.312	0.881	0.935
H-Be-Be-H (13)	2.086	0.919	0.455	0.705	1.053
Cp-Be-Be-Cp (14)	2.028	0.941	.3098	0.926	1.019
Al_2H_4 (D2h) (15)	2.641 (2.622)	0.868	0.336	0.901	0.856
Al_2H_4 (D2d) (16)	2.604	0.881	0.353	0.916	0.870
$\text{Al}_2\text{H}_6^{2-}$ (17)	2.756	0.102	0.394	1.027	1.052
$\text{H}_6\text{C}_2\text{B}_4\text{-Al-Al-C}_2\text{B}_4\text{H}_6$ (18)	2.520	0.865	-0.226	0.966	0.682
$\text{H}_{11}\text{C}_2\text{B}_9\text{-Al-Al-C}_2\text{B}_9\text{H}_{11}$ (19)	2.522	0.888	-0.672	0.937	0.470
Ga_2H_4 (D2h) (20)	2.586 (2.525)	0.769	0.307	0.879	0.791
Ga_2H_4 (D2d) (21)	2.543	0.810	0.328	0.900	0.809
$\text{Ga}_2\text{H}_6^{2-}$ (22)	2.695	0.112	0.376	1.026	0.980
$\text{H}_6\text{C}_2\text{B}_4\text{-Ga-Ga-C}_2\text{B}_4\text{H}_6$ (23)	2.445 (2.397)	0.738	-0.062	0.951	0.552
$\text{H}_{11}\text{C}_2\text{B}_9\text{-Ga-Ga-C}_2\text{B}_9\text{H}_{11}$ (24)	2.444	0.754	-0.185	0.926	0.464

[2.4] Conclusions

The trend that group 13 metals prefer pentagonal-bipyramidal skeleton, rather than an icosahedron, is well explained by the orientation of the π -orbitals of the ring in both cases. In $B_7H_7^{2-}$, the π MOs of the B_5H_5 ring will span too large an area to have optimum overlap with the MOs of the two BH fragments. A B_4H_4 ring or caps with more diffuse orbitals would have been better suited for such interaction. Thus, the B-H bonds of the B_5H_5 ring would bend out of the B_5 plane, rehybridizing the orbitals so that the larger lobe is directed toward the group with more diffuse orbitals. The overlap of fragment MOs in $B_{11}H_{11}^{2-}$ requires rehybridization for better overlap with the metal atom. This leads to the distortion of *exo*-polyhedral B-H bonds farther away from the metal so that there is a better orbital match. The overlap between ring π -orbitals and the cap orbitals is improved by the out-of-plane bending of ring hydrogens. The five-membered ring of a pentagonal-bipyramid makes better overlap with the diffuse orbital of metals more effectively than that of an icosahedron. Five-membered faces of the $C_2B_4H_6$ ring can be more easily brought together to form a sandwich because the B-H and the C-H bonds of the five-membered rings are bent away from the central metal atom. This explains the relative stability of the single-atom sharing complexes involving $C_2B_4H_6$ over their icosahedral analogues. The binuclear metallocenes with $C_2B_4H_6^{2-}$ ligands are more stable than those having $C_2B_9H_{11}^{2-}$ because of their strong metal-metal σ -bonding, as is indicated by NBO analysis.

[2.5] References

1. (a) Grimes, R. N.; in *Advanced Inorganic Chemistry*; ed. Cotton, F. A.; Wilkinson, G.; Murillo, C. A.; Bochmann, M. Wiley-Interscience, 6th edition, Chapter 5, New York, 1999. (b) Casanova, J. *The Borane, Carborane, Carbocation Continuum*; ed. John Wiley, New York, 1998. (c) Grimes, R. N.; Wilkinson, G., Stone, F. G. A, Abel, E. W. *Comprehensive Organometallic Chemistry II*; Oxford: Elsevier Science Ltd 1995; Vol. 1, Chapter 9. (d) Grimes, R. N. Ed. In *Metal Interactions with Boron Clusters*; Plenum: New York, 1982, 269.
2. (a) Hosmane, N. S. *Pure and Appl. Chem.* **1991**, 63, 375. (b) Saxena, A. K.; Maguire, J. A.; Banewicz, J. J.; Hosmane, N. S. *Main Group Chem. News* **1993**, 1, 14. (c) Hosmane, N. S.; Maguire, J. A. *Adv. Organomet. Chem.* **1990**, 30, 99. (d) Hosmane, N. S.; Maguire, J. A. *J. Cluster Science* **1993**, 4, 297. (e) Hosmane, N. S. In “*Main Group Elements and Their Compounds*”, Das, V. G. K., Ed. Narosa/Springer-Verlag: New Delhi, India, **1996**, 299. (f) Saxena, A. K.; Maguire, J. A.; Hosmane, N. S. *Chem. Rev.* **1997**, 97, 2421. (g) Hosmane, N. S.; Zhang, H.; Lu, K. -J.; Maguire, J. A.; Cowley, A. H.; Mardones, M. A. *Struct.Chem.* **1992**, 3, 183 (h) Maguire, J. A.; Hosmane, N. S.; Saxena, A. K.; Zhang, H.; Gray, T. G. *Phosphorus, Sulfur, and Silicon* **1994**, 87, 129. (i) Grimes, R. N.; Rademaker, W. J., *J. Am. Chem. Soc.* **1969**, 91, 6498.
3. (a) Allen, F. H.; Kennard, O. *Chem. Des. Autom. News* **1993**, 8, 31. (b) Grimes, R. N.; Rademaker, W. J.; Denniston, M. L.; Bryan, R. F.; Greene, P. T.; *J. Am. Chem. Soc.* **1972**, 94, 1865. (c) Hosmane, N. S.; Lu, K. -J.; Zhang, H.; Jia, L.; Cowley, A.

- H.; Mardones, M. A. *Organometallics* **1991**, *10*, 963. (d) Hosmane, N.S. et al. *Organometallics* **1995**, *14*, 5104. (e) Hosmane, N.S.; Kai-Juan Lu, Zhang, H.; Maguire, J.A.; *Organometallics* **1997**, *16*, 5163. (f) Hosmane, N.S.; Kai-Juan Lu, Saxena, A.K.; Zhang, H.; Maguire, J.A.; Cowley, A.H.; Schluter, R.D. *Organometallics* **1994**, *13*, 979. (g) Young, D. A. T.; Wiersema, R. J.; Hawthorne, M. F. *J. Am. Chem. Soc.* **1971**, *93*, 5687. (h) Getman, T.D.; Shore, S.G. *Inorg.Chem.* **1988**, *27*, 3439. (i) Churchill, M.R.; Reis Juniorv A. H. *J.Chem.Soc.,Dalton Trans.* **1972**, 1317. (j) Schubert, D. M.; Bandman, M.A.; Rees Junior, W. S.; Knobler, C.B.; Wonwoo, P. Lu. N, Hawthorne, M. F. *Organometallics* **1990**, *9*, 2046. (k) Manning, M.J.; Knobler, C.B.; Hawthorne, M.F.; Youngkyu D. *Inorg.Chem.* **1991**, *30*, 3589. (l) Bandman, M. A.; Knobler, B.; Hawthorne, M. F. *Inorg.Chem.* **1989**, *28*, 1204. (m) Franken, A.; Ormsby, D.L.; Kilner, C.A.; Clegg, W.; Thornton-Pett, M.; Kennedy, J. D. *J.Chem.Soc.,Dalton Trans.* **2002**, 2807. (n) Stibr, B.; Tok, O.L.; Milius, W.; Bakardjiev, M.; Holub, Hnyk, J. D.; Wrackmeyer, B. *Angew.Chem.,Int.Ed.* **2002**, *41*, 2126.
4. (a) Young, D. A. T.; Willey, G. R.; Hawthorne, M. F; Churchill, M. R.; Reis, A. H.; *J. Am. Chem. Soc.* **1970**, *92*, 6663.
5. (a) Churchill, M. R.; Reis, A. H., Jr.; Young, D. A. T.; Willey, G. R.; Hawthorne, M. F. *J. Chem. Soc., Chem. Commun.* 1971, 298. (b) Jutzi, P. *Adv. Organomet. Chem.* **1986**, *26*, 217. (c) Churchill, M.; Reis. A. H. *J. Chem. SOC. Dalton Trans.* **1972**, 1317. (d) Rees, W. S., Jr.; Schubert, D. M.; Knobler, C. B.; Hawthorne, M. F. *J. Am. Chem. Soc.* **1986**, *108*, 5369. (e) Schubert, D. M.; Rees, W. S., Jr.; Knobler, C. B.;

- Hawthorne, M. F. *Organometallics* **1987**, 6, 201. (f) Schubert, D. M.; Rees, W. S., Jr.; Knobler, C. B.; Hawthorne, M. F. *Organometallics* **1987**, 6, 203. (g) Schubert, D. M.; Knobler, C. B.; Hawthorne, M. F. *Organometallics* 1987, 6, 1353. (h) Bandman, M. A.; Knobler, C. B.; Hawthorne, M. F. *Inorg.Chem.* **1988**, 27, 2399.
6. (a) Howard, J. W.; Grimes, R. N.; *J. Am. Chem. Soc.* **1969**, 91, 6499 (b) Grimes, R. N., *J. Am. Chem. Soc.* **1971**, 93, 261. (c) Howard, J. W.; Grimes, R. N., *Inorg. Chem.* **1972**, 11, 263.
7. (a) Wade, K. *Chem. Commun.* **1971**, 792. (b) Wade, K. *Adv. Inorg. Chem. Radiochem.* **1976**, 18, 1.
8. (a) Jemmis, E. D.; Balakrishnan, M. M.; Pancharatna, P. D. *J. Am. Chem. Soc.* **2001**, 123, 4313. (b) Jemmis, E. D.; Balakrishnan, M. M.; Pancharatna, P. D. *Chem. Rev.* **2002**, 102, 93. (c) Jemmis, E. D.; Jayasree, E. G. *Acc. Chem. Res.* **2003**, 36, 816.
9. (a) Resa, I.; Carmona, E.; Gutierrez-Puebla, E.; Monge, A. *Science* **2004**, 305, 1136.
- (b) A semi-popular review of this critical discovery (Reference [10a]) has been made by Parkin, G.; *Science* **2004**, 305, 1117. (c) Schnepf, A.; Himmel, H. -J. *Angew. Chem., Int. Ed.* **2005**, 44, 3006. (d) Schnepf, A.; Himmel, H. -J. *Angew. Chem.* **2005**, 117, 3006.
- 10.(a) Honle, W.; Gerlach, G.; Weppner, W.; Simon, A. *J Solid State Chem* **1986**, 61, 171. (b) Uhl, W. *Angew. Chem. Int. Ed.* **1993**, 32, 1386. (c) Uhl, W.; Hiller, W.; Layh, M.; Schwarz, W. *Angew. Chem. Int. Ed.* **1992**, 31, 1364. (d) Uhl, W.; Layh.

- M.; Hildenbrand, T. *J Organomet. Chem.* **1989**, 364, 289. (e) He, X.; Bartlett, R. A.; Olmstead, M. M.; Senge, K. R.; Sturgeon, B. E. ; Power, P. P. *Angew. Chem.Int. Ed.* **1993**, 32, 717. (f) Schluter, R. D.; Cowley, A. H.; Atwood, D. A.; Jones, R. A.; Bond, M. R.; Carrano, C. J.; *J. Am. Chem. Soc.* **1993**, 115, 2070.
11. Saxena, A.K.; Zhang, H.; Maguire, J.A.; Hosmane, N.S.; Cowley, H. *Angew. Chem., Int. Ed.* **1995**, 34, 332.
12. Jutzi, P.; Galow, P. *J. Organomet. Chem.* **1987**, 319, 139.
13. (a) Spencer, J. L.; Green, M.; Stone, F. G. A. *J. Chem. Soc., Chem. Commun.* **1972**, 1178.
14. (a) Tour, J. M.; *Chem. Rev.* **1996**, 96, 537. (b) Schwab, P. F. H.; Levin, M. D.; Michl, J. *Chem. Rev.* **1999**, 99, 1863. (c) Herzog, A.; Jalisatgi, S. S.; Knobler, C. B.; Wedge, T. J.; Hawthorne, M. F. *Chem. A. Eur. J.* **2005**, 11, 7155.
15. (a) Becke, A. D. *J. Chem. Phys.* **1993**, 98, 5648. (b) Becke, A. D. *Phys. Rev. A* **1988**, 38, 2398. (c) Lee, C.; Yang, w.; Parr, R. G. *Phys. Rev. B* **1988**, 37, 785.
16. Gaussian 03, Revision B.03, Frisch, M. J.; Trucks, G. W.; Schlegel, H. B.; Scuseria, G. E.; Robb, M. A.; Cheeseman, J. R.; Montgomery, Jr., J. A.; Vreven, T; Kudin, K. N.; Burant, J. C.; Millam, J. M.; Iyengar, S. S.; Tomasi, J. Barone, V.; Mennucci, B.; Cossi, M.; Scalmani, G.; Rega, N.; Petersson, G. A.; Nakatsuji, H.; Hada, M.; Ehara, M.; Toyota, K.; Fukuda, R.; Hasegawa, J.; Ishida, M.; Nakajima, T.; Honda, Y.; Kitao, O.; Nakai, H.; Klene, M.; Li, X.; Knox, J. E.; Hratchian, H. P.; Cross, J. B.; Adamo, C.; Jaramillo, J.; Gomperts, R.; Stratmann, R. E.; Yazyev, O.; Austin, A. J.; Cammi, R.; Pomelli, C.; Ochterski, J. W.; Ayala, P. Y.; Morokuma, K.; Voth,

- G. A.; Sthis alvador, P. Dannenberg, J. J.; Zakrzewski, V. G.; Dapprich, S.; Daniels, A. D.; Strain, M. C.; Farkas, O.; Malick, D. K.; Rabuck, A. D.; Raghavachari, K.; Foresman, J. B.; Ortiz, J. V.; Cui, Q.; Baboul, A. G.; Clifford, S.; Cioslowski, J.; Stefanov, B. B.; Liu, G.; Liashenko, A.; Piskorz, P.; Komaromi, I.; Martin, R. L.; Fox, D. J.; Keith, T.; Al-Laham, M. A.; Peng, C. Y.; Nanayakkara, A.; Challacombe, M.; Gill, P. M. W.; Johnson, B.; Chen, W.; Wong, M. W.; Gonzalez, C.; Pople, J. A. Gaussian, Inc., Pittsburgh PA, 2003.
17. (a) Canadell, E.; Eisenstein, O.; Rubio, J. *Organometallics* 1984, **3**, 759. (b) Maguire, J. A.; Hosmane, N. S.; Saxena, A. K.; Zhang, H.; Gray, T. G. *Phosphorus, Sulfur, Silicon* **1994**, 87, 1299.
18. (a) Río, D.; Galindo, A.; Resa, I.; Carmona, E. *Angew. Chem. Int. Ed.* **2005**, 44, 1244. (b) Xie, Y. -M.; Schaefer III, H. F.; King, R. B. *J. Am. Chem. Soc.* **2005**, 127, 2818. (c) Xie, Z. -Z.; Fang, W. H. *Chem. Phys. Lett.* **2005**, 404, 212 (d) Xie, Y. -M.; Schaefer III, H. F.; Jemmis, E. D. *Chem. Phys. Lett.* **2005**, 402, 414.
19. Boys, S. F.; Bernardi, F. *Mol. Phys.* **1970**, 19, 553.
20. Reed, A. E.; Curtiss, L. A.; Weinhold, F. *Chem. Rev.* **1988**, 88, 899.
21. Wiberg, K. *Tetrahedron* **1968**, 24, 1083.
22. (a) Mayer, I. *Chem. Phys. Letters* **1983**, 97, 270. (b) Mayer, I. *Int. J. Quantum Chem.* **1984**, 26, 151.
23. Mulliken, R. S. *J. Chem. Phys.* **1955**, 23, 1833.

CHAPTER 3

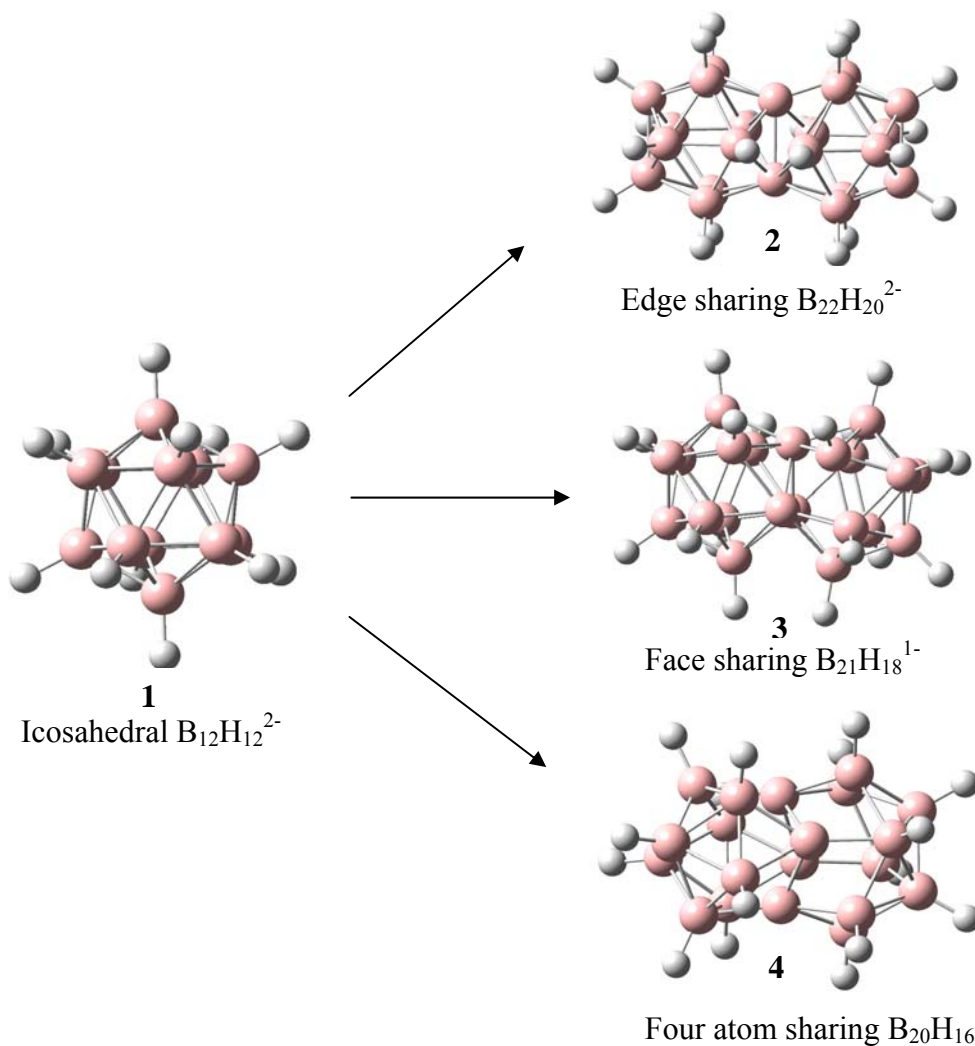
CONDENSED 2- AND 3-DIMENSIONAL AROMATIC SYSTEMS: A
THEORETICAL STUDY ON THE RELATIVE STABILITIES OF ISOMERS
OF $\text{CB}_{19}\text{H}_{16}^+$, $\text{B}_{20}\text{H}_{15}\text{Cl}$ AND $\text{B}_{20}\text{H}_{14}\text{Cl}_2$ AND COMPARISON TO $\text{B}_{12}\text{H}_{10}\text{Cl}_2^{2-}$,
 $\text{C}_6\text{H}_4\text{Cl}_2$, $\text{C}_{10}\text{H}_7\text{Cl}$ AND $\text{C}_{10}\text{H}_6\text{Cl}_2$

[3.0] Abstract

DFT studies (B3LYP/6-31G*) on mono- and dichloroderivatives of benzene, naphthalene, $B_{12}H_{12}^{2-}$, four atom sharing condensed systems $B_{20}H_{16}$, and mono-carborane isomers of $B_{20}H_{16}$, are used to compare the variation of relative stability and aromaticity between condensed aromatics. The trends in the variation of the relative energies and aromaticity in these 2- and 3-Dimensional systems are similar. Aromaticity, estimated by NICS values, does not change considerably with condensation or substitution. The minor variation in the relative energies of the isomers of chloro derivatives are explained by the topological charge stabilization rule of Gimarc. The compatibility of cap and ring orbitals decide the relative stability of $CB_{19}H_{16}^+$.

[3.1] Introduction

Benzene and $B_{12}H_{12}^{2-}$ are important prototypes of two- and three-dimensional aromatic compounds in the carbon and boron families.¹ Condensation of two benzenes sharing an edge gives naphthalene, which has a well-developed chemistry of its own. The properties of benzene and naphthalene are contrasted frequently in the early days of aromaticity.² The variation of aromaticity and reactivity has been especially noted. In contrast, the chemistry of condensed polyhedral borane is only being developed.³ Among the possible condensation products of $B_{12}H_{12}^{2-}$ (**1**), such as the edge sharing $B_{22}H_{20}^{2-}$ (**2**), face sharing $B_{21}H_{18}^{1-}$ (**3**) and four-atom sharing $B_{20}H_{16}$ (**4**) (Scheme 1), the latter is synthesized and characterized.⁴ The electronic requirements of these condensed products are now understood by the *mno* Rule.⁵ Though $B_{20}H_{16}$ is one of the borane equivalent of naphthalene, there is limited information available on $B_{20}H_{16}$.⁶ A major part of the development in the chemistry of polyhedral boranes came from the study of carboranes.⁷ While borane cations are not common, we compare here the isomers of $C_2B_{10}H_{12}$ and $CB_{19}H_{16}^+$. We find that such cross comparisons between two and three dimensional structures are very useful. A recent comparison of the benzyl cation-tropylium cation system to the corresponding carboranes⁸ led to the report of synthesis of $CB_9H_{10}^-$ derivatives.⁹ We also study here the structure and stability of the chloroderivatives of $B_{12}H_{12}^{2-}$ and of the condensed product $B_{20}H_{16}$ and compare them to the benzenoid systems. The present results will also trigger new experiments in the area.



Scheme 1

[3.2] Computational Details

We have optimized the structures of mono and dichloro derivatives of benzene, naphthalene, $B_{12}H_{12}^{2-}$ and $B_{20}H_{16}$ at B3LYP/6-31g* level¹⁰ using Gaussian 03 program package.¹¹ All the monocarborane isomers ($CB_{19}H_{16}^+$) of four atom sharing condensed $B_{20}H_{16}$ are studied at the same level of theory. Nucleus Independent Chemical Shifts

(NICS)¹² values are calculated at ring centers for benzene, naphthalene and at cage centers for $B_{12}H_{12}^{2-}$ and $B_{20}H_{16}$ and at the centroid of $B_{20}H_{16}$ at the GIAO-HF/6-31+g*/B3LYP/6-31g* level.¹²

[3.3] Results and Discussion

[3.3.1] Comparison of $C_2B_{10}H_{12}$ and $CB_{19}H_{16}^+$

The most studied disubstituted boranes are the carboranes. Three isomers of the icosahedral carborane $C_2B_{10}H_{12}$ are known. Thermal isomerization and equilibrium studies involving the three isomers 1,2-, 1,7-, and 1,12-dicarba-*closo*-dodecaborane(12), o-, m-, and p-carborane respectively, established their relative stability. The 1,2-isomer, is the least stable one and isomerizes to the next stable 1,7- isomer (meta) at 500 °C. This in turn goes to the most stable 1,12-isomer (para) above 615 °C.¹³ Theoretical studies at various level have confirmed these experimental trends (Table 1).¹⁴

There is only one monosubstituted carborane possible viz $CB_{11}H_{12}^-$. There are three isomers possible for $C_2B_{10}H_{12}$. There has been several attempts at explaining the stability of positional isomers of carboranes, such as Gimarc's topological charge index, Williams rule, and optimization of ring cap overlap.¹⁵ According to Gimarc rule of topological charge index of carborane, more electronegative incoming atoms prefer to be located at sites of higher electron density while more electropositive elements prefer sites of lower electron density. The Mulliken atomic charges in $CB_{11}H_{12}^-$ are B12(-0.079), B7(-0.005) and B2(0.005) respectively. Therefore the topological charge index

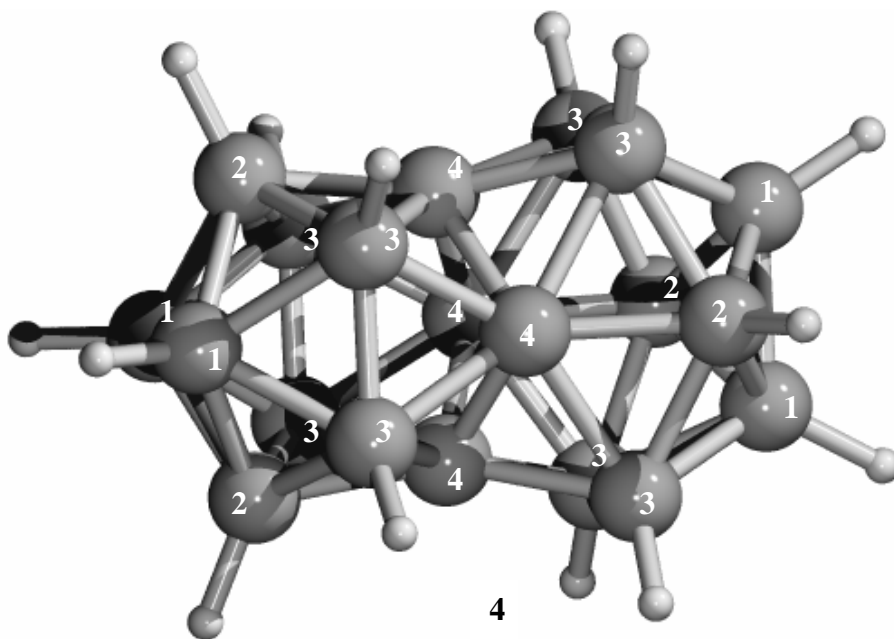


Figure 1: Molecular structure of four atoms sharing condensed $B_{20}H_{16}$, showing the numbering used.

explains their relative stability. The propensity of the chemistry of $C_2B_{10}H_{12}$ in comparison to that of $B_{12}H_{12}^{2-}$ comes from the lack of charge. However, there are some unique characteristics of $B_{12}H_{12}^{2-}$ and $CB_{11}H_{11}^{1-}$ that arise from the negative charge.¹⁶ In contrast, $B_{20}H_{16}$ is neutral. Replacement of one B by C^+ leads to $CB_{19}H_{16}^+$, with four isomers. A stable large carborane with a positive charge is sure to generate unique chemistry of its own.

The four isomers generated by carbon substitution are: 1- $CB_{19}H_{16}^+$, 2- $CB_{19}H_{16}^+$, 3- $CB_{19}H_{16}^+$ and 4- $CB_{19}H_{16}^+$. Out of these, 1- $CB_{19}H_{16}^+$ is the most stable (Table 1). The least stable, 4- $CB_{19}H_{16}^+$, is 33.10 kcal/mol higher in energy. This is indeed a large range, compared to that in the $C_2B_{10}H_{12}$ series. The Mulliken charges calculated on the

four different boron atoms in $B_{20}H_{16}$ [B1(-0.059), B2(-0.012), B3(-0.035) and B4(-0.019)] allow the prediction of the relative stability of the carborane cations $CB_{19}H_{16}^+$, as substitution at $B1 > B3 > B4 > B2$. However this is not supported by the results. The relative stability of these carboranes could be explained by the ring-cap orbital compatibility used in explaining relative stability of $C_2B_{10}H_{12}$ isomers.^{15c} According to this caps with less diffuse orbital prefer small rings. Thus three- and four-membered rings prefer the CH group as a cap. The interaction of CH cap with a four membered boron ring requires orbital reorientation by tilting B–H groups towards the cap. The interaction between a CH cap and B5 ring is even less favourable. The CH group in carborane ($CB_{19}H_{16}^+$) isomers can be considered as a case of a CH cap on different five-membered rings of the skeleton.

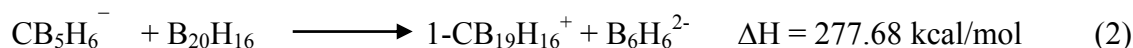
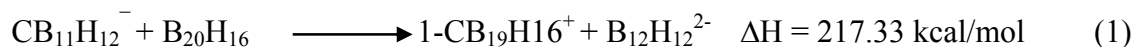
Table 1: Relative stabilities of isomers of the monocarborane $CB_{19}H_{16}^+$ and $C_2B_{10}H_{12}$.

Compounds	Relative Energy (kcal/mol)	Compounds	Relative Energy (kcal/mol)
1- $CB_{19}H_{16}^+$	0.00	1,12- $C_2B_{10}H_{12}$	0.00
2- $CB_{19}H_{16}^+$	5.71	1,7- $C_2B_{10}H_{12}$	2.82
3- $CB_{19}H_{16}^+$	16.01	1,2- $C_2B_{10}H_{12}$	18.70
4- $CB_{19}H_{16}^+$	33.10		

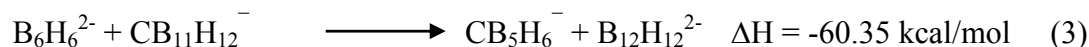
The redirection of orbitals of the five membered rings towards carbon by tilting the B–H bonds towards the C–H cap helps in increasing the overlap between the ring and CH cap. This flexibility is maximum when all the substituents on the B5 rings are hydrogens as in 1- $CB_{19}H_{16}^+$. This is calculated to be the most stable isomer. One boron atom (B4) of the five membered ring that interact with CH in 2- $CB_{19}H_{16}^+$ bridges the

two polyhedra and hence cannot be effective in redirecting the orbitals as much as in 1-CB₁₉H₁₆⁺. Therefore 2-CB₁₉H₁₆⁺ is less stable by 5.71 kcal/mol. Similarly the CH in 3-CB₁₉H₁₆⁺ has to interact with a B5 ring, two borons of which bridge the two polyhedra. Thus positional isomers 2-CB₁₉H₁₆⁺ and 3-CB₁₉H₁₆⁺ are higher in energy than 1-CB₁₉H₁₆⁺. The fourth isomer 4-CB₁₉H₁₆⁺, where carbon forms a part of a bridge and heptavalent, is expected to be the least stable one as indeed as calculated (Table 1).

The differences in relative stabilities that arise on replacing a –CH by an isoelectronic –BH group is quite interesting. We have used isodesmic equations (equation 1-2) to estimate the relative stability of various boranes (B_nH_n²⁻, B₂₀H₁₆) and their carboranes (CB₁₉H₁₆⁺).



The large endothermicity of these reactions is a reflection of the high separation of charges in the products. The lower endothermicity of equation 1 may be a reflection of the inherent extra stability of B₁₂H₁₂²⁻ or the extra stability of an octahedral carborane, CB₅H₆⁻. This is further estimated using equation (3), obtained by subtracting equation 2 from equation 1.



The preference of carbon for a smaller polyhedron is obvious. Thus there is no major inherent difference in the stability of CB₁₁H₁₂⁻ and CB₁₉H₁₆⁺.

Table 2: Data for $B_nH_n^{2-}$ ($n=5-7, 12$), $B_{20}H_{16}$ and for their most stable *closo*-carborane derivatives.¹⁷ [^aTotal energies (hartrees); ^bZero point energy (ZPE) (kcal/mol) and ^c Total energy + zero point energy (T.E + ZPE) (hartrees): calculated at B3LYP/6-31g*)]

Molecules	Total Energy ^a	ZPE ^b	T.E+ZPE ^c
$B_5H_5^{2-}$	-127.09272	36.67	-127.03428
$B_6H_6^{2-}$	-152.65161	47.10	-152.57656
$B_7H_7^{2-}$	-178.14319	56.30	-178.05348
$B_{12}H_{12}^{2-}$	-305.69026	105.00	-305.52293
$B_{20}H_{16}$	-506.90851	154.28	-506.66264
$1-CB_{19}H_{16}^+$	-519.86261	155.80	-519.61433
$1,5-C_2B_3H_5$	-153.77382	44.86	-153.70234
$1,6-C_2B_4H_6$	-179.24479	54.44	-179.15804
$2,4-C_2B_5H_7$	-204.73130	63.93	-204.62942
$1,12-C_2B_{10}H_{12}$	-318.99437	108.82	-318.82096
$CB_4H_5^-$	-140.53863	41.33	-140.47277
$CB_5H_6^-$	-166.05271	51.42	-165.97076
$2-CB_6H_7^-$	-191.53405	60.54	-191.43757
$CB_{11}H_{12}^-$	-318.99437	108.82	-318.82096

[3.3.2] $B_{12}H_{11}Cl^{2-}$, $B_{12}H_{10}Cl_2^{2-}$, C_6H_5Cl and $C_6H_4Cl_2$

Chlorinated derivatives ($B_{12}H_{11}Cl^{2-}$, $B_{12}H_6Cl_6^{2-}$ and $B_{12}Cl_{12}^{2-}$) of $B_{12}H_{12}^{2-}$ have been prepared in the early seventies by reaction with chlorine.¹⁸ The dianion $B_{12}H_{12}^{2-}$ reacts smoothly in aqueous or alcoholic solutions with chlorine to give derivatives in which all hydrogen atoms have been replaced sequentially by halogens. Conversion of $B_{12}H_{12}^{2-}$ to chlorinated derivatives can also be effected with the addition of hydrogen chloride.

We have selected the mono- and dichloroderivatives to make comparison between the $B_{12}H_{12}^{2-}$ and $B_{20}H_{16}$ vis-à-vis C_6H_6 and $C_{10}H_8$. The relative stability of 1,2-, 1,7-, 1,12- isomers of $B_{12}H_{10}Cl_2^{2-}$ are given in the Table 3. The relative stabilities of these may be related to the charge distribution in the mono-chlorinated species. Thus the preference for the replacement of the second hydrogen by chlorine will be for the hydrogen that has maximum negative charge. Calculated charges (Table 4) indicate the order p-> m-> o- as is seen in Table 3.

Table 3: Relative stabilities of di-chloro isomers of $B_{12}H_{12}^{2-}$ and C_6H_6 (NICS = values at the center of the ring cage).

Molecules	Relative Energy (kcal/mol)	NICS	Compounds	Relative Energy (kcal/mol)	NICS
$B_{12}H_{12}^{2-}$	—	-34.4	C_6H_6	—	-11.5
1,2- $B_{12}H_{10}Cl_2^{2-}$	1.38	-35.9	1,2- $C_6H_4Cl_2$	2.50	-12.5
1,7- $B_{12}H_{10}Cl_2^{2-}$	0.00	-35.8	1,3- $C_6H_4Cl_2$	0.08	-12.8
1,12- $B_{12}H_{10}Cl_2^{2-}$	0.11	-35.5	1,4- $C_6H_4Cl_2$	0.00	-12.7

The energy difference between the ortho-isomer, and the para and meta isomers is similar to that for the corresponding dichlorobenzenes. In both cases the para and meta isomers are close to each other in energy. The charges on the hydrogens in C_6H_5Cl are indicators of the preferred positions for second chlorine substitution. Though there is a basic difference between two and three dimensional aromaticity of having definite sigma and pi framework in the former, substitution effects are comparable. Similarly the substituent positions do not effect the extend of aromaticity as indicated by NICS values. The differences in energy between para and meta isomers are very small that we do not attempt any interpretation.

Table 4: Mulliken atomic charges in 1-chloro-B₁₂H₁₁²⁻, 1-chlorobenzene. The number in the second row corresponds to the charge on the corresponding hydrogens.

Atoms	B2	B7	B12	Atoms	C2	C3	C4
Charges	0.0025	0.0032	-0.0001	Charges	-0.128	-0.127	-0.126
	-0.1378	-0.1601	-0.1621		0.155	0.140	0.137

[3.3.3] B₂₀H₁₆, B₂₀H₁₅Cl, B₂₀H₁₄Cl₂, C₁₀H₈, C₁₀H₇Cl, and C₁₀H₆Cl₂

The relative stability of monochloro isomers of B₂₀H₁₆ are given in Table 5. Mulliken atomic charges in B₂₀H₁₆ are H1(0.033), H2(0.035) and H3(0.046) (Table 6). As we know substitution of electronegative atom is more favorable at the site which has larger electron density. In B₂₀H₁₆, H1 is more electro negative than H2 and which is in turn more than H3 and but that is not the order of their relative stability (Table 5). Based on the relative energy values of monochloro isomers, we try to understand the stability pattern of B₂₀H₁₄Cl₂. Substitution at 1-position is more favorable than 3-position and 3- is more favorable than 2. Numbering of dichloroderivatives needs further clarification. We consider 1,1-isomer when both substitutions take place in 1-position of the same polyhedron but if substitution takes place in same position but on different polyhedra then it is 1,1'-isomer. If these substituents are adjacent to each other in the same polyhedron then it is 1,1a-isomer if far then it is 1,1b- and if it is farther then it is 1,1c- and so on. Similarly if substituents are adjacent to each other but in different polyhedra then it is 1,1'a-isomer. Thus, as a first approximation we can predict the stability order as 1,1->1,3->1,2->3,3->2,3->2,2-. The calculated values show that only two isomers do not follow this order: 1,2- and 3,3'- (Table 7). The 3,3'- isomer has two Cl atoms close

to each other and this is the least stable among all $B_{20}H_{14}Cl_2$ isomers. In general among the same category, the substitution at different cages is more favorable than that at the same cage.

Thus, 1,1'-substitution is more favorable than 1,1-, 1,3'- > 1,3- 1,2'- > 1,2-, 3,3'- > 3,3-. 1,2a- $B_{20}H_{16}$ is less stable as steric factor plays a vital role here than any other factors. In the case of 1,1a-isomer steric interaction is less as the distance between two boron atoms is more (2.847 Å) than the any others normal B-B bond distance (1.780 Å) in $B_{20}H_{16}$. The low difference in energy between the chloro- and dichloro- $B_{20}H_{16}$ derivatives is also reflected in the energetics of chloro- and dichloronaphthalenes. Though there is some structural difference between these condensed systems, substitution effects are comparable with their parent systems. There are very minor changes in terms of aromaticity when a substitution of this type takes place.

Table 5: Relative stabilities of mono-chloro isomers of $B_{20}H_{16}$ and $C_{10}H_7Cl$ (*NICS1 = values at the center of the first cage/ring, NICS2 = values at the center of the next cage/ring, NICS3 = values at the center of the four atom sharing ring).

Molecules	Relative Energy (kcal/mol)	NICS1	NICS2	NICS3
$B_{20}H_{16}$	–	-30.9	-30.9	-68.3
1- $B_{20}H_{15}Cl$	0.00	-31.7	-31.0	-68.3
3- $B_{20}H_{15}Cl$	0.74	-31.3	-31.7	-68.3
2- $B_{20}H_{15}Cl$	1.29	-30.3	-30.7	-67.7
$C_{10}H_8$	–	-11.4	-11.4	–
2- $C_{10}H_7Cl$	0.00	-12.0	-11.4	–
1- $C_{10}H_7Cl$	0.93	-11.9	-11.6	–

Table 6: Mulliken atomic charges in B₂₀H₁₆ and C₁₀H₈.

B4	B1	B2	B3	Atoms	C1	C2
Charges at B	-0.059	-0.012	-0.035	Charges at C	-0.1910	-0.1350
Charges at H	0.033	0.035	0.046	Charges at H	0.1290	0.1295

These are to be compared to the chloronaphthalenes. The 2-chloronaphthalene is more stable than 1-chloro naphthalene by 0.9 kcal/mol. 1-position (also called alpha - position) is sterically more favorable than the 2-position (beta -position) because the Cl-H non-bonded distances are 2.675 Å and 2.814 Å whereas in 2-chloronaphthalene these Cl-H distances are 2.854 Å and 2.861 Å. The relative energies (Table 8) of dichloronaphthalenes follow the order 2,6=2,7 > 1,6- > 1,7- > 1,3-> 1,5- > 1,4- > 2,3- > 1,2- > 1,8-. As 2-chloronaphthalene is more stable than the 1-chloronaphthalene by 0.93 kcal/mol, it is clear that further substitution on 2-chloronaphthalene will be more favorable than in 1-chloronaphthalene. But taking steric factor in account, further substitution in the same ring is not favorable. Thus, 2,3-dichloronaphthalene is less stable by 3.25 kcal/mol. Similarly substitution in 1- chloronaphthalene makes 1,6-dichloronaphthalene and 1,7- dichloronaphthalene less stable by around 1.00 kcal/mol. The 1,2-dichloronaphthalene, 1,3-dichloronaphthalene and 1,4-dichloronaphthalene are less stable due to substitution in the same ring.

Table 7: Relative energies (R.E) and NICS values of all dichloro isomers of B₂₀H₁₆. (NICS1 = values at the center of the first cage, NICS2 = values at the center of the next cage, NICS3 = values at the center of the four atom sharing ring).

Molecules	R.E (kcal/mol)	NICS1	NICS2	NICS3
1,1'a-B ₂₀ H ₁₄ Cl ₂	0.00	-31.8	-31.8	-68.3
1,1a-B ₂₀ H ₁₄ Cl ₂	0.14	-32.6	-31.0	-68.7
1,3'b-B ₂₀ H ₁₄ Cl ₂	0.68	-31.5	-31.3	-67.9
1,3'a-B ₂₀ H ₁₄ Cl ₂	0.74	-31.5	-31.3	-67.9
1,3b-B ₂₀ H ₁₄ Cl ₂	0.83	-32.0	-30.7	-67.8
1,3a-B ₂₀ H ₁₄ Cl ₂	1.21	-31.9	-30.7	-67.9
1,2'b-B ₂₀ H ₁₄ Cl ₂	1.29	-31.4	-30.3	-67.6
3,3'd-B ₂₀ H ₁₄ Cl ₂	1.41	-31.0	-30.7	-67.3
3,3'b-B ₂₀ H ₁₄ Cl ₂	1.46	-31.0	-30.9	-67.4
3,3'c-B ₂₀ H ₁₄ Cl ₂	1.46	-32.6	-31.0	-67.4
3,3b-B ₂₀ H ₁₄ Cl ₂	1.51	-31.5	-30.5	-67.4
1,2a-B ₂₀ H ₁₄ Cl ₂	1.68	-30.8	-30.8	-67.7
3,3a-B ₂₀ H ₁₄ Cl ₂	1.68	-31.5	-30.5	-67.4
3,3c-B ₂₀ H ₁₄ Cl ₂	1.96	-31.1	-30.4	-67.2
2,3'b-B ₂₀ H ₁₄ Cl ₂	2.01	-30.0	-31.0	-67.2
2,3b-B ₂₀ H ₁₄ Cl ₂	2.05	-30.6	-30.5	-67.2
2,3'a-B ₂₀ H ₁₄ Cl ₂	2.16	-30.0	-31.0	-67.2
2,3a-B ₂₀ H ₁₄ Cl ₂	2.36	-30.6	-30.5	-67.4
2,2b-B ₂₀ H ₁₄ Cl ₂	2.47	-30.0	-30.5	-67.2
2,2'a-B ₂₀ H ₁₄ Cl ₂	2.58	-30.0	-30.0	-67.1
3,3'a-B ₂₀ H ₁₄ Cl ₂	2.94	-30.9	-30.9	-67.2

There is a greater steric interaction in 1,8-dichloronaphthalene making Cl-C-C bond angle 124°. Following guidelines emerge from the studies to determine the stability of dichloronaphthalenes: (a) substitution at adjacent carbons are not favorable, (b) 2-position is more stable than the 1-position, (c) substitution at different rings are better than that at the same ring.

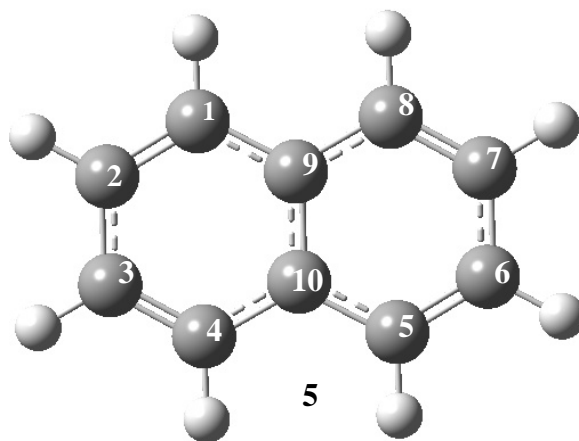


Figure 2: Molecular structure of naphthalene

The 1,8-dichloro isomer, where both Cl occupy an alpha- position, is the least stable. Non bonded Cl-Cl distance of 3.11 Å here is below the range of vander Walls radii (3.5 Å) making it the least stable. Next stable isomer is where chlorine atoms are substituted at adjacent positions, i.e., 1,2- and 2,3-. Among these two isomers, 2,3- is more stable

Table 8: Relative stabilities of di-chloro isomers of naphthalene.

Molecules	Relative Energy (kcal/mol)	C-Cl bond length (Å)	NICS1	NICS2
2,6-C ₁₀ H ₆ Cl ₂	0.00	1.76	-12.0	-12.0
2,7-C ₁₀ H ₆ Cl ₂	0.00	1.76	-12.0	-12.0
1,6-C ₁₀ H ₆ Cl ₂	0.88	1.76	-11.9	-11.9
1,7-C ₁₀ H ₆ Cl ₂	1.00	1.76	-11.9	-11.9
1,3-C ₁₀ H ₆ Cl ₂	1.45	1.76	-12.5	-12.5
1,5-C ₁₀ H ₆ Cl ₂	2.13	1.76	-12.1	-12.1
1,4-C ₁₀ H ₆ Cl ₂	2.28	1.76	-12.3	-11.9
2,3-C ₁₀ H ₆ Cl ₂	3.25	1.75	-12.5	-11.3
1,2-C ₁₀ H ₆ Cl ₂	4.02	1.75	-12.0	-11.7
1,8-C ₁₀ H ₆ Cl ₂	10.49	1.76	-12.2	-12.2

because both the Cl are at beta -positions. Then there are two isomers where Cl atoms are at alpha -positions, i.e., 1,4- and 1,5-. The 1,5-isomer, where substitutions are at

different rings, is more stable than the 1,4-isomers where both the Cl atoms are at the same ring. Next three isomers contain one alpha -Cl and one beta -Cl substituents (1,3-1,6- and 1,7-). The 1,3-isomer is the least stable among these three because both Cl are at same ring.

Table 9: Mulliken atomic charges in 1-chloronaphthalene. Second row shows the charges on the corresponding hydrogens.

	C1	C2	C3	C4	C5	C6	C7	C8
Charges	-0.141	-0.139	-0.133	-0.185	-0.192	-0.130	-0.134	-0.192
	-0.019	0.153	0.139	-0.185	0.134	0.134	0.136	0.157

The 1,7-isomer is 0.02 kcal/mol more stable than 1,6-. Most stable isomers are found where Cl's are substituted at beta -position of the different rings: 2,6- and 2,7-. Substitution does not change aromaticity considerably as judged from NICS values. In view of the similarity in energetics, it is anticipated that a chemistry of condensed polyhedral boranes as elaborate as those of naphthalene must be in the realm of the possible.

[3.4] Conclusions

We have studied the structures and relative stability of all the four mono-carborane isomers ($\text{CB}_{19}\text{H}_{16}^+$) of $\text{B}_{20}\text{H}_{16}$. The relative stability order ($1-\text{CB}_{19}\text{H}_{16}^+ > 2-\text{CB}_{19}\text{H}_{16}^+ > 3-\text{CB}_{19}\text{H}_{16}^+ > 4-\text{CB}_{19}\text{H}_{16}^+$) of these positional isomers are explained based on the ring-cap orbital overlap criterion. Comparisons are made between the mono- and

dichloroderivatives of two- and three-dimensional aromatic systems. The stability order of all the chloro- isomers are explained based on the Gimarc's topological charge stabilization rule. The energy difference between the ortho-, para-, and meta-isomer of dichloro-B₁₂H₁₂²⁻ is similar to that for corresponding dichlorobenzenes. Though there is a basic difference between two- and three-dimensional aromaticity (of having definite σ and π -framework in the former), substitution effects are comparable. Similarly we found the substituent position do not effect the extend of aromaticity significantly.

[3.5] References

1. (a) March, J. *Advanced Organic Chemistry: Reactions, Mechanisms, and Structure*, 5th Ed, John Wiley and Sons, New York, 1999. (b) Grimes, R. N. *Advanced Inorganic Chemistry*, Sixth Edition, Cotton, F. A. and Wilkinson, G. 6th Ed., Wiley Interscience. 1999. Chapter 5.
2. Finar, I. L. *Organic Chemistry*, Volume 1, 5th Ed, John Wiley and Sons, New York, 1992.
3. (a) Casanova, J. *The Boranes, Carboranes, carborane continuum*: Edition, John Wiley & Sons, 1998. (b) Shea, S. L.; Bould, J.; Londesborough, M. G. S.; Perera, S. D.; Franken, A.; Ormsby, D. L.; Jelinek, T.; Stibr, B; Holub, J.; Kilner, C. A.; Thornton-Pett, M.; Kennedy, J. D. *Pure Appl. Chem.* **2003**, 75, 1239.
4. (a) Miller, N. E.; Muetterties, E. L. *J. Am. Chem. Soc.* **1963**, 85, 3506. (b) Friedman, L. B.; Dobrott, R. D.; Lipscomb, W. N., *J. Am. Chem. Soc.* **1963**, 85, 3505. (c) Miller, N. E., Miller, C. H.; Muetterties, E. L., *Inorg. Chem.* **1964**, 3, 1690. (d) Dobrott, R. D.; Friedman, L. B.; Lipscomb, W. N. *J. Chem. Phys.* , **1964**, 40, 866.
5. (a) Jemmis, E. D.; Balakrisnanarajan, M. M.; Pancharatna, P. D. *J. Am. Chem. Soc.* **2001**, 123, 4313. (b) Jemmis, E. D.; Balakrisnanarajan, M. M.; Pancharatna, P. D. *Chem. Rev.* **2002**, 102, 93. (c) Jemmis, E. D.; Jayasree, E. G. *Acc. Chem. Res.* **2003**, 36, 816.
6. (a) Kaur, P.; Perera, S. D.; Jelinaek, T.; Stibr, B.; Kennedy, J. D.; Clegg, W.; Thornton-Pett, M. *J. Chem. Soc., Chem. Commun.* **1997**, 217. (b) Enemark, J.;

- Friedman, L. B.; Hartsuck, J. A.; Lipscomb, W. N. *J. Am. Chem. Soc.*, **1966**, 88, 3659.
7. (a) Hawthorne, M. F. *Angw. Chem. Int. Ed. Engl.* **1993**, 32, 950 (b) Bregadze, V. I., *Chem. Rev.* **1992**, 92, 209. (c) Grimes, R. N. *Carboranes, Anti-Crowns, Big Wheels, and Supersandwiches, in Organic Synthesis Highlights III*, Mulzer, J. and Waldmann, H., Eds., Wiley -VCH. **1998**. 406.
8. Jemmis, E. D.; Jayasree, E. G. *Inorg. Chem.* **2003**, 42, 7725.
9. Laromine, A.; Teixidor, F.; Vinas, C. *Angew. Chem. Int. Ed.* **2005**, 44, 2220.
10. (a) Becke, A. D. *J. Chem. Phys.* **1993**, 98, 5648. (b) Becke, A. D. *Phys. Rev. A* **1988**, 38, 2398. (c) Lee, C.; Yang, w.; Parr, R. G. *Phys. Rev. B* **1988**, 37, 785.
11. Gaussian 03, Revision C.02, Frisch, M. J.; Trucks, G. W.; Schlegel, H. B.; Scuseria, G. E.; Robb, M. A.; Cheeseman, J. R.; Montgomery, Jr., J. A.; Vreven, T.; Kudin, K. N.; Burant, J. C.; Millam, J. M.; Iyengar, S. S.; Tomasi, J.; Barone, V.; Mennucci, B.; Cossi, M.; Scalmani, G.; Rega, N.; Petersson, G. A.; Nakatsuji, H.; Hada, M.; Ehara, M.; Toyota, K.; Fukuda, R.; Hasegawa, J.; Ishida, M.; Nakajima, T.; Honda, Y.; Kitao, O.; Nakai, H.; Klene, M.; Li, X.; Knox, J. E.; Hratchian, H. P.; Cross, J. B.; Bakken, V.; Adamo, C.; Jaramillo, J.; Gomperts, R.; Stratmann, R. E.; Yazyev, O.; Austin, A. J.; Cammi, R.; Pomelli, C.; Ochterski, J. W.; Ayala, P. Y.; Morokuma, K.; Voth, G. A.; Salvador, P.; Dannenberg, J. J.; Zakrzewski, V. G.; Dapprich, S.; Daniels, A. D.; Strain, M. C.; Farkas, O.; Malick, D. K.; Rabuck, A. D.; Raghavachari, K.; Foresman, J. B.; Ortiz, J. V.; Cui, Q.; Baboul, A. G.; Clifford, S.; Cioslowski, J.; Stefanov, B. B.; Liu, G.;

- Liashenko, A.; Piskorz, P.; Komaromi, I.; Martin, R. L.; Fox, D. J.; Keith, T.; Al-Laham, M. A.; Peng, C. Y.; Nanayakkara, A.; Challacombe, M.; Gill, P. M. W.; Johnson, B.; Chen, W.; Wong, M. W.; Gonzalez, C.; and Pople, J. A.; Gaussian, Inc., Wallingford CT, **2004**.
12. Scheleyer, P. v. R.; Maerker, C.; Dransfeld, A.; Jiao, H.; Hommes, N. J. v. E. *J. Am. Chem. Soc.* **1996**, *118*, 6317.
13. (a) Salinger, R. M.; Frye, C. L. *Inorg. Chem.* **1965**, *4*, 1815 (b) Bohn, R. K.; Bohn, M. D. *Inorg. Chem.* **1971**, *2*, 350.
14. (a) Ott, J. J.; Gimarc, B. M. *J. Comput. Chem* **1986**, *7*, 673 (b) Jemmis, E. D.; Kiran, B.; Coffe, D. Jr. *Chem. Ber.* **1997**, *130*, 1147.
15. (a) Ott, J. J.; Gimarc, B. M. *J. Am. Chem. Soc.* **1986**, *108*, 4303. (b) Williams, R. E.; Gerhart, F. J. *J. Am. Chem. Soc.* **1965**, *87*, 3513. (c) Jemmis, E. D. *J. Am. Chem. Soc.* **1982**, *104*, 7017.
16. (a) King, B. T.; Noll, B. C.; McKinely, A. J.; Michl, J. *J. Am. Chem. Soc.* **1996**, *118*, 10902. (b) Srivastava, R. R.; Hamlin, D. K.; Wilbur, D. S. *J. Org. Chem.* **1996**, *61*, 9041. (c) Tsang, C.; Yang, Q.; Tung-Po Sze, E.; Mak, T. C. W.; Chan, D. T. W.; Xie, Z. *Inorg. Chem.* **2000**, *39*, 5851. (d) King, B. T.; Michl, J. *J. Am. Chem. Soc.* **2000**, *122*, 10255. (e) Xie, W.; Bau, R.; Reed, C. A. *Inorg. Chem.* **1995**, *34*, 5403. (f) Xie, W.; Bau, R.; Benesi, A. *Science* **1993**, *262*, 402. (g) Reed, C. A. *Acc. Chem. Res.* **1998**, *31*, 133. (h) Strauss, S. H. *Chem. Rev.* **1993**, *93*, 927. (i) Bullen, N. J.; Franken, A.; Kilner, C. A.; Kennedy, J. D., *Chem. Commun.* **2003**, 1684.

17. (a) Schleyer, P. v. R.; Najafian, K. *Inorg. Chem.* **1998**, 37, 3454 (The relative energies of all the positional isomers of the *closo*-monocarboranes, $\text{CB}_{n-1}\text{H}_n^-$ ($n=5-12$), and the *closo*-dicarboranes, $\text{C}_2\text{B}_{n-2}\text{H}_n$ ($n=5-12$) are discussed at RMP2(fc)/6-31G* level of theory (b) Jemmis, E. D.; Ramalingam, M.; Jayasree, E. G. *J. Comp. Chem.* **2001**, 22, 1542.
18. (a) Knoth, W. H.; Miller, H. C.; Sauer, J. C.; Balthis, J. H.; Chia, Y. T.; Muetterties, E. L. *Inorg. Chem.* **1963**, 3, 159. (b) Morrison, J. A. *Chem. Rev.* **1991**, 91, 35.

CHAPTER 4

THE INTRAMOLECULAR ACTIVATION OF C_β-H BOND BY TRANSITION METAL COMPLEXES

[4.0] Abstract

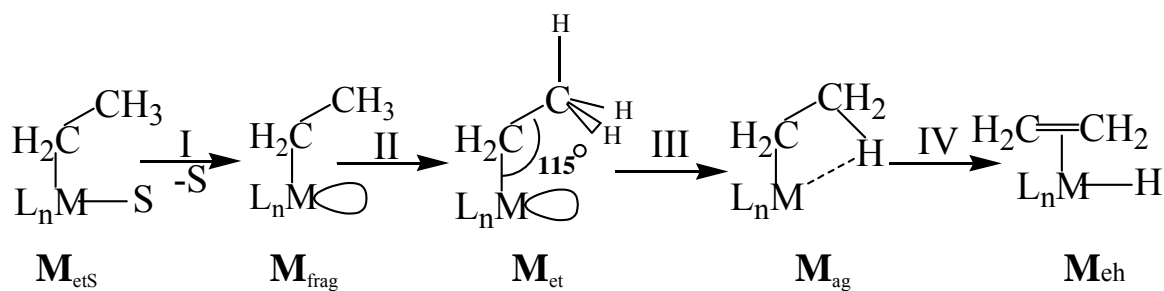
The frontier molecular orbitals of any transition metals can be brought close to that of the C_β-H bond so that the formation of the agostic and the ethylene hydride complex is possible. The relative energies between the metal-agostic and metal-ethylene-hydride complexes show that the former complex is most stable with the first-row transition metals and the stability decreases for their heavier group analogues but increases for the latter complexes. The preference of heavier group metal to form ethylene-hydride complex over their agostic is explained on the basis of the metal's atomic radius and steric factor arises from the ligands. The transition states located for the conversion of the agostic complex to the ethylene-hydride complex is generally found to be late for lighter transition metal complexes and early for their heavier group analogues. Isodesmic equation 1 calculated at the B3LYP/LANL2Z and BP86/LANL2DZ supports the trends that the lighter metals prefer agostic complexes and heavier metals prefer ethylene-hydride complexes.

[4.1] Introduction

The activation of inert C-H bonds by a transition metal is of fundamental interest for stoichiometric and catalytic reactions particularly for functionalization of hydrocarbons.¹ The development of catalytic variants of these high barrier reactions allows for efficient syntheses of many types of organic molecules.² Binding a transition metal to the C-H bond is the first step in the activation of C-H bonds and leads to the formation of agostic complexes.² Agostic interaction, a term first introduced by Brookhart and Green, is described³ as an attractive interaction between metal atom and the CH fragment of an appended ligand. The C-H activation reactions proceed from the initially formed agostic complex in various directions leading to the different products. Agostic interactions have been found to play an important role in the olefin polymerization reactions⁴ and also in the isomerization and dynamics⁵ of alkyl groups. Most of the time a hydrocarbon group already attached to the metal is involved in agostic interaction and C-H bond activation. The different possible agostic complexes are labeled as α -, β -, γ - etc based on the position of the C-H bonds which interacting with the metal atoms. If the initial product is a result of a C-H bond addition, the oxidation numbers of the metal changes for all excepts the C_{β} -H bond complex. In the latter case the product is an olefin hydride complex. One of the remarkable aspects of C-H bond activation is the following. The C-H bond energy does not vary considerably from molecule to molecule. The energy levels of the metal on the other hand vary substantially across the periodic table and yet several metals form agostic complexes.

The way in which the different ligands combinations prepare any metal of the periodic table to interact with the C-H bond effectively is fascinating and prompted this study.

Among the vast variety of reactions involving agostic complexes, the one involving β -hydrogen is chosen for the current study. The β -agostic complexes are involved in the β -hydride elimination which is of prime importance in catalytic hydrogenation, hydroformylation,⁶ isomerization,⁷ metathesis,⁸ and oligomerization⁹ of olefins as well as in the hydrogenolysis¹⁰ and other heterogeneous catalytic reactions of hydrocarbons. The first step of the β -hydride elimination is an activation of the C_β -H bond of a metal-alkyl complex, which is unique because addition does not change oxidation state of the metal. This step involves the transformation of metal-ethyl complex (M_{ets} , Scheme 1) to β -agostic complex (M_{ag} , Scheme 1) which go on to form an ethylene-hydride complex (M_{eh} , Scheme 1), from which many other processes can continue. For example, in the polymerization reaction, agostic complex is the resting state, from where propagation, termination or hydride exchanges can occur.



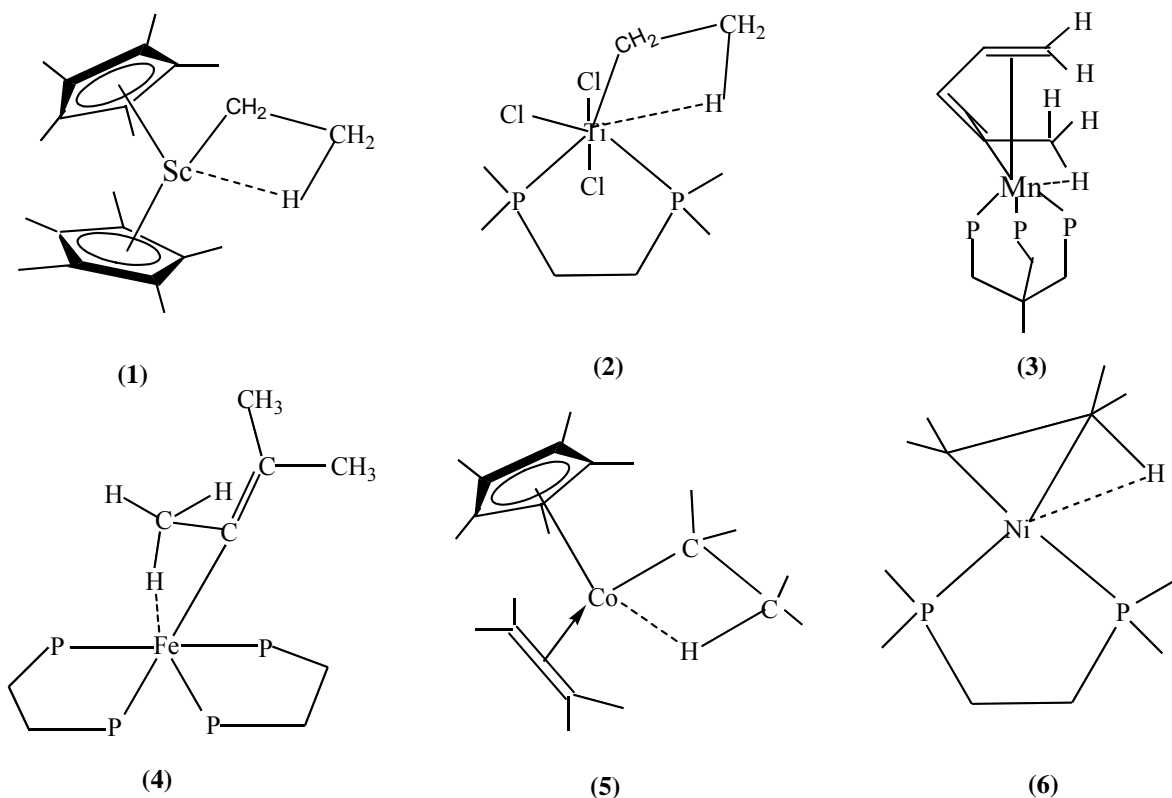
Scheme 1

The available crystal structures of metal-alkyl β -agostic complexes point to the occurrence of β -agostic interactions as an intermediate across the periodic table (Table 1). We would like to understand the way in which the differing ligand combinations on different metals lead to appropriate frontier orbitals that stabilize the agostic interactions.

Two different types of M-C-C bonded β -agostic structures exist in the literature: (i) Metal-alkyl (M-C-C $_{\beta}$ -H), and (ii) Metal-alkenyl (M-C=C $_{\beta}$ -H) where the carbons are unsaturated. Here we have restricted our study within the metal-alkyl β -agostic complex. Even though the agostic-complexes are widely studied, there are only a few structurally characterized transition metal-alkyl β -agostic complexes are reported in the literature (Table 1). 16 of these are characterized using X-ray or neutron diffraction methods. Others are assigned using spectroscopic methods in solutions or in matrix. Interestingly, most of the β -agostic complexes (18) are from the first row transition metals. This numbers decrease sharply in the second-row transition metals (8) and further in the third row transition metal complexes (4). Here, we would like to investigate if there are any specific reasons for the diverse experimental trends. Our objective is to study and compare the agostic structure and the β -hydride addition reactions catalyzed by transition metal complexes along the groups and across the row of a periodic table. In addition, we have searched for the ground state agostic and ethylene-hydride structures. We predict based on their ground state structure whether a given metal complex will be more suitable for polymerization reactions or β -hydride elimination reactions.

Table 1: List of experimentally characterized (CCSD and Spectroscopy studies) structures of all transition metals reported in the literature that feature metal-alkyl β -agostic ($M\cdots H-C_{\beta}$) interactions along with selected geometrical parameters.

Molecular Formula		Connecting group $M\cdots HC-R$	$C_{\beta}-H$	$C_{\alpha}-C_{\beta}$	$M-C_{\alpha}-C_{\beta}$
¹¹ Sc(Cp*) ₂ Et (1)		-CH ₂ -			
¹² TiCl ₃ (dmpe)Et (2)	(CCSD)	-CH ₂ -	1.036	1.500	84.56
¹³ Ti(Cp) ₂ Et		-CH ₂ -			
¹⁴ Ti(η^5 -C ₂ B ₉ H ₁₁)(Cp*)(Et)		-CH ₂ -			
¹⁵ [Fe(dmpe) ₂ (CH ₂ CH(ⁱ Pr))] (4)	(CCSD)	-CH=	1.143	1.490	78.49
¹⁶ [CoCp*(P(o-tolyl) ₃ Et)] ⁺		-CH ₂ -	1.317	1.480	74.46
(CCSD)		-CH ₂ -			
[CoCp*(PPh ₃ Et)] ⁺		-CH ₂ -			
[CoCp*PMe ₃ Et] ⁺		-CH ₂ -			
¹⁷ [Co(C ₅ H ₅)Et(C ₂ H ₄)] ⁺ (5)	(CCSD)	-CH ₂ -			
¹⁷ [Co(C ₅ Me ₄ Et)Et(C ₂ H ₄)] ⁺		-CH ₂ -			
¹⁷ [Co(C ₅ Me ₅)Et(C ₂ H ₄)] ⁺		-CH ₂ -			
¹⁷ [Co(C ₅ Me ₄ Et)Et(C ₂ H ₄)] ⁺		-CH ₂ -			
¹⁸ [CoCp*(P(OMe) ₃ Et)] ⁺		-CH ₂ -			
¹⁹ [Ni(LL)Et] ⁺	(CCSD)	-CH ₂ -	1.016	1.435	74.01
²⁰ [Ni(Me ₂ NN)Et]		-CH ₂ -			
²⁰ [Ni(Me ₂ NN)C ₃ H ₇]		-CH ₂ -			
²¹ [Ni(diimine)C ₃ H ₇] ⁺	(CCSD)	-CH ₂ -			
²¹ [Ni(diimine)CH ₂ CH(CH ₃)] ⁺		-CH ₂ -			
²² Cp ₂ *YCH ₂ CH ₂ CH(CH ₃) ₂		-CH ₂ -			
²² [Y(Cp*)(μ -CH ₂ CH ₂ R)] ₂	(CCSD)	-CH ₂ -	0.935	1.534	84.81
²³ [Zr(Cp*) ₂ (CH ₂ CH ₂ R)PMe ₃] ⁺	(CCSD)	-CH ₂ -	0.940	1.518	83.69
²⁴ [Zr(Cp*) ₂ (CH ₂ CH ₃)RCN] ⁺		-CH ₂ -			
²⁵ Tp ^{Me2} NbCl(<i>i</i> -Pr)(PhC \equiv CMe)	(CCSD)	-CHR-	1.106	1.476	87.010
^{17b} [Rh(C ₅ Me ₅)Et(C ₂ H ₄)] ⁺		-CH ₂ -			
²⁶ [Pd(C ₂ H ₅)(1,2-(CH ₂ PBu ^t) ₂ C ₆ H ₄)] ⁺		-CH ₂ -			
²⁷ [(N \wedge N)Pd(C ₂ H ₄)(C ₃ H ₇)] ⁺		-CH ₂ -			
²⁸ [P ₂ N ₂]Ta(C ₂ H ₄)(CH ₂ CH ₃)]	(CCSD)	-CH ₂ -	1.024	1.449	81.82
²⁹ OsCl(C(C(CH ₃)CHPh)(PPh ₃) ₂ C ₉ H ₈)	(CCSD)	-C=	1.219	1.520	89.86
³⁰ Pt(η^2 -C ₇ H ₁₀)(L-L)	(CCSD)	-CH ₂ -	1.280	1.480	78.36
³¹ [Pt(^t Bu ₂ P(CH ₂) ₃ ^t Bu)(C ₂ H ₅)] ⁺		-CH ₂ -			



Scheme 2

The three possible intermediate species involved for the C-H bond activation (or β -hydride elimination) process are (i) metal-ethyl (16 electrons or less), (ii) metal-agostic (18 electrons or less) and (iii) metal-ethylene-hydride (18 electrons or less). The β -agostic complex is a very crucial intermediate for the bond activation process in many aspects. We have used the experimentally characterized metal-alkyl β -agostic structures in designing the appropriate agostic complex for each metal. In the absence of such experimental guidelines, we have tuned the possible combination of ligands around the metal such that ligands stabilize the agostic interactions for each metal. With these model compounds, we have studied the CH addition step. Two sets of complexes where

all the metal complexes are either neutral or cationic maintaining the total number of valence electron count of 14 for early and 16 for late transition metals are considered here. Among the many possible ligand-metal combinations are considered, we have chosen the ones which gave local minima for all the three species involved in the step.

The previous theoretically studies on the C $_{\beta}$ -H bond activation did not attempt to make such kind of generalization across the periodic table. In 1980, Hoffmann *et al.* first theoretically observed³² the C $_{\alpha}$ -H bond elongation in the Ta-alkylidene complex using extended Hückel calculations. In 1984, morokuma *et al.* reported^{33a} the first theoretical evidence of C $_{\beta}$ -H...M interaction found in the model Ti(C $_2$ H $_5$)(Cl) $_2$ (H)(PH $_3$) $_2$ complex using *ab initio* molecular orbital calculation. Later, in 1985, they studied^{33b} the role of agostic complex in the β -hydride-elimination of Ni- and Pd-complexes. Our earlier study shows³⁴ that the cationic Co- β -agostic [Co(C $_5$ H $_5$)(PH $_3$)(C $_2$ H $_5$)] complex is more stable than the corresponding ethylene-hydride [Co(C $_5$ H $_5$)(PH $_3$)(C $_2$ H $_4$)H] $^+$ complex. Spencer *et al.* theoretically studied³⁵ the model [Co(C $_5$ H $_5$)(PH $_3$)(C $_2$ H $_5$)] $^+$ complex to support the experimental observation of dynamic inversion of chirality at Co-center and β -hydrogen-elimination reaction. In 1994, Guest *et al.* studied³⁶ the β -H exchange process of the Rh-agostic [Rh(Cp)(C $_2$ H $_4$)(C $_2$ H $_5$)] complex and found that ethylene-hydride complex is higher in energy than the β -agostic complex. Morokuma³⁷ *et al.* found that the formation of the β -agostic complex is an important step for the Ti-, Zr-, Ni- and Pd-catalyzed ethylene polymerization reactions. Zeigler *et al.* found³⁸ that the β -agostic complex is the most stable complex and found to be the resting state for the

polymerization reactions. They found that the β -hydrogen elimination and termination has a great impact on the transition metal-catalyzed polymerization reactions. In 1998, Scherer *et al.* theoretically studied³⁹ (DFT) three model complexes $[\text{EtTiCl}_2]^+$, EtScCl_2 , and EtTiCl_2 and concluded that that agostic stabilization derives not from $\text{C-H} \rightarrow \text{M}$ electron donation but from delocalization of the M-C bonding orbital, usually the HOMO in d^0 complexes. Their study points out that factors such as the Lewis acidity or VE count of the metal center are not important; instead, the form and rigidity of the metal-ligand framework appear to be crucial factors in permitting or inhibiting the development of the agostic interaction. Very recently, Köppel *et al.* studied⁴⁰ the dynamics of migratory insertion and β -hydrogen elimination in the cationic complex $[\text{CpRh}(\text{PH}_3)\text{H}(\text{C}_2\text{H}_4)]^+$ from a quantal point of view. Their study shows that the geometrical parameters changes considerably for the four atoms where the bonds are broken and formed whereas the others remain constant. Even though the β -agostic complexes are extensively studied theoretically, there are no systematic study for the transition metal catalyzed $\text{C}_\beta\text{-H}$ bond activation process.

[4.2] Computational Details

The neutral first row complexes $\text{Sc}(\text{Cp})_2\text{Et}$, $\text{TiCpEt}(\text{PH}_3)_2$, $\text{VCpEt}(\text{NO})$, $\text{Cr}(\text{PH}_3)_2\text{CpEt}$, $\text{MnEt}(\text{PH}_3)_4$, $\text{FeEt}(\text{PH}_3)_2\text{NO}$, $\text{CoC}_6\text{H}_6\text{Et}$, and $\text{Ni}(\text{Cp})\text{Et}$ and the cationic first row complexes $[\text{ScCp}(\text{C}_6\text{H}_6)\text{Et}]^+$, $[\text{TiCpEt}(\text{NO})]^+$, $[\text{V}(\text{Cp})\text{Et}(\text{PH}_3)_2]^+$, $[\text{Cr}(\text{Cp})_2\text{Et}]^+$, $[\text{MnEt}(\text{PH}_3)_2\text{NO}]^+$, $[\text{FeEt}(\text{PH}_3)_4]^+$, $[\text{CoCpEt}(\text{PH}_3)]^+$, and $[\text{Ni}(\text{C}_6\text{H}_6)\text{Et}]^+$ are considered in this study. The combination of ligands used around the metal centre is from the group

Cp, C₆H₆, -PH₃, and -NO ligands. The same set of ligand combinations are used for heavier group metals. We use the following labels for the structures: M_{ets} for the metal-ethyl complex with a coordinated PH₃ as a labile ligand (solvent); M_{frag} for the metal fragment where the solvent molecule is separated; M_{et} for non-agostic metal-ethyl complex; M_{ag} for the agostic intermediate; and M_{eh} for the product metal-ethylene-hydride complex. The geometries of M_{ets}, M_{ag}, and M_{eh} are optimized at B3LYP/LANL2DZ⁴¹⁻⁴³ level using Gaussian 03 program package.⁴⁴ The single point calculation done on the M_{frag} structures which is a non-optimized structure of corresponding M_{ets} without the solvent molecule. The model metal-ethyl (M_{et}) structures are optimized imposing some geometrical constraints [$\angle\text{M-C}_\alpha\text{-C}_\beta=115.0^\circ$ and dihedral angle $\text{M-C}_\alpha\text{-C}_\beta\text{-H}=180.0^\circ$] to avoid any kind of interaction between the C_β-H of ethyl and metal fragments. The nature of the stationary points is characterized by vibrational frequency calculations. For comparisons and calibration, we have done optimization as well as frequency calculation at TZVP basis set using same method for the all first row transition metal-complexes and results are found to be similar.

[4.3] Results and Discussions

The formation of the agostic complex in β -hydride elimination reaction is preceded by the release of a solvent molecule or a labile ligand attached to the metal (Scheme 1, Step I). The stability of agostic structure is decided by many factors such as the oxidation number, electrophilicity around the metal center, spatial orientation of the ligands, number of d-electrons, and electron density around the M \cdots HC bond etc. The agostic

complexes can go on to form the metal-ethylene-hydride complex (Scheme 1, Step II) under favorable reaction conditions. The reaction profile for the β -hydride elimination reaction catalyzed by transition metal complexes is shown in the Figure 1.

Table 2: The relative energies (R.E.; Kcal/mol) between the neutral Metal-agostic (M_{agostic}) and Metal-ethyl (M_{ethyl}) (A), and Metal-ethylene-hydride (M_{eh}) and Metal-agostic (M_{agostic}) (B) are calculated at B3LYP/LANL2DZ level for the first (1R), second (2R) and third row (3R) of transition metal complexes. (3G, 4G, etc. indicates III-, IV-, groups respectively and 1R, 2R, 3R for the 1st, 2nd and 3rd row respectively).

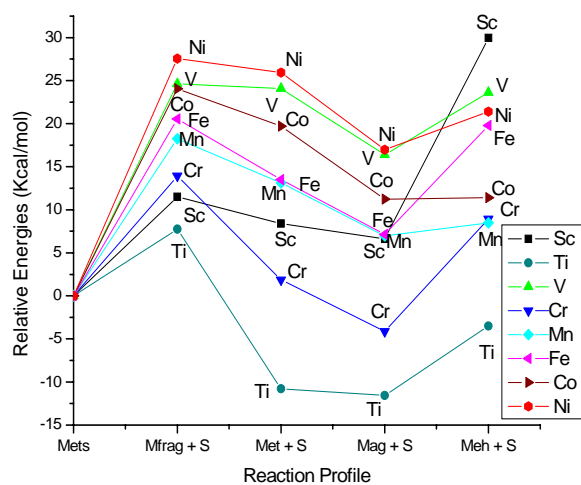
ΔE		3G	4G	5G	6G	7G	8G	9G	10G
		$M(\text{Cp})_2\text{Et}$	$M(\text{Cp})(\text{PH}_3)_2\text{Et}$	$M(\text{Cp})(\text{NO})\text{Et}$	$M(\text{PH}_3)_2(\text{Cp})\text{Et}$	$M(\text{PH}_3)_4\text{Et}$	$M(\text{PH}_3)_2(\text{NO})\text{Et}$	$M(\text{C}_6\text{H}_6)\text{Et}$	$M(\text{Cp})\text{Et}$
(A)	1R	-1.62	-0.09	-7.03	-5.13	-5.84	-5.92	-8.34	-9.00
$(E_{\text{agostic}} - E_{\text{ethyl}})$	2R	-2.12	-1.79	-7.20	-10.74	-8.03	-1.36	-2.04	-1.66
	3R	-2.98	0.76	-3.54	-9.31	-7.41	-0.89	-1.39	-1.35
(B)	1R	20.44	6.26	5.65	11.80	0.76	12.14	-0.93	2.78
$(E_{\text{product}} - E_{\text{agostic}})$	2R	16.96	-4.78	-5.30	-4.55	-8.22	4.26	-7.02	-1.89
	3R	15.74	-11.92	-15.45	-14.42	-15.86	-9.76	-20.17	-8.49

We have considered the endothermic dissociation of the solvent, i.e., $M_{\text{etS}} \rightarrow M_{\text{frag}} + S$, is the first step in the bond activation process. In the reaction profile (Figure 1), M_{frag} is a non-optimized structure, left behind while detaching the solvent (S) from the optimized saturated M_{ets} complex. The coordinatively unsaturated metal-fragment (M_{frag}) complex will always try to form a saturated stable metal-agostic (M_{ag}) complex. The formation of the agostic complex is prevented to get an estimate of the energy in

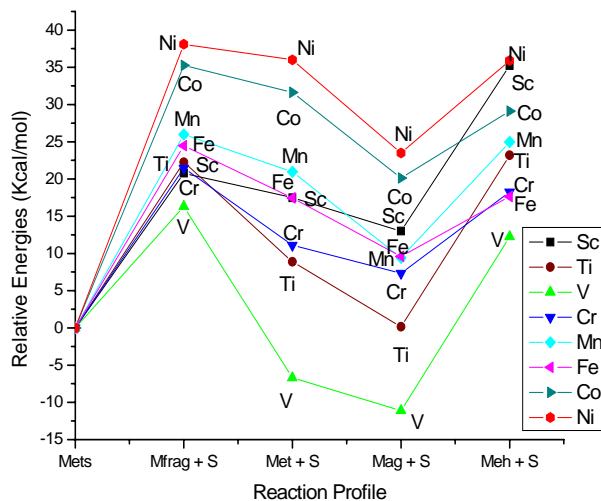
the absence of it, by optimizing the M_{frag} keeping $\angle MC_\alpha C_\beta = 115^\circ$ and dihedral $MC_\alpha C_\beta H = 180^\circ$. This structure is indicated by M_{et} . If the $\angle MC_\alpha C_\beta$ and dihedral $MC_\alpha C_\beta H$ angles are relaxed, the agostic complex M_{ag} is obtained. The agostic complex of varying stability is the intermediate on the way to the stable ethylene-hydride complex, M_{eh} . The reaction profile shows (Figure 1) that the extent of stabilization of metal-ethyl, metal-agostic and metal-ethylene hydride complexes are different for different transition metals. The variation of the preference of each of these complexes is discussed in the following sections.

Table 3: The relative energies (R.E.; Kcal/mol) between the cationic Metal-agostic ($M_{agostic}$) and Metal-ethyl (M_{ethyl}) (A), and Metal-ethylene-hydride (M_{eh}) and Metal-agostic ($M_{agostic}$) (B) are calculated at B3LYP/LANL2DZ level for the first (1R), second (2R) and third row (3R) of transition metal complexes. (3G, 4G, etc. indicates III-, IV-, groups respectively and 1R, 2R, 3R for the 1st, 2nd and 3rd row respectively).

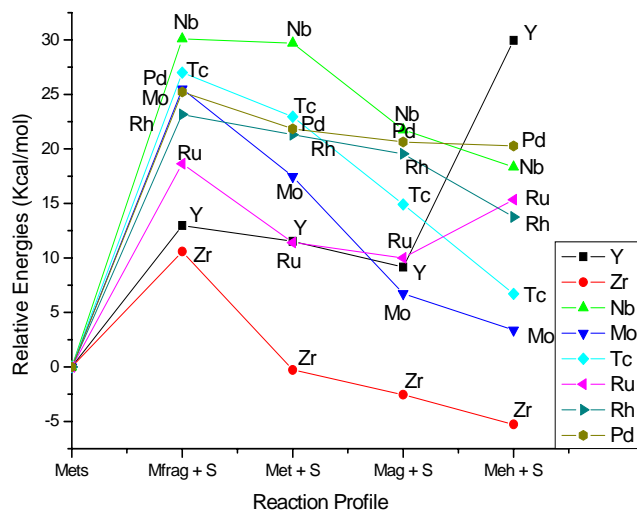
ΔE		3G [MCp(C ₆ H ₆)Et] ⁺	4G [MCp(NO)Et] ⁺	5G [MCp(PH ₃) ₂ Et] ⁺	6G [M(Cp) ₂ Et] ⁺	7G [M(PH ₃) ₂ (NO)Et] ⁺	8G [M(PH ₃) ₄ Et] ⁺	9G [M(Cp)(PH ₃)Et] ⁺	10G [M(C ₆ H ₆)Et] ⁺
(A)	1R	-3.99	-7.72	-3.52	-3.12	-10.82	-7.30	-11.26	-12.43
(E _{agostic}	2R	-4.46	-6.63	-5.69	-11.37	-11.10	-8.16	-6.57	-5.15
- E _{ethyl})	3R	-3.45	-2.76	-3.56	-8.11	-7.72	-10.96	-5.02	-5.84
(B)	1R	19.52	20.20	21.79	9.03	13.28	6.81	7.48	10.56
(E _{product}	2R	15.99	16.77	10.87	-4.06	7.78	-3.34	-0.55	5.70
- E _{agostic})	3R	16.27	14.93	0.23	-11.22	3.13	-12.29	-10.23	-8.56



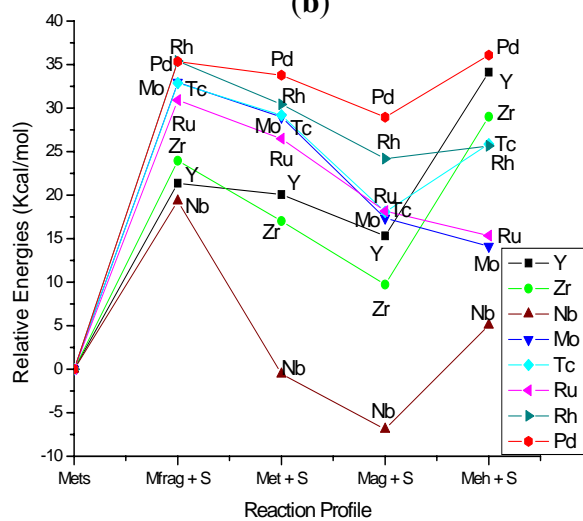
(a)



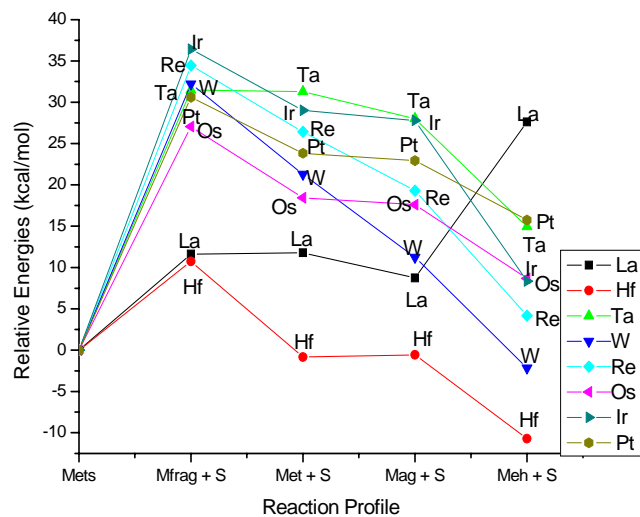
(b)



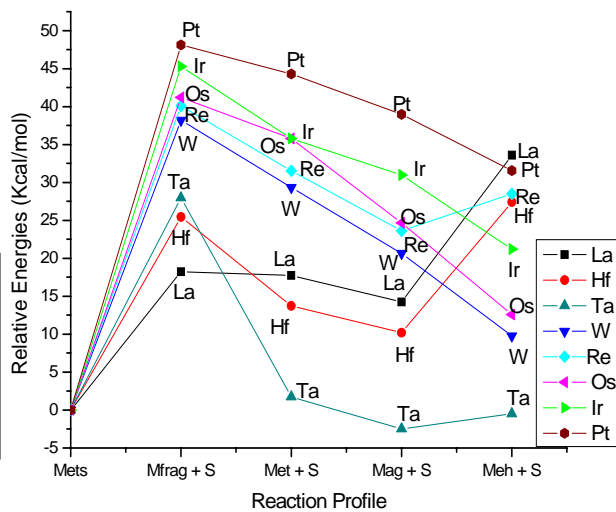
(c)



(d)



(e)



(f)

Figure 1: Reaction profile for the transition metal catalyzed reaction $M_{\text{ets}} \rightarrow M_{\text{frag}} + S \rightarrow M_{\text{et}} + S \rightarrow M_{\text{ag}} + S \rightarrow M_{\text{eh}} + S$; where S is the slovent (PH_3). The figure 1(a) and 1(b) are for neutral and cationic first row transition metal complexes. Similarly, 1(c) and 1(d) for second row and 1(e) and 1(f) for third row transition metal complexes. See text for details of the ligands.

Table 4: The relative energies (kcal/mol) between the metal-agostic and metal-ethylene-hydride and corresponding transition state calculated at the B3LYP/LANL2DZ level of theory. (3G, 4G, etc. indicates III-, IV-, groups respectively and 1R, 2R, 3R for the 1st, 2nd and 3rd row respectively).

			3G	4G	5G	6G	7G	8G	9G	10G
Neutral	1R	Agostic	0.00	0.00	0.00	0.00	0.00	0.00	0.00	0.00
		TS	20.78	16.17	13.95	13.09	3.82	14.63	7.84	8.23
		Product	20.44	6.26	5.65	11.80	0.76	12.14	-0.93	2.78
	2R	Agostic	0.00	0.00	–	–	–	0.00	0.00	–
		TS	17.77	13.20	–	–	–	14.13	7.48	–
		Product	16.96	-4.78	–	–	–	4.26	-7.02	–
	3R	Agostic	0.00	0.00	–	–	0.00	0.00	0.00	0.00
		TS	16.34	11.34	–	–	1.77	10.17	3.37	7.13
		Product	15.34	-11.92	–	–	-15.86	-9.76	-19.45	-8.49
Cationic	1R	Agostic	–	–	0.00	0.00	–	0.00	0.00	0.00
		TS	–	–	22.66	11.21	–	6.84	9.23	10.56
		Product	–	–	21.79	10.90	–	6.81	8.98	12.54
	2R	Agostic	0.00	–	0.00	–	–	0.00	0.00	0.00
		TS	16.49	–	15.26	–	–	2.66	4.31	9.78
		Product	15.99	–	10.87	–	–	-3.34	0.55	5.70
	3R	Agostic	0.00	–	0.00	0.00	0.00	0.00	0.00	0.00
		TS	17.13	–	11.09	1.22	4.53	1.29	0.22	2.56
		Product	16.27	–	0.23	-10.88	3.13	-12.08	-10.23	-8.56

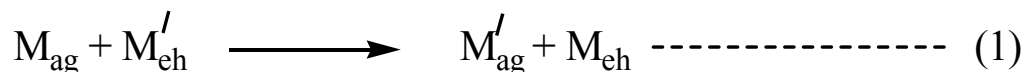


Table 5: Energies of the reaction (equation 1) calculated at B3LYP/LANL2DZ level of theory (Values are in parentheses calculated at BP86/LANL2DZ level of theory). Here, M is a first row transition metal and M' is the corresponding heavier group metals from the second (2R) and third row respectively (3R).

M' (Neutral)	M=Sc	Ti	V	Cr	Mn	Fe	Co	Ni
2R	3.48	11.04 (8.28)	10.96 (10.26)	16.35 (10.32)	9.73 (7.51)	7.88 (2.61)	6.09 (6.94)	4.67 (4.38)
3R	4.70	18.17 (13.96)	20.57	26.22	16.64 (13.48)	21.90 (14.17)	19.23 (18.65)	11.28
M' (Cationic)	M=Sc	Ti	V	Cr	Mn	Fe	Co	Ni
2R	9.73	3.43	10.93 (7.76)	13.10 (9.26)	7.79	10.16 (7.20)	6.93	4.86 (5.95)
3R	9.46	5.27	21.56 (15.80)	20.26 (14.98)	10.71	19.10 (14.92)	17.71	19.12 (18.39)

[4.3.1] Metal-ethyl, Metal-agostic and Metal-ethylene-hydride Complexes

The model metal-ethyl complexes considered are either 14 (Sc-, Ti-, and V-group complexes) or 16-electron complexes. These coordinatively unsaturated metal-ethyl complexes always have a tendency to form a saturated metal-agostic complex which could end up with a metal-ethylene-hydride complex in the process of β -hydrogen

addition to the metal center. In order to find out the feasibility of ethylene-hydride complex formation, we have calculated the potential energy barrier by locating the transition state (Table 4) between the metal-agostic and ethylene-hydride complexes. We have used isodesmic equation 1 to estimate the relative stabilities (Table 5) of metal-agostic and metal-ethylene-hydride complexes when the metal is substituted by its heavier group analogues.

The agostic stabilization energy is calculated as the energy difference between the agostic structure and the non-agostic structure ($\Delta E_{\text{agostic}} = E_{\text{ag}} - E_{\text{et}}$). We have plotted a series of graphs (Figure 2) which explain the agostic stabilization energy based on the energy difference between the metal vacant orbital and σ -CH orbital of the metal-ethyl complexes.

The relative stabilities between the M_{et} , M_{ag} and M_{eh} complexes are studied for two sets of transition metal complexes: neutral- and cationic so adjusted with ligands to be isoelectronic as mentioned under methods above. The agostic stabilization energy calculated for the neutral Sc(III)-complex is -1.62 kcal/mol (Table 2) which further increases in magnitude to -2.12 kcal/mol and -2.98 kcal/mol for the corresponding yttrium- and lanthanum-complexes respectively. The agostic stabilization (Figure 2) found to be more when the energy difference between the metal vacant orbital and σ -CH orbital of the metal-ethyl complex is less and vice versa. The neutral Sc-group agostic complexes are more stable in comparison to their corresponding ethylene-hydride complexes. The relative stabilization energies are -20.44, -16.96 and -15.74 kcal/mol for the corresponding Sc-, Y and La-complexes respectively. We have located

the transition state between the agostic and ethylene-hydride complexes. The potential energy barrier (Table 4) for the formation of ethylene hydride complex is 20.78, 17.77, and 16.34 kcal/mol for the Sc-, Y- and La-incorporated complexes respectively. So, the barrier for ethylene-hydride formation decreases down the group and the stability of ethylene-hydride complex increases. The transition state located for the conversion of the agostic complex to the ethylene-hydride complex is only about 0.34-0.81 kcal/mol higher than the product. This indicates a very late transition state; expected the geometry of the TS is very close to that of the product (Table 7). In all the complexes, the C_α - C_β bond distances (Table 6) in the agostic, TS, and ethylene-hydride complexes are within 1.545-1.539, 1.374-1.355, and 1.359-1.356 Å respectively. So, the C_α - C_β bond distance of TS is very close to the ethylene-hydride structure. The M-H bond distance in the TS (1.821-2.167 Å) is close to that in the ethylene-hydride (1.804-2.169 Å) complex than in the agostic (2.246-2.556 Å) complex. The C_β -H bond distances in the agostic, TS, and ethylene-hydride are 1.135-1.142, 2.107-3.253, and 2.565-3.587 Å respectively; supports the late transition state. The other structural parameters (\angle M- C_α - C_β , \angle C_α - C_β -H and dihedral angle M- C_α - C_β -H) do not change significantly (Table 6 and 7). So, these data are not discussed in the following sections. The relative stability of agostic and ethylene-hydride complexes within the same group is probed by the isodesmic equation 1. Endothermicity of this equation indicates that the lighter metals prefer agostic complexes and heavier metals prefer ethylene-hydride complexes. The endothermicity (3.48 kcal/mol) of the reaction (equation 1, when M=Sc and M'=Y, Table 5) shows that Sc-agostic complex is more preferred than the Y-agostic and Y-

ethylene-hydride complex more than the Ti-ethylene-hydride complexes. Similarly, the reaction energies 4.70 kcal/mol supports the stability of Sc-agostic complex over La-agostic and La-ethylene-hydride over Sc-ethylene-hydride complexes. Our results show that the agostic complex is the most preferred structure for the neutral Sc-group complexes. Available experiments support these results.^{11,22} The ground state β -agostic structure involving scandium, ScCp^*_2Et (1) has been identified by Burger *et al.* from the slow rate of ethylene insertion into the Sc-C bond (Scheme 2).¹¹ The rates of ethylene insertion into the Sc-C bond for Cp^*_2ScR ($\text{Cp}^* = (\eta^5\text{-C}_5\text{Me}_5)$, $\text{R} = \text{CH}_3$, CH_2CH_3 , $\text{CH}_2\text{CH}_2\text{CH}_3$) have been measured at -80°C by ^{13}C NMR and their second order rate constants ($\text{M}^{-1}.\text{s}^{-1}$) are as follows: $\text{R} = \text{CH}_3$, $8.1 (2) \times 10^{-4}$; $\text{R} = \text{CH}_2\text{CH}_3$, $4.4 (2) \times 10^{-4}$; $\text{R} = \text{CH}_2\text{CH}_2\text{CH}_3$, $6.1 (2) \times 10^{-4}$. They show the second order rates of ethylene insertion into the Sc-C bond are slowest when R is an $-\text{C}_2\text{H}_5$ group. So, the β -agostic complex reduces the approach of ethylene which in turn supports the extra stability of β -agostic complex. Two experimentally characterized Y-incorporated β -agostic complexes are also reported (Table 1) in the CCSD.²² To the best of our knowledge, the La-incorporated β -agostic complexes are not reported in the literature. Similarly, the agostic stabilization energy has been studied for the cationic Sc-group complexes. The stabilization energies are -3.99, -4.46 and -3.45 kcal/mol (Table 3) for the corresponding Sc-, Y- and La-complexes respectively. So, the agostic stabilization energy increases (Table 3) for the cationic set of the complexes in comparison to their neutral set of complexes (Table 2). For the cationic Sc-group complexes, the agostic form is the most preferred structure in relative to their ethylene-hydride complexes. The

agostic Sc-, Y- and La-incorporated complexes are stable by 19.52, 15.99 and 16.27 kcal/mol respectively than their ethylene-hydride complexes. We have located the transition state (TS) for the formation of ethylene-hydride complexes and the energy barriers (Table 4) are 16.49 and 17.13 kcal/mol for the cationic Y- and La-incorporated complexes respectively. The transition state located for the conversion of the agostic complex to the ethylene-hydride complex is only about 0.50-0.86 kcal/mol higher than the product. So, the energy of the transition state is more close to the product. This suggests a late transition state; expected the geometry of the TS is very close to that of the product (Table 7). In the Y- and La-incorporated complexes, the C_{α} - C_{β} bond distances (Table 7) are within 1.542-1.540, 1.383-1.384, and 1.363-1.361 Å for the agostic, TS, and ethylene-hydride complexes respectively. So, the C_{α} - C_{β} bond distance of TS is very close to the ethylene-hydride structure, supports the prediction of late transition state. Other structural parameters, such as M-H and C_{β} -H bond distances also support the late transition state. The M-H bond distance in the TS (1.981-2.128 Å) is more close to the product (1.959-2.106 Å) than in the agostic (2.334-2.548 Å). The C_{β} -H bond distances in the agostic, TS, and ethylene-hydride are 1.147-1.140, 2.038-2.001, and 2.611-2.718 Å respectively; confirms the late transition state. Though the agostic form is the most stable form for these complexes, the stability of the agostic complex decreases down the group. The high endothermicity values 9.73 kcal/mol (equation 1; when M=Sc, M'=Y, Table 5) favor the stability of cationic Sc-agostic complex over the Y-agostic and Y-ethylene-hydride over Sc-ethylene-hydride complex. Similarly, the reaction energy 9.46 kcal/mol (M=Sc, M'=La) supports the stability of Sc-agostic

The Intra-molecular Activation

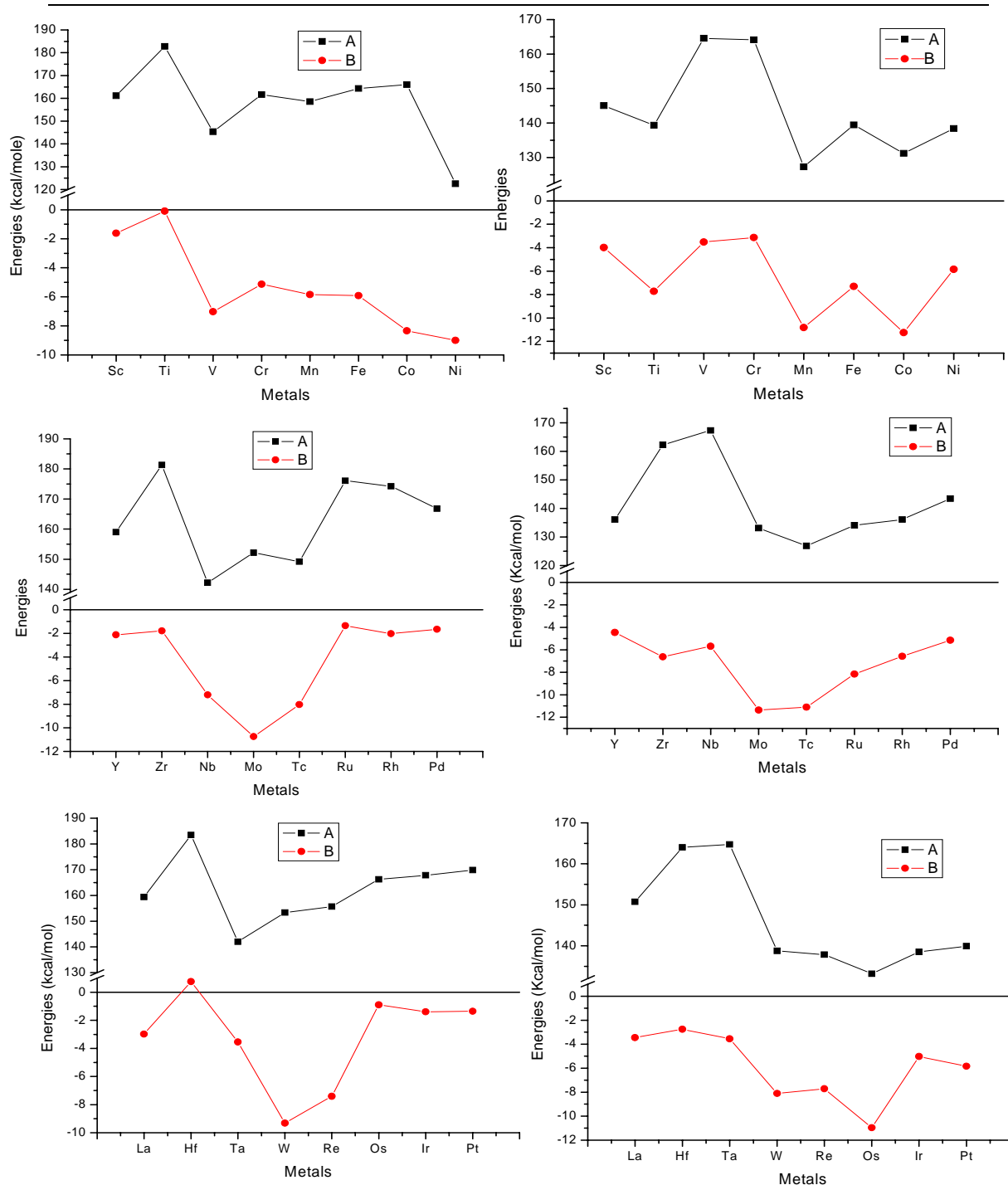


Figure 2: The energy difference between the metal vacant orbital and σ -CH orbital of the metal-ethyl complexes (A). The agostic stabilization energy for the transition metal complexes (B). The figures 2(a) and 2(b) are for neutral and cationic first row transition metal complexes. Similarly, 2(c) and 2(d) for second row and 2(e) and 2(f) for third row transition metal complexes.

complex over La-agostic as well as La-ethylene-hydride over Sc-ethylene-hydride complex. Surprisingly, our crystal structure database search did not list any β -agostic complex reported for the cationic Sc-group complexes. It could be due to the less synthetic effort directed for the cationic Sc-group complexes.

Among the neutral group-4 complexes, the agostic stabilization energy is maximum (-1.79 kcal/mol) for the neutral Zr(II)-complex. In this group, the agostic complex is the most stable structure for Ti- by 6.26 kcal/mol but ethylene-hydride complexes are lower in energy for the Zr- and Hf- complexes by 4.78 and 11.92 kcal/mol respectively. The transition state for the formation of ethylene-hydride complex decreases from Ti- to Zr-complexes by 2.97 kcal/mol which further decreases by 4.83 kcal/mol for the Hf-complexes. Obviously, the preference for the metal-ethylene-hydride complexes increases down the group. The TS of the Ti-complex is more close to the product (9.91 kcal/mol) than the agostic (16.17 kcal/mol) but agostic is close for the Zr- and Hf-complexes. The C_{β} -H bond distance in the transition state is an important geometrical parameter for confirming the nature of the TS whether close to the reactant or product. On the other hand, the C_{α} - C_{β} bond distances do not as it increases considerably when the metal's back-bonding and diffuseness of d-orbital's increases. The C_{β} -H bond distance in the TS decreases by 0.046 Å from Ti to Zr which further decreases by 0.047 Å from Zr to Hf complex. So the elongated C_{β} -H bond distances in the Zr- and Hf-supports the structure of TS close to the product. The reaction energy 10.96 kcal/mol (equation 1, M=Ti, M'=Zr) supports the stability of Ti-agostic complex over Zr-agostic and Zr-ethylene-hydride over Ti-ethylene-hydride complex. The reaction energy

increases to 20.57 kcal/mol (equation 1, M=Ti, M'=Hf) when the Zr-complexes are replaced by Hf-complexes. The preference of heavier group metal to form ethylene-hydride complex over their agostic can be explained on the basis of the metal's atomic radius and steric factor arises from the ligands. The larger size of the metal atom gives enough room to hold both the ethylene and hydride resulting ethylene-hydride complex. So, the tilting equilibrium between the agostic and ethylene-hydride complexes depend on the steric effect manifested by the ligands and the atomic radius of the metal involved. The preference for Ti-agostic complex has been reported experimentally.¹² The neutral β -agostic $\text{TiCl}_3(\text{dmpe})\text{Et}$ (**2**) complex, synthesized by Green *et al.*¹² is attributed to the inability of the complex to undergo β -hydride elimination reaction. There are two other β -agostic Ti-complexes reported in the literature.¹³⁻¹⁴

In the cationic Ti-group complexes, the agostic stabilization energy is maximum (7.72 kcal/mol) for the Ti-complex which decreases in magnitude to 6.63 kcal/mol for the Zr-complex and further decreases to 2.76 kcal/mol for the Hf-complex. In group 4 metals, the agostic stabilization energy is higher for the cationic set of complexes (Table 3) in comparison to their neutral-set (Table 2). The stability of metal-agostic complexes increases as the metal's electrophilic nature increases. The relative stabilities between the agostic and ethylene-hydride complexes show that the agostic complex is stable by 20.20, 16.77, and 14.93 kcal/mol for the Ti-, Zr-, and Hf-complexes respectively. So, the relative stabilities show that the metal-agostic form is the most stable form for these group complexes (Table 3) but the stability of metal-ethylene-hydride complex increases for heavier group complexes. In these cationic group 4 complexes, we could

Table 6: Selected geometric parameters of the neutral structures optimized at B3LYP/LANL2DZ. (3G, 4G, etc. indicates III-, IV-, groups respectively and 1R, 2R, 3R for the 1st, 2nd and 3rd row respectively).

Bond (Å)	Compound		3G	4G	5G	6G	7G	8G	9G	10G
	Oxidation State		+3	+2	+1	+2	+1	0	+1	+2
	Valance Electrons		16	16	16	18	18	18	18	18
C _β -H	Agostic	1R	1.135	1.122	1.155	1.148	1.172	1.145	1.171	1.171
		2R	1.142	1.134	1.167	1.166	1.184	1.125	1.141	1.144
		3R	1.142	1.129	1.171	1.174	1.196	1.128	1.160	1.115
	TS	1R	2.107	1.694	1.966	1.934	1.581	1.784	1.668	1.783
		2R	2.050	1.648	-	-	-	1.692	1.558	-
		3R	3.253	1.601	-	-	1.434	1.587	1.432	1.514
	Hydride	1R	2.565	2.731	2.925	2.285	2.215	2.081	2.424	2.543
		2R	2.698	3.123	3.330	2.399	2.388	2.510	2.553	2.675
		3R	3.587	3.108	3.130	2.407	2.418	2.530	2.464	2.592
M-H	Agostic	1R	2.246	2.264	1.971	1.927	1.845	1.931	1.761	1.763
		2R	2.370	2.287	2.071	2.006	1.949	2.322	2.079	2.083
		3R	2.556	2.335	2.069	2.003	1.944	2.336	2.017	2.444
	TS	1R	1.821	1.712	1.639	1.583	1.604	1.550	1.491	1.481
		2R	2.023	1.891	-	-	-	1.674	1.612	-
		3R	2.167	1.876	-	-	1.774	1.749	1.692	1.660
	Hydride	1R	1.804	1.733	1.616	1.588	1.596	1.517	1.473	1.465
		2R	2.007	1.900	1.766	1.703	1.687	1.672	1.532	1.550
		3R	2.169	1.874	1.763	1.716	1.703	1.707	1.571	1.560
C _α -C _β	Agostic	1R	1.545	1.549	1.525	1.523	1.524	1.528	1.515	1.516
		2R	1.546	1.549	1.523	1.518	1.523	1.543	1.540	1.527
		3R	1.539	1.560	1.538	1.524	1.530	1.553	1.541	1.551
	TS	1R	1.374	1.460	1.392	1.417	1.455	1.436	1.439	1.421
		2R	1.381	1.470	-	-	-	1.442	1.449	-
		3R	1.355	1.486	-	-	1.484	1.470	1.479	1.466
	Hydride	1R	1.359	1.457	1.397	1.413	1.424	1.433	1.427	1.409
		2R	1.359	1.483	1.413	1.443	1.436	1.438	1.431	1.533
		3R	1.356	1.509	1.432	1.466	1.452	1.466	1.461	1.439
M-C _α -C _β	Agostic	1R	88.0	90.2	83.1	81.4	78.809	83.103	79.5	79.073
		2R	88.8	88.1	84.1	82.6	80.323	93.142	87.0	87.226
		3R	91.5	89.9	83.8	82.5	79.935	92.881	85.3	97.639
C _α -C _β -H	Agostic	1R	113.8	112.8	112.7	112.1	113.0	111.4	110.5	111.4
		2R	114.4	113.6	112.9	111.9	113.7	111.6	114.1	111.3
		3R	114.4	113.6	113.2	111.8	113.9	112.0	110.9	112.0

not locate any transition state between the agostic and ethylene-hydride complexes. The endothermicity values 3.43 kcal/mol (equation 1; M=Ti, M'=Zr) and 5.37 kcal/mol

(M=Ti, M'=Hf) show the cationic Ti-agostic complex preferred over their heavier group metal-agostic complexes and Hf-ethylene-hydride complex preferred over their lighter group analogues. To the best of our knowledge, there are two examples²³⁻²⁴ (Table 1) from the cationic Zr-complexes where $[\text{Zr}(\text{Cp}^*)_2(\text{PMe}_3)\text{Et}]^+$, identified as a ground state structure and believed to be a catalyst resting state during the polymerization reaction.²³

The neutral vanadium(I)-complexes has -7.03 kcal/mol agostic stabilization energy which increases in magnitude to -7.20 kcal/mol for Nb(I)-complex and decreases to -3.54 kcal/mol for the Ta(I)-complex. The agostic form is the most stable form for the neutral vanadium complexes but ethylene-hydride complexes are lower in energy by 5.30 and 15.45 kcal/mol for the Nb- and Ta-complexes respectively. We have located the transition state between the V-agostic and V-ethylene-hydride complexes. The high barrier 13.09 kcal/mol predicts the transition state to be close to the product and the difference is 8.30 kcal/mol. The $\text{C}_\alpha\text{-C}_\beta$ and $\text{C}_\beta\text{-H}$ bond distances in the TS (1.392, 1.966 Å) are more close to the ethylene-hydride (1.397, 2.925 Å) than to the agostic (1.525, 1.155 Å) complex. Again, the high endothermicity (10.96 kcal/mol, M=V, M'=Nb) and 20.57 kcal/mol) of the reaction (equation 1) favors the V-agostic complex in comparison to the Nb-agostic and Nb-ethylene-hydride over V-ethylene-hydride. The endothermicity value increases to 20.57 kcal/mol when Nb- is replaced by Ta. Though our study shows that the metal-ethylene-hydride complex is the most stable form for the Nb- and Ta-incorporated complexes but there are two experimentally characterized β -agostic complexes $[(\text{Tp}^{\text{Me}_2}\text{NbCl}(i\text{-Pr})(\text{PhC}\equiv\text{CMe})$ and $[\text{P}_2\text{N}_2]\text{Ta}(\text{C}_2\text{H}_4)(\text{CH}_2\text{CH}_3)]$]^{25,28} are reported in the literature. This could be due to the presence of bulkier ligands which

reduce the available space around the metal center to hold an ethylene and hydride group simultaneously.

Similarly, the cationic V-group complexes are studied in greater details. The agostic stabilization energies are -3.52, -5.69 and -3.56 kcal/mol for the V-, Nb- and Ta-complexes respectively. The relative energies between agostic and ethylene-hydride complex show that V-, Nb and Ta-agostic complexes are lower in energy by 21.79, 10.87, and 0.23 respectively. So, the agostic form is the relatively most stable form for these set of complexes as previously seen in the cationic Sc- and Ti-group complexes. The energy barriers for the conversion of the agostic complex to the ethylene hydride complex (Table 4) are 22.66, 15.26 and 11.09 kcal/mol for the V-, Nb- and Ta-complexes respectively. The energy barrier decreases considerably for heavier group metal complexes as seen in the earlier group complexes. The relative energies between the TS and product is maximum 10.86 kcal/mol for Ta which decreases to 4.39 kcal/mol for Nb and further decreases to 0.87 kcal/mol for the V. So, the vanadium-TS energy is only 0.87 kcal/mol higher than the product, predicts a late transition state. The C_{β} -H and C_{α} - C_{β} bond distances in TS (2.028, 1.424 Å) is close to the product (2.434, 1.420 Å) than to the agostic (1.128, 1.534 Å), supports such prediction. The C_{β} -H and C_{α} - C_{β} bond distances in the Niobium-TS (1.789, 1.454 Å) structure is close to the product (2.421, 1.443 Å) than to the agostic (1.142, 1.540 Å). Though the niobium-TS energy is close to the product but it has higher energy difference in comparison to the V-complex. Such energy differences have been reflected in their geometrical parameters too. The difference in the C_{β} -H bond length between the TS and agostic is 0.900 Å for V, 0.647

for Nb and 0.526 Å for Ta. So, the Niobium-TS structure is close to the product but little bit shifted towards the agostic structure and tantalum-TS shifted further towards the agostic. The high reaction energy 10.93 kcal/mol (equation 1; M=V, M'=Ta; Table 5) shows that cationic V-agostic and Nb-ethylene-hydride complex are stable over Nb-agostic and V-ethylene-hydride respectively. The reaction energy increases to 21.56 kcal/mol when the V-complexes are compared with the Ta-complexes. To the best of our knowledge, the cationic V-group β -agostic complexes are not yet characterized experimentally.

The neutral Cr-group complexes show similar kind of trend observed in the previous group complexes. The agostic stabilization energies are considerably high and the values are -5.13, -10.74, and -9.31 kcal/mol for the Cr-, Mo-, and W-complexes respectively. The agostic complex is the most stable structure for Cr- by 11.80 kcal/mol (Table 2) but ethylene-hydride complexes are lower in energy for the Mo- and W-complexes by 4.55 and 14.42 kcal/mol respectively. So, the stability of ethylene-hydride complexes increases from Cr to W, as seen in the previous group complexes. We have located the transition state for the Cr-complexes and the barrier (Table 4) is 13.09 kcal/mol. The transition states located for the conversion of the agostic to the ethylene hydride complex is only 1.29 kcal/mol higher than the product. This indicates a very late transition state; expected the geometry of the TS is very close to that of the product. The C $_{\beta}$ -H and C $_{\alpha}$ -C $_{\beta}$ bond distances in TS (1.934, 1.417 Å) is more close to the product (2.285, 1.413 Å) than to the agostic (1.148, 1.523 Å), supports the prediction of late transition state. The high reaction energies (equation 1, Table 5) 16.35 (M=Cr, M'=Mo)

Table 7: Selected geometric parameters of the cationic structures optimized at B3LYP/LANL2DZ. (3G, 4G, etc. indicates III-, IV-, groups respectively and 1R, 2R, 3R for the 1st, 2nd and 3rd row respectively).

Bond (Å)		Compound	3G	4G	5G	6G	7G	8G	9G	10G
		Oxidation State	+3	+2	+3	+4	+1	+2	+3	+2
		Valance Electrons	16	16	16	18	18	18	18	18
C _β -H	Agostic	1R	1.141	1.141	1.128	1.143	1.168	1.170	1.173	1.173
		2R	1.147	1.146	1.142	1.188	1.180	1.187	1.168	1.148
		3R	1.140	1.147	1.144	1.206	1.190	1.223	1.190	1.177
	TS	1R	-	-	2.028	1.787	-	1.727	1.817	1.955
		2R	2.038	-	1.789	-	-	1.555	1.615	1.815
		3R	2.001	-	1.670	1.436	1.720	1.444	1.452	1.574
	Hydride	1R	2.560	2.857	2.434	2.084	2.210	2.081	2.080	2.511
		2R	2.611	3.055	2.421	2.306	2.293	2.299	2.342	2.590
		3R	2.718	3.011	2.802	2.334	2.309	2.399	2.374	2.615
M-H	Agostic	1R	2.197	2.095	2.131	2.015	1.852	1.842	1.512	1.766
		2R	2.334	2.255	2.181	1.977	1.180	1.932	1.962	2.075
		3R	2.548	2.234	2.160	1.952	1.973	1.897	1.945	1.961
	TS	1R	-	-	1.597	1.557	-	1.543	1.486	1.447
		2R	1.981	-	1.760	-	-	1.683	1.622	1.549
		3R	2.128	-	1.781	1.775	1.727	1.746	1.700	1.615
	Hydride	1R	1.766	1.649	1.611	1.540	1.561	1.526	1.473	1.425
		2R	1.959	1.812	1.756	1.663	1.663	1.617	1.562	1.513
		3R	2.106	1.811	1.476	1.679	1.685	1.650	1.591	1.529
C _α -C _β	Agostic	1R	1.540	1.532	1.534	1.526	1.514	1.520	1.512	1.501
		2R	1.542	1.538	1.540	1.514	1.518	1.513	1.515	1.509
		3R	1.540	1.548	1.549	1.520	1.528	1.517	1.525	1.516
	TS	1R	-	-	1.424	1.413	-	1.425	1.413	1.404
		2R	1.383	-	1.454	-	-	1.450	1.438	1.412
		3R	1.384	-	1.472	1.476	1.422	1.476	1.471	1.446
	Hydride	1R	1.362	1.384	1.420	1.395	1.379	1.401	1.398	1.396
		2R	1.363	1.384	1.443	1.422	1.379	1.410	1.404	1.403
		3R	1.361	1.393	1.476	1.438	1.384	1.428	1.425	1.425
M-C _α -C _β	Agostic	1R	87.0	83.6	88.1	83.5	79.5	80.2	78.4	79.7
		2R	88.4	86.0	87.2	81.3	81.4	81.4	82.7	87.8
		3R	91.8	86.2	86.5	80.5	81.0	79.7	82.1	83.9
C _α -C _β -H	Agostic	1R	114.2	115.8	112.8	112.7	113.1	113.0	111.9	111.0
		2R	114.6	116.0	113.3	113.5	111.7	112.5	112.2	110.8
		3R	114.5	115.7	113.3	113.6	113.7	113.3	112.0	111.2

and 26.22 kcal/mol ($M=Cr$, $M'=W$) favor the Cr-agostic complex over the heavier group (Mo-, W-) analogues and W-ethylene-hydride over lighter group (Cr-, Mo) analogues. Three Mo-incorporated β -agostic complexes are reported in the CCSD where the β -H comes from an acyl $[-C(=O)CH_3]$ group. To the best of our knowledge, there are no experimentally characterized Cr- and W-incorporated β -agostic complexes reported in the literature but the equilibrium between the metal-agostic and metal-ethylene-hydride complexes reported for this group of complexes. Wrighton and co-workers^{7d} observed that near UV radiation on $(\eta^5-C_5R_5')M(CO)_3R$ ($R' = H, Me$; $M = Mo, W$; $R = CH_3, C_2H_5, n\text{-pentyl}$) results in efficient dissociative loss of CO. The resulting 16 valence electron species from CO loss has been characterized by infrared spectroscopy. For the R groups having β -hydrogens, optical and infrared spectroscopy give evidence for a species which is not completely coordinatively unsaturated and is proposed to be an intermediate precursor for β -hydrogen transfer. This species does not react rapidly with CO or PPh_3 at the same reaction condition as do the $(\eta^5-C_5R_5')M(CO)_2CH_3$. On warming β -hydrogen transfer takes place leading to a metal-alkene-hydride. This β -hydrogen transfer is proposed to involve a pre-equilibrium between the 16-valence-electron species and a *cis*-alkene-hydride complex that isomerizes to the *trans*-alkene-hydride in the rate-determining step. Similar results are also obtained⁴⁵ with Fe- and Ru-metal complexes.

The agostic stabilization energy in the cationic Cr-group complexes is highest (11.37 kcal/mol) for Mo- and lowest (3.12 kcal/mol) for Cr- complex. The Cr-agostic complex is relatively stable by 9.03 kcal/mol than the ethylene-hydride complex but the latter

form is stable by 4.06 and 11.22 kcal/mol for the Mo- and W-complexes respectively. The transition states located for the conversion of the agostic complex to the ethylene-hydride complex for the Cr- and W-metals. The energy barrier is 11.21 kcal/mol for Cr- and 1.22 kcal/mol for W-complexes. The chromium-TS energy is 2.18 kcal/mol higher than the product whereas tungsten-TS is 12.44 kcal/mol higher than the product. So we predict a late transition state for Cr- but early transition state for W-complexes. In the chromium complexes, the C β -H bond distances are 1.143, 2.084, 2.015 Å in the agostic, TS, and product respectively. So the C β -H bond distance in the TS is close to the product, supports the late transition state. In the W-complexes, the C β -H bond distances are 1.206, 1.436, 2.334 Å in the agostic, TS, and product respectively. Here, the C β -H bond distance in the TS is close to the agostic, supports an early transition state. The cationic Cr-group complexes show (equation 1) that the stability of Cr-agostic complex and Mo-ethylene-hydride is preferred over Mo-agostic and Cr-ethylene-hydride complex by 13.10 kcal/mol. The value increases to 20.16 kcal/mol when Mo-complexes are replaced by the heavier group analogues. Our CCSD search did not show any cationic Cr-group β -agostic structure reported in the literature.

For the neutral Mn-group complexes, the agostic stabilization energies are -5.84, -8.03 and -7.41 kcal/mol for the Mn-, Tc-, and Re-complexes respectively. So, the stabilization energy increases down the group. The trend is same which has observed in their earlier group metal-complexes too. The relative stabilities show the Mn-agostic complex is stable by 0.76 kcal/mol than the ethylene-hydride form. The down the group Tc- and Re-complexes prefer their ethylene-hydride form by 8.22 and 15.86 kcal/mol

respectively. We have located corresponding transition state for the Mn- and Re-complexes and the energy barriers are 3.82 and 1.77 kcal/mol respectively. The low barriers of ethylene-hydride formation support their kinetic stability in addition to their thermodynamic stability. The energy of the transition state is more close to the product with a difference of 3.06 kcal/mol in the case of Mn-complex, while it is more close to reactant with a difference of 1.77 kcal/mol in the case of Re- complex. This is further supported by the similarities in the geometrical parameters of transition state with agostic or ethylene hydride complexes. For Mn- complex, the C_{β} -H bond distances (Table 6) changes from 1.172 to 1.581 to 2.215 Å while going from agostic to TS to ethylene-hydride complexes respectively. The C_{α} - C_{β} and M-H distances (Table 6) in agostic (1.530, 1.845 Å), TS (1.455, 1.604 Å) and product (1.424, 1.596 Å) show that the TS is more close to the product. But for Re- complex, the C_{β} -H bond distances changes from 1.196 to 1.434 to 2.418 Å from agostic to TS to product respectively. The C_{β} -H bond distance in the TS is more close to the agostic structure than to the product, supports the prediction of early transition state. The high endothermicity values 9.73 and 16.64 kcal/mol indicate that lighter metals prefer agostic complex and heavier metals prefer ethylene-hydride complexes, as seen in the previous group complexes.

The agostic stabilization energy for the cationic Mn-group complexes is considerably high in comparison to the earlier cationic group complexes. The stabilization energy is maximum (-11.10 kcal/mol) for Tc-complex and minimum (-7.72 kcal/mol) for Re-complex. The agostic complex is the most stable structure for the cationic Mn-group complexes. The relative stabilities between the agostic and ethylene-hydride complexes

show the stability of Mn-agostic is maximum (13.28 kcal/mol) and minimum (3.13 kcal/mol) for Re- complexes. We have found the transition state for Re-complex and the barrier is 4.53 kcal/mol. The low barrier of transition state shows that TS is more close to that of the agostic complex, which is further supported by the C β -H bond distances of TS (1.720 Å) which is close to the agostic (1.190 Å) than that of the ethylene hydride 2.309 Å. The endothermicity value (equation 1) 7.79 kcal/mol (M=Mn, M'=Tc) supports the preference in stability of Mn-agostic complex over Tc-agostic and Tc-ethylene hydride over Tc-agostic complex. Similarly, the reaction (equation 1) energy 10.71 kcal/mol (M=Mn, M'=Re) supports the stability of Mn-agostic complex over Re-agostic and Re-ethylene hydride over Re-agostic complexes. An agostic structure with manganese, (η^5 -pentadienyl)Mn[(Me₂PCH₂)₃CMe]⁺PF₆⁻ (**3**), has been experimentally identified as a ground state, where as the product η^5 -pentadienely-metal-hydride is the ground state structure⁴⁶ for the corresponding rhenium system [(η^5 -2,4-dimethyl-pentadienyl)Re[(Me₂PPh)₃]⁺BF₄], supports our results.

Among in the neutral Fe-group complexes, the agostic stabilization energy (Table 2) is maximum (-5.92 kcal/mol) for Fe-complex and minimum (-0.89 kcal/mol) for Os-complex. So, in this group, the agostic stabilization energy decreases for down the group. The relative stabilities calculated between metal-agostic and metal-ethylene-hydride complexes show that Fe- and Ru-agostic complexes are stable by 12.14 and 4.26 kcal/mol respectively but Os-ethylene-hydride stable by 9.76 kcal/mol. We have located the transition state for Fe-, Ru- and Os-complexes. The energy barrier for the formation of Fe-ethylene-hydride complex is 14.63 kcal/mol which decreases to 14.13

for Ru-complexes and further decreases to 10.17 kcal/mol for the Os-complexes. The iron-TS energy is higher by 2.49 kcal/mol than the product; expecting a late transition state. The difference increases in magnitude to 9.87 for Ru- and 19.93 kcal/mol for Os-transition state. So, the Ru and Os-transition state will be more close to the reactant than the product. In the Fe-complexes, the C_{β} -H bond distances in TS (1.784 Å) is close to the product (2.081 Å) than to the agostic (1.145 Å). Similarly the C_{α} - C_{β} and M-H (Table 6) distances support a late transition state. In the Ru-complexes, the C_{β} -H bond distances in TS (1.692 Å) is close to the agostic (1.125 Å) than to the product (2.510 Å); supports a early transition state. The C_{β} -H bond distances in the Os-transition state (1.587 Å) is more close to the agostic (1.128 Å) than in the Ru-complexes. The trend is similar as seen in the previous group complexes. The isodesmic equation 1 shows that the Fe-agostic and Ru-ethylene-hydride complex is stable by 7.88 kcal/mol in comparison to their Fe-ethylene-hydride and Ru-agostic complexes respectively. Similarly, the endothermicity value increases to 21.90 kcal/mol when Fe- is replaced by Os- metal atom in their complexes.

For the cationic Fe-group complexes (Table 3), the agostic stabilization energies for Fe, Ru- and Os-complexes are -7.30, -8.16 and -10.96 kcal/mol respectively. So, among in these group complexes, the stabilization energy increases for heavier group metal complexes. The relative stabilities between agostic and ethylene-hydride complexes show that Fe-agostic is most stable by 6.81 kcal/mol but Ru- and Os-ethylene-hydride complexes are stable by 3.34 and 12.29 kcal/mol respectively. The transition states located between theses complexes show that the energy barrier for the ethylene hydride

formation is maximum 6.84 kcal/mol for Fe- which decrease to 2.66 kcal/mol for Ru- and further decreases to 1.29 kcal/mol for Os-complexes. The relative energies between the TS and product increase for down the group complexes. So, we predict a late TS for lighter metals and early TS for the heavier group analogues. The trend is similar to the neutral Fe-group complexes and explanations can be given similarly. The isodesmic equation 1 used for comparing the relative stabilities between the complexes of lighter and heavier group elements show that the combination of cationic Fe-agostic and Ru-ethylene-hydride complexes preferred over the combination of cationic Ru-agostic complex and Fe-ethylene-hydride complexes by 10.16 kcal/mol. The endothermicity value increases to 19.10 kcal/mol when Ru-complexes are replaced by Os-complexes. Even though the iron β -agostic complex, $[\text{Fe}(\text{dmpe})_2(\text{CH}_2\text{CH}(\text{iPr}))^+]$ (**4**), has reported, no information is available on the β -hydride elimination reaction and nothing has been discussed about its ground state structure.¹⁵ Tolman,⁴⁷ and Ittel *et al.* studied⁴⁷ the C-H bond cleavage at sp^2 carbon while reaction of iron and ruthenium with anthracene suggests that the 1,3-diene structure is more stable thermodynamically than the anthryl hydride for Fe. The reverse is true for Ru, which again supports indirectly that the bond activation process is more feasible in presence of second or third-row transition metals in comparison to first row.

The agostic stabilization energies for the neutral Co-, Rh- and Ir-complexes are -8.34, -2.04, and -1.39 kcal/mol respectively. The stabilization energy decreases from Co- to Ir-complexes. The relative energies between the agostic and ethylene-hydride shows that the ethylene-hydride complex is the most stable structure by 0.93, -7.02 and -20.17

kcal/mol for the Co-, Rh- and Ir-complexes respectively. The energy barrier for the Co-ethylene-hydride complex formation is 7.84 kcal/mol and decreases to 7.48 kcal/mol for Rh-complex which further decreases to 3.37 kcal/mol for the Ir-complexes. The energy of the cobalt-TS is close to the agostic (7.84 kcal/mol) than to the product (8.77 kcal/mol). Similarly, the energy of Rh- and Ir-TS complexes is more close to the agostic by 7.48 and 3.37 kcal/mol than to the product by 14.50, and 23.54 kcal/mol respectively. We predicts a early transition state for all these complexes and the TS structure will be more close to the corresponding agostic for Ir- than to the Rh- than to the Co-. This is supported by the $\Delta C_{\beta-H}$ [$C_{\beta-H} = C_{\beta-H}(TS) - C_{\beta-H}(agostic)$] bond distances. The $\Delta C_{\beta-H}$ value is maximum 0.497 Å for Co-, decreases to 0.417 Å for Rh- and minimum for 0.272 Å for Ir-; supports the early transition for heavier group and late transition for lighter group analogues. The endothermicity values (equation 1) are 6.09 and 19.23 kcal/mol indicating the preferred stability of Co-agostic complex over Rh- and Ir-agostic complexes. Similarly the Rh- and Ir-ethylene-hydrides are more stable than the Co-ethylene-hydride complexes.

The agostic stabilization energy decreases as -11.26, -6.57 and -5.02 kcal/mol for the cationic Co-, Rh- and Ir-complexes respectively (Table 3). The Co-agostic form is relatively most stable form over its ethylene-hydride form by 7.48 kcal/mol but the ethylene-hydrides are relatively most stable complexes for Rh- and Ir- by 0.55 and 10.23 kcal/mol respectively. The transition states between the agostic and ethylene-hydride complexes are located and the energy barriers are 9.23, 4.31 and 0.22 kcal/mol for the Co-, Rh- and Ir-complexes respectively. Similar trend has been found in the

neutral-Co-group complexes too. Similar kind of explanations can be given here. The high endothermicity values (equation 1) 6.93 and 17.71 kcal/mol corresponds to the stability of Co-agostic complex in comparison to their heavier group analogues respectively. Our theoretical results are close to the experimental results. Brookhart *et al.* experimentally calculated^{17b} the free energies of activation of $[M(C_5R_5)(C_2H_4)(CH_3CH_2-\mu-H)]^+$ ($R=H, CH_3$; $M=Co, Rh$) complex for the conversion of agostic to ethylene-hydride complex. The barrier is 5.3 kcal/mol for Co but decreases to 3.7 for the Rh-complexes. They observed^{17b} that the energy difference between the agostic and the olefin-hydride structure is higher for the Co-complex and the difference is very small for the corresponding rhodium system. Such observations lead to conclude that the second row metal complex will favor terminal-hydride structures relative to their first row analogues. Later, they found third row metal complex will favor terminal-hydride structures relative to their second row analogues. This trend has been further supported from the activation barrier of alkyl migration reaction in the metal hydride complexes where Brookhart *et al.* proposed¹⁸ that the barrier for alkyl migration reaction is lower in the bridged-hydride (agostic type) rather than in the terminal hydride complexes. The equilibrium between 18 electron metal-agostic and metal-ethylene-hydride systems was first found by Brookhart *et al.* in the $[Co(C_2H_4-H)(\eta^5-C_5H_5)(C_2H_4)]BF_4$ complex.^{17a} They interpreted^{17a} the β -agostic cobalt-complex $[Co(Cp^*)(C_2H_4)Et]^+$ (**5**) in terms of a ground state with an agostic ethyl group where as NMR data on the related rhodium $[C_5H_5Rh(PR_3)(C_2H_4)H]^+$, ruthenium $[C_6H_6Ru(PR_3)(C_2H_4)H]^+$, osmium $[C_6H_6Os(PR_3)(C_2H_4)H]^+$, and

$\text{Os}(\text{PR}_3)_2(\text{CO})\text{Cl}(\text{C}_2\text{H}_4)\text{H}]$ complexes have been interpreted in terms of hydrido olefin complexes.⁴⁸

In the neutral Ni-group complexes (Table 2), the agostic stabilization energy is maximum (-9.00 kcal/mol) for Ni-complex and minimum (-1.35 kcal/mol) for Pt-complex. The stabilization energy decreases down the group. The relative stabilities between the agostic and ethylene-hydride show that Ni-agostic is the most stable structure by 2.78 kcal/mol but Pd- and Pt-ethylene-hydride complexes are more stable by 1.89 and 8.49 kcal/mol respectively. The transition states located for Ni- and Pt-complexes and the energy barriers are 8.23 and 7.13 kcal/mol respectively. The TS are predicted to be a late transition state and can be confirmed from the geometrical parameters. The results are similar as seen in the previous group complexes. The isodesmic equation 1 gives endothermicity values of 4.67 and 11.28 kcal/mol in support of lighter favor agostic and heavier metal prefers ethylene-hydride complexes.

For the cationic Ni-group complexes, the agostic stabilization energies are -12.43, -5.15, and -5.84 kcal/mol for the Ni-, Pd- and Pt-complexes respectively. The relative stabilities between the agostic and ethylene-hydride complexes show Ni- and Pd-agostic complexes are stable by 10.56 and 5.70 kcal/mol respectively but Pt-ethylene-hydride is stable by 8.56 kcal/mol. The transition states between agostic and ethylene-hydride complexes are calculated for these group complexes. The transition state energy barriers for the cationic Ni-, Pd- and Pt-incorporated complexes are 12.54, 9.78 and 2.56 kcal/mol respectively. The barrier decreases down the group. Same trend has been found in the previous group complexes. The explanations are similar. The isodesmic

equation 1 used for the relative stabilities between the lighter and heavier group complexes show that the cationic Ni- and Pd-ethylene-hydride complexes preferred over the Pd-agostic and Ni-ethylene-hydride complexes by 4.86 kcal/mol. The endothermicity increases to 19.12 kcal/mol when Pd-complexes are replaced by Pt-complexes. Our results are similar to the experimental results. Spencer *et al.* characterized¹⁹ $[M(L_2)(Et)]^+$ (where M= Ni, Pd) (**6**) the β -agostic metal-ethyl complex as stable structures. However, the alkene-hydride form is found to be thermodynamically more stable for the Pt-complex. Even though agostic structures are lower in energy for Ni and Pd-system, the activation barrier to β -hydride addition reaction is much lower for Pd than the Ni-system. Kougut *et al.* also identified that the neutral Ni-alkyl β -agostic complex $[(Me_2NN)Ni(Et)]$ is a ground state during the ethylene oligomerization catalysis, lowering in energy than the hydride complex.²⁰

The extent of agostic stabilization is different for different transition metal complexes. This is due to the various combination of ligands, charge and oxidation state present in the metal center. Though the ligand combinations around the metal centers vary across the periodic table but each and every metals form a stable agostic complex. So, this is the ligands combinations which bring the frontier levels of any transition metal fragment close to that of the C_{β} -H bond so that the formation of the agostic complex is possible.

In the polymerization reactions, the β -agostic complexes are stable and supposed to be the resting state. For the polymerization reaction, the stability of the β -agostic complex should be optimum so that the transformation of the agostic complex to the ethylene-

hydride complex will be easier. In our study, we found the first row transition metal β -agostic complexes are most stable complexes and the stability of the β -agostic complexes decreases down the group. The extent of stability can be tuned by varying the steric effect manifested by the ligands. If the first-row transition metal β -agostic complexes are stable by a large margin then the second-row or third-row β -agostic complexes can have an optimum stability to be a better candidate for the polymerization reaction within the same set of ligands.

[4.4] Conclusion

It is possible to bring the frontier levels of any transition metal fragment close to that of the C_{β} -H bond so that the formation of the agostic and the ethylene hydride complex is possible. The relative energies of the complexes depend on the steric effect manifested by the ligands and the atomic radius of the metal involved. The larger size of the metal atom gives enough room to hold both the ethylene and hydride resulting ethylene-hydride complex. So, the tilting equilibrium between the agostic and ethylene-hydride complexes depends on the steric effect manifested by the ligands and the atomic radius of the metal involved.

The reaction profile shows (Figure 1) that there is a major stability changes in the conversion of metal-agostic to metal-ethylene-hydride complexes across the periodic table. The graph (Figure 1) goes upwards for the first-row, becomes almost parallel for the second-row, and goes downwards for the third row complexes. So, our detailed study across the periodic stable shows that the first row transition metals prefer agostic

form but the stability of ethylene-hydride complexes increase for the second row complexes which further increases for the third row complexes. The relative stability of agostic and ethylene-hydride complexes within the same group is probed by the using of isodesmic equation 1 also. High endothermicity of this equation supports that the lighter metals prefer agostic complexes and heavier metals prefer ethylene-hydride complexes. The transition states barrier for the conversion of the metal-agostic to metal-ethylene decreases down the group. The early or late transition state has been predicted on the basis of low energy differences between the TS with agostic or product. The early and late TS have been confirmed from their geometrical parameters.

[4.5] References

1. (a) Labinger, J. A.; Bercaw, J. E. *Nature* **2002**, *417*, 507. (b) Crabtree, R. H. *J. Chem. Soc., Dalton Trans.* **2001**, 2437. (c) Shilov, A. E.; Shul'pin, G. B. *Chem. Rev.* **1997**, *97*, 2879. (d) Hall, C.; Perutz, R. N. *Chem. Rev.* **1996**, *96*, 3125. (e) Ryabov, A. D. *Chem. Rev.* **1990**, *90*, 403. (c) *Activation and Functionalization of Alkanes*; Hill, C. L., Ed.; John Wiley and Sons: New York, 1989.
2. (a) Arndtsen, B. A.; Bergman, R. G.; Mobley, T. A.; Peterson, T. H.; *Acc. Chem. Res.* **1995**, *28*, 154. (b) Shilov, A. E.; Shulpin, G. B. *Chem. Rev.* **1997**, *97*, 2879. (c) Dyker, G. *Angew. Chem. Int. Ed.* **1999**, *38*, 1698.
3. (a) Brookhart, M.; Green, M. L. H. *J. Organomet. Chem.* **1983**, *250*, 395. (b) Brookhart, M.; Green, M. L. H.; Wong, L.-L. *Prog. Inorg. Chem.* **1988**, *36*, 1-124.
4. (a) Keim, W.; Appel, R.; Storeck, A.; Kruger, C.; Goddard, R. *Angew. Chem., Int. Ed. Engl.* **1981**, *20*, 116-117. (b) Möhring, V. M.; Fink, G. *Angew. Chem., Int. Ed. Engl.* **1985**, *24*, 1001-1003. (c) Ostoja Starzewski, K. A.; Witte, J. *Angew. Chem.* **1985**, *97*, 610-612. (d) Klabunde, U.; Ittel, S. D. *J. Mol. Catal.* **1987**, *41*, 123-134. (e) Brookhart, M.; DeSimone, J. M.; Grant, B. E.; Tanner, M. J. *Macromolecules* **1995**, *28*, 5378-5380. (f) Small, B. L.; Brookhart, M.; Bennett, A. M. A. *J. Am. Chem. Soc.* **1998**, *120*, 4049-4050. (g) Small, B. L.; Brookhart, M. *Macromolecules* **1999**, *32*, 2120-2130. (h) Britovsek, G. J. P.; Gibson, V. C.; Kimberly, B. S.; Maddox, P. J.; McTravish, S. J.; Solan, G. A.; White, A. J. P.; Williams, D. J. *Chem. Commun.* **1998**, 849-850. (i) Britovsek, G. J. P.; Gibson, V. C.; Wass, D. F. *Angew. Chem., Int. Ed.* **1999**, *38*, 429-447. (j) Younkin, T. R.; Connor, E. F.;

- Henderson, J. I.; Friedrich, S. K.; Grubbs, R. H.; Bansleben, D. A. *Science* **2000**, 287, 460-462. (k) Hicks, F. A.; Brookhart, M. *Organometallics* **2001**, 20, 3217-3219. (l) Ittel, S. D.; Johnson, L. K.; Brookhart, M. *Chem. Rev.* **2000**, 100, 1169-1203. (m) Piers, W. E.; Bercaw, J. E. *J. Am. Chem. Soc.* **1990**, 112, 9406. (n) Krauledat, H.; Brintzinger, H. -H. *Angew. Chem., Int. Ed Engl.* **1990**, 29, 1412. (o) Barta, N.; Kirk, B. A.; Stille, J. R. *J. Am. Chem. Soc.*, 1994, 116, 8912. (p) Grubbs, R. H.; Coates, G. W. *Acc. Chem. Res.* **1996**, 29, 85. (q) Tanner, M. J.; Brookhart, M.; DeSimone, J. M. *J. Am. Chem. Soc.*, **1997**, 119, 7617.
5. (a) Green, M. L. H.; Sella, A.; Wong, L.-L. *Organometallics* **1992**, 11, 2650. (b) Brookhart, M.; Hauptman, E.; Lincoln, D. M. *J. Am. Chem. Soc.* **1992**, 114, 10394 (c) Brookhart, M.; Lincoln, D. M.; Volpe, A. F.; Schmidt, G. F. *Organometallics* **1989**, 8, 1212. (d) Casey, C. P.; Yi, C. S. *Organometallics* **1991**, 10, 33. (e) Burger, B. J.; Thompson, M. E.; Cotter, W. D.; Bercaw, J. E. *J. Am. Chem. Soc.* **1990**, 112, 1566; (f) Tempel, D. J.; Brookhart, M. *Organometallics* **1998**, 17, 2290.
6. (a) Fryzuk, M. D.; Johnson, S. A.; Rettig, S. J. *Organometallics* **2000**, 19, 3931. (b) Collman, J. P.; Hegedus, L. S. In *Principles and Applications of Organotransition Metal Chemistry*; Kelly, A, Ed.; University Science Books: Mill Valley, CA, **1980**. (c) Koga, N.; Daniel, C.; Han, J.; Fu, X. Y.; Morokuma, K. *J. Am. Chem. Soc.* **1987**, 109, 3455. (d) Daniel, C.; Koga, N.; Han, J.; Fu, X. Y.; Morokuma, K. *J. Am. Chem. Soc.* **1988**, 110, 3773. (e) Koga, K.; Morokuma, K. *Chem. Rev.* **1991**, 91, 823. (f) Musaev, D. G.; Morokuma, K. In *Advances in Chemical Physics*; Rice, S. A., Prigogine, I., Eds.; John Wiley & Sons: New York, **1996**; Vol. XCV, p 61. (g)

- Siegbahn, P. E. M.; Blomberg, M. R. A. In *Theoretical Aspects of Homogeneous Catalysts, Applications of Ab Initio Molecular Orbital Theory*; van Leeuwen, P. W. N. M., van Lenthe, J. H., Morokuma, K., Eds.; Kluwer Academic Publishers: Hingham, MA, **1995**. (h) Ziegler, T. *Chem. Rev.* **1991**, *91*, 651. (i) Salahub, D. R.; Castro, M.; Fournier, R.; Calaminici, P.; Godbout, N.; Goursot, A.; Jamorski, C.; Kobayashi, H.; Martinez, A.; Papai, I.; Proynov, E.; Russo, N.; Sirois, S.; Ushio, J.; Vela, A. In *Theoretical and Computational Approaches to Interface Phenomena*; Sellers H., Olab, J., Eds.; Plenum Press: New York, 1995; p 187. (j) Siegbahn, P. E. M. In *Advances in Chemical Physics*; Rice, S. A., Prigogine, I., Eds.; John Wiley & Sons: New York, 1996; Vol. XCIII, p 333. (k) *Transition Metal Hydrides*, Edited by Dedieu, A., VCH Publishers: **1992**. (l) *Theoretical Aspects of Homogeneous Catalysis, Applications of Ab Initio Molecular Orbital Theory*; van Leeuwen, P. W. N. M., van Lenthe, J. H., Morokuma, K., Eds.; The Netherlands, 1994. (m) Yoshida, S.; Sakaki, S.; Kobayashi, H. *Electronic Processes in Catalyst*; VCH: New York, 1992.
7. (a) Shultz, L. H.; Tempel, D. J.; Brookhart, M. *J. Am. Chem. Soc.* 2001, *123*, 11539. (b) Leatherman, M. D.; Svejda, S. A.; Johnson, L. K.; Brookhart, M. *J. Am. Chem. Soc.* 2003, *125*, 3068-3081. (c) Woo, T. K.; Margl, P. M; Lohrenz, J. C. W.; P. E. Bloch, Ziegler, T. *J. Am. Chem. Soc.* 1996, *118*, 13021-13030 (d) Kazlauskas, R. J.; Wrighton; M. S. *J. Am. Chem. Soc.* 1982, *104*, 6005-6015 (e) Chirik, P. J.; Day, M. W.; Labinger, J. A.; Bercaw, J. E. *J. Am. Chem. Soc.* 1999, *121*, 10308-10317. (f) Jaffart, J.; Etienne, M.; Maseras, F.; McGrady, J. E.; Eisenstein, O. *J.*

- Am. Chem. Soc.* 2001, *123*, 6000-6013. (g) Musaev, D. G.; Froese, R. D. J.; Morokuma, K. *Organometallics* 1998, *17*, 1850-1860. (h) Tempel, D. J.; Brookhart, M. *Organometallics* 1998, *17*, 2290-2296. (i) Casey, C. P. J. A; Lee, T. Ting-Yu; Carpenetti II, D. W. *Organometallics* 2002, *21*, 389-396. (j) Stern, D.; Sabat, M.; Marks, T. J. *J. Am. Chem. Soc.* 1990, *112*, 9558-9575. (k) Ozerov, O. V.; Watson, L. A.; Pink, M.; Caulton, K. G. *J. Am. Chem. Soc.* 2003, *125*, 9604-9605. (l) Yang K. G.; Peters, K. S. Vaida, V. *J. Am. Chem. Soc.* 1986, *108*, 2511-25139.
8. (a) Brookhart, M.; Schmidt, G. F.; Lincoln, D.; Rivers, D. Olefin Insertion Reactions: The Mechanism of Co(II) Catalyzed Polymerization. In *Transition Metal Catalyzed Polymerization: Ziegler-Natta and Metathesis Polymerization*; Quirk, R. P., Ed.; Cambridge Press: Oxford, **1988**. (b) Brookhart, M.; Schmidt, G. F.; Lincoln, D.; Rivers, D. Olefin Insertion Reactions: The Mechanism of Co(III) Catalyzed Polymerization. In *Transition Metal Catalyzed Polymerization: Ziegler-Natta and Metathesis Polymerization*; Quirk, R. P., Ed.; Cambridge Press: Cambridge, 1988. (c) Ivin, K. J. Olefin Metathesis, Academic Press, New York, 1983 (d) Ostoj-Starzewski, K.A.; Witte, J. in: R.P. Quirk (Ed.), *Transition Metal Catalyzed Polymerizations-Ziegler-Natta and Metathesis Polymerization*, Cambridge University Press, Cambridge, 1988, p. 472. (e) Schmidt, G. F.; Brookhart, M. *J. Am. Chem. Soc.* **1985**, *107*, 1443.
9. (a) Mohring, V. M.; Fink, G. *Angew. Chem., Int. Ed. Engl.* **1985**, *24*, 1001-1003 (b) Schubbe, R.; Angermund, K.; Fink, G.; Goddard, R. *Makromol. Chem. Phys.* 1995, *196*, 467-468. (c) Killian, C. M.; Johnson, L. K.; Brookhart, M. *Organometallics*

- 1997, *16*, 2005-2007. (d) Tempel, D. J. Ph.D. Dissertation, University of North Carolina at Chapel Hill, 1998. (e) Svejda, S. A.; Brookhart, M. *Organometallics* 1999, *18*, 65-74. (e) Thompson, M. E.; Barter, S. M.; Bulla, A. R.; Burger, B. J.; Nolan, M. C.; Santareiero, B. D.; Schaefer, W. P.; Bercaw, J. E. *J. Am. Chem. Soc.* 1987, *109*, 203. (f) Burger, B. J.; Thompson, M. E.; Cotter, W. D.; Bercaw, J. E. *J. Am. Chem. Soc.* 1990, *112*, 1566. (g) Parkin, C.; Bunel, E.; Burger, B. J.; Trimmer, M. S.; Van Asselt, A.; Bercaw, J. E. *J. Mol. Catal.* 1987, *41*, 21. (h) Wilke, G. *Angew. Chem., Int. Ed. Engl.* **1988**, *27*, 185-206. (i) Keim, W.; Behr, A.; Limbacker, B.; Kruger, C. *Angew. Chem., Int. Ed. Engl.* **1983**, *22*, 503. (j) Peuckert, M.; Keim, W. *Organometallics* **1983**, *2*, 594-597. (k) Cavell, K. J.; Masters, A. F. *Aust. J. Chem.* **1986**, *39*, 1129-1134. (l) Rix, F. C.; Brookhart, M. *J. Am. Chem. Soc.* **1995**, *117*, 1137-1138. (m) Desjardins, S. Y.; Cavell, K. J.; Jin, H.; Skelton, B. W.; White, A. H. *J. Organomet. Chem.* **1996**, *515*, 233-243. (n) Desjardins, S. Y.; Cavell, K. J.; Hoare, J. L.; Skelton, B. W.; Sobolev, A. N.; White, A. H.; Keim, W. *J. Organomet. Chem.* **1997**, *544*, 163-174. (o) Svedja, S. A.; Brookhart, M. *Organometallics* **1999**, *18*, 65-74.
10. (a) Kemball, C. *Catal. Rev.* **1971**, *5*, 33. (b) Clarke, J. K. A, Rooney, J. J. *Adv. Catal.* **1976**, *27*, **125**.
11. (a) Thompson, M. E.; Baxter, S. M.; Bulla, A. R.; Burger, B. J.; Nolan, M. C.; Santarsiero, B. D.; Schaefer, W. P.; Bercaw, J. E. *J. Am. Chem. Soc.* **1987**, *109*, 203. (b) (a) Barbara J. Burger, Mark E. Thompson, W. Donald Cotter, and John E. Bercaw, *J. Am. Chem. Soc.* 1990, *112*, 1566-1577.

12. (a) Dawoodi, Z.; Green, M. L. H.; Mtetwa, V. S. B.; Prout, K. *Chem. Commun.* **1982**, 802. (b) Cotton, F. A.; Petrukhina, M. A. *Inorg. Chem. Commun.* **1998**, 1, 195. (c) Scherer, W.; Priermeier, T.; Haaland, A.; Volden, H. V.; McGrady, G. S.; Downs, A. J.; Boese, R.; Blaser, D. *Organometallics* **1998**, 17, 4406. d) Scherer, W.; Hieringer, W.; Spiegler, M.; Sirsch, P.; McGrady, G.S.; Downs, A.J.; Haaland, A.; Pedersen, B. *Chem. Commun.* **1998**, 2471. e) Dawoodi, Z.; Green, M. L. H.; Mtetwa, V. S. B.; Prout, K.; Schultz, A. J.; Williams, J. M.; Koetzle, T. F. *J. Chem. Soc., Dalton Trans.* **1986**, 1629.
13. Lukens, W. W.; Smith III, M. R.; Andersen, R. A. *J. Am. Chem. Soc.* **1996**, 118, 1719-1728.
14. Bei, X.; Young, V. G. Jr., Jordan, R. F. *Organometallics* **2001**, 20, 355-358.
15. Hills, A.; Hughes, D. L.; Jimenez-Tenorio, M.; Leigh, G. J.; McGeary, C. A.; Rowley, A. T.; Bravo, M.; McKenna, C. E.; McKenna, M.-C. *J. Chem. Soc., Chem. Commun.* **1991**, 522.
16. Cracknell, R. B.; Orpen, A. G.; Spencer, J. L. *Chem. Commun.* **1984**, 326-328.
17. (a) Brookhart, M.; Green, M. L. H.; Pardy, R. B. A. *J. Chem. Soc. Chem. Comm.*, 1983, 691-693 (b) Brookhart, M.; Lincoln, D. M.; Bennett, M. A.; Pelling, S. *J. Am. Chem. Soc.* 1990, 112, 2691-2694.
18. Schmidt, G. F.; Brookhart, M. *J. Am. Chem. Soc.* **1985**, 107, 1443-1444.
19. Conroy-Lewis, F. M.; Mole, L.; Redhouse, A. D.; Litster, S. A. Spencer, J. L. *Chem. Commun.* **1991**, 1601.

20. Kogut, E.; Zeller, A.; Warren, T. H.; Strassner, T. *J. Am. Chem. Soc.* **2004**, *126*, 11984-11994.
21. (a) Johnson, L. K.; Killian, C. M.; Brookhart, M. *J. Am. Chem. Soc.* **1995**, *117*, 6414. (b) Svejda, S. A.; Johnson, L. K.; Brookhart, M. *J. Am. Chem. Soc.* **1999**, *121*, 10634. (c) Tempel, D. J.; Johnson, L. K.; Huff, R. L.; White, P. S.; Brookhart, M. *J. Am. Chem. Soc.* **2000**, *122*, 6686. (d) Shultz, L. H.; Tempel, D. J.; Brookhart, M. *J. Am. Chem. Soc.* **2001**, *123*, 11539. (e) Shultz, L. H.; Brookhart, M. *Organometallics* **2001**, *20*, 3975. (f) Leatherman, M. D.; Svejda, S. A.; Johnson, L. K.; Brookhart, M. *J. Am. Chem. Soc.* **2003**, *125*, 3068. (g) Tempel, D. J.; Brookhart, M. *Organometallics* **1998**, *17*, 2290.
22. Voth, P.; Arndt, S.; Spaniol, T. P.; Okuda, J.; Ackerman, L. J.; Green, M. L. H. *Organometallics*, **2003**, *22*, 65-76.
23. (a) Jordan, R. F.; Bradley, P. K.; Baenziger, N. C.; LaPointe, R. E. *J. Am. Chem. Soc.*, **1991**, *112*, 1289-1291. (b) Sun, Y.; Piers, W. E.; Rettig, S. J. *Chem. Commun.*, **1998**, 127-128.
24. Alelyunas, Y. W.; Guo, Z.; LaPointe, R. E.; Jordan, R. F.; *Organometallics* 1993, *12*, 544-553.
25. Jaffart, J.; Mathieu, R.; Etienne, M.; McGrady, J. E.; Eisenstein, O.; Maseras, F. *Chem. Commun.* **1998**, 2011.
26. Clegg, W.; Eastham, G. R.; Elsegood, M. R. J.; Heaton, B. T.; Iggo, J. A.; Tooze, R. P.; Whyman, R.; Zacchini, S. *Organometallics* 2002, *21*, 1832-1840.

-
27. Tempel, D. J.; Johnson, K. L.; Huff, R. L.; White, P. S.; Brookhart, M. *J. Am. Chem. Soc.* **2000**, *122*, 6686-6700.
28. Fryzuk, M. D.; Johnson, S. A.; Rettig, S. J. *J. Am. Chem. Soc.* **2001**, *123*, 1602.
29. Wen, T. B.; Zhou, Z. Y.; Lau, Chak-Po; Jia, G. *Organometallics* **2000**, *19*, 3466-3468.
30. (a) Carr, N.; Dunne, B. J.; Mole, L.; Orpen, A. G.; Spencer, J. L. *J. Chem. Soc., Dalton Trans.* **1991**, 863. (b) Carr, N.; Dunne, B. J.; Orpen, A. G.; Spencer, J. L. *Chem. Commun.* **1988**, 926-928.
31. Mole, L.; Spence, J. L.; Carr, N.; Orpen, A. G. *Organometallics* **1991**, *10*, 49-52.
32. Goddard, R. J.; Hoffmann, R.; Jemmis, E. D. *J. Am. Chem. Soc.* **1980**, *102*, 7667.
33. (a) Koga, N.; Obara, S.; Morokuma, K. *J. Am. Chem. Soc.* **1984**, *106*, 4625. (b) Obara, S.; Koga, N.; Morokuma, K. *J. Organomet. Chem.* **1984**, *270*, C33.
34. Pavankumar, P. N. V.; Ashok, B.; Jemmis, E. D. *J. Organomet. Chem.* **1986**, *315*, 361.
35. Cracknell, R. B.; Orpen, A. G.; Spencer, J. L. *Chem. Commun.* **1986**, 1005-1006.
36. Lin, Z.; Hall, M. B.; Guest, M. F.; Sherwood, P. J. *J. Organomet. Chem.* **1994**, *478*, 197.
37. (a) Yoshida, T.; Koga, N.; Morokuma, K. *Organometallics* **1995**, *14*, 746. (b) Yoshida, T.; Koga, N.; Morokuma, K. *Organometallics* **1996**, *15*, 766. (c) Musaev, D. G.; Froese, R. D. J.; Morokuma, K. *Organometallics* **1998**, *17*, 1850-1860 (d) Froese, R. D. J.; Musaev, D. G.; Morokuma, K. *J. Am. Chem. Soc.* **1998**, *120*, 1581-1587. (e) Vyboishchikov, S. F.; Musaev, D. G.; Froese, R. D. J.; Morokuma, K.;

- Organometallics* **2001**, *20*, 309-323. (f) Froese, R. D. J.; Musaev, D. G.; Matsubara, T.; Morokuma, K. *J. Am. Chem. Soc.* **1997**, *119*, 7190-7196. (g) Musaev, Svensson, D. G. M.; Morokuma, K.; Strömberg, S.; Zetterberg, K.; Siegbahn, P. E. M. *Organometallics* **1997**, *16*, 1933-1945.
38. (a) Woo, T. K.; Fan, L.; Ziegler, T. *Organometallics* **1994**, *13*, 2252. (b) Fan, L.; Harrison, D.; Woo, T. K.; Ziegler, T. *Organometallics* **1995**, *14*, 2018. (c) Fan, L.; Harrison, D.; Deng, L.; Woo, T. K.; Swerhone, D.; Ziegler, T. *Can. J. Chem.* **1995**, *73*, 989. (d) Lohrenz, J. C. W.; Woo, T. K.; Fan, L.; Ziegler, T. *J. Organomet. Chem.* **1995**, *497*, 91. (e) Peter Margl, Liqun Deng, and Tom Ziegler *J. Am. Chem. Soc.* 1999, *121*, 154-162;
39. Haaland, A.; Scherer, W.; Ruud, K.; McGrady, G. S.; Downs, A. J.; Swang, O. *J. Am. Chem. Soc.* **1998**, *120*, 3762-3772.
40. (a) Bittner, M.; Köppel, H.; Gatti, F. *J. Phys. Chem. A* **2007**, *111*, 2407-2419. (b) Bittner, M.; Köppel, H. *J. Phys. Chem. A* **2004**, *108*, 11116-11126
41. Hehre, W.; Radom, L.; Schleyer, P. v. R.; Pople, J. A. *Ab Initio Molecular Orbital Theory*; Wiley: New York, 1986.
42. Hehre, W.; Radom, L.; Schleyer, P. v. R.; Pople, J. A. *Ab Initio Molecular Orbital Theory*; Wiley: New York, 1986.
43. (a) Becke, A. D. *J. Chem. Phys.* **1993**, *98*, 5648. (b) Becke, A. D. *Phys. Rev. A* **1988**, *38*, 3098. (c) Lee, C.; Yang, W.; Parr, R.G. *Phys. Rev. B*, **1988**, *37*, 785. (d) Vosko, S. H.; Wilk, L.; Nusair, M. *Can. J. Phys.* **1980**, *58*, 1200. (e) Hay, P. J.; Wadt, W. R. *J. Chem. Phys.* **1985**, *82*, 270.

44. Gaussian 03, Revision B.03, Frisch, M. J.; Trucks, G. W.; Schlegel, H. B.; Scuseria, G. E.; Robb, M. A.; Cheeseman, J. R.; Montgomery, Jr., J. A.; Vreven, T.; Kudin, K. N.; Burant, J. C.; Millam, J. M.; Iyengar, S. S.; Tomasi, J. Barone, V.; Mennucci, B.; Cossi, M.; Scalmani, G.; Rega, N.; Petersson, G. A.; Nakatsuji, H.; Hada, M.; Ehara, M.; Toyota, K.; Fukuda, R.; Hasegawa, J.; Ishida, M.; Nakajima, T.; Honda, Y.; Kitao, O.; Nakai, H.; Klene, M.; Li, X.; Knox, J. E.; Hratchian, H. P.; Cross, J. B.; Adamo, C.; Jaramillo, J.; Gomperts, R.; Stratmann, R. E.; Yazyev, O.; Austin, A. J.; Cammi, R.; Pomelli, C.; Ochterski, J. W.; Ayala, P. Y.; Morokuma, K.; Voth, G. A.; Sthis alvador, P. Dannenberg, J. J.; Zakrzewski, V. G.; Dapprich, S.; Daniels, A. D.; Strain, M. C.; Farkas, O.; Malick, D. K.; Rabuck, A. D.; Raghavachari, K.; Foresman, J. B.; Ortiz, J. V.; Cui, Q.; Baboul, A. G.; Clifford, S.; Cioslowski, J.; Stefanov, B. B.; Liu, G.; Liashenko, A.; Piskorz, P.; Komaromi, I.; Martin, R. L.; Fox, D. J.; Keith, T.; Al-Laham, M. A.; Peng, C. Y.; Nanayakkara, A.; Challacombe, M.; Gill, P. M. W.; Johnson, B.; Chen, W.; Wong, M. W.; Gonzalez, C.; Pople, J. A. Gaussian, Inc., Pittsburgh PA, 2003.
45. Kazlauskas, R. J.; Wrighton, M. S. *Organometallics*, **1982**, 1, 602-611.
46. Bleeke, J. R.; Kotyk, J. J.; Moore, D. A.; Rauscher, D. J. *J. Am. Chem. Soc.* **1987**, *109*, 417-423.
47. Tolman, C. A.; Ittel, S. D.; English, A. D.; Jesson, J. P. *J. Am. Chem. Soc.* **1979**, *101*, 1742.

48. (a) Werner, H.; Feser, R. *J. organomet. Chemistry*, 1982, 232, 351-370. (b) Werner, R.; Werner, H. *Chem. Ber*, 1983. 116, 2074. (c) Esteruelas, M. A.; Werner, H. *J. organomet. Chemistry*, **1986**, 303, 221-231.

CHAPTER 5

BOND LENGTH AND BOND MULTIPLICITY: σ

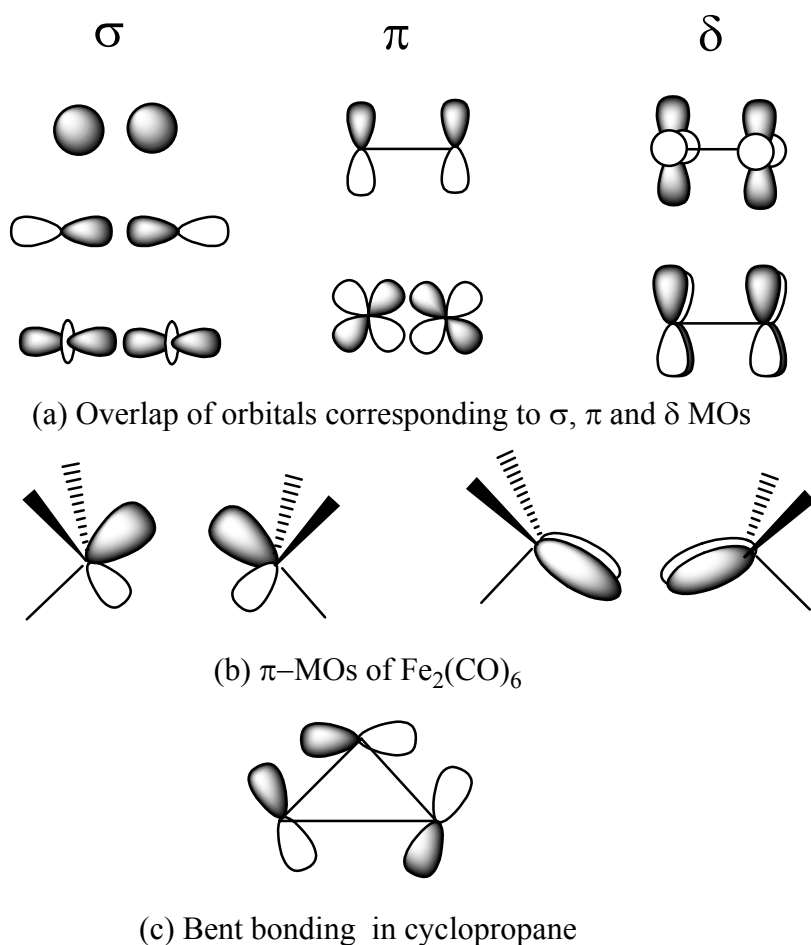
BOND PREVENTS SHORT π BONDS

[5.0] Abstract

The unusual shortness of the bond length in the several main group and transition metal compounds is explained on the basis of their π -alone bonding. The detailed electronic structure calculation on C_2 , HBBH, and $Fe_2(CO)_6$ shows that each of them have two π -alone bonds (unsupported by an underlying σ -bond) while B_2 has two-half π -bonds. The C-C bond length in C_2 is 1.240 Å, shorter than any C-C double ($\sigma + \pi$, in C_2H_4 , C-C=1.338 Å) bonded species. The B-B bond distance in B_2 (1.590 Å, two half- π bonds) is shorter than any B-B single σ -bonded (~ 1.706 Å) species. The calculated Fe-Fe bond distance of 2.002 Å in $Fe_2(CO)_6$ is shorter than those of some experimentally known M-M single bonded compounds in the range of 2.904–3.228 Å. Here, our detailed studies on the second and third row diatomics (five, six, seven and eight valance electrons species) and transition metal complexes show that π -alone bonds left to themselves are shorter than σ -bonds; in many ways σ -bonds prevent π -bonds from adopting their optimal shorter distances.

[5.1] Introduction

The concept of σ -, π - and δ -bonds is ingrained into the thought process of chemists. The cylindrically symmetrical σ -bond is traditionally estimated to be stronger than the π -bond, which in turn is stronger than the δ -bond. The linear overlap of orbitals in the σ -bond is supposed to be more effective than the sideways overlap available in the π - and δ -bonds [Scheme 1a]. Closely related to the discussion of σ -, π - and δ -bonds and their bond strengths is the issue of bond length.



Scheme 1: Overlapping Orbitals

The decrease of bond length in going from a single σ -bond to multiple bonds involving σ and π components are exemplified by $\text{H}_3\text{C}-\text{CH}_3$, $\text{H}_2\text{C}=\text{CH}_2$, and $\text{HC}\equiv\text{CH}$ with C-C bond length of 1.538Å, 1.338Å and 1.203Å, respectively.^{1a,b,c} In transition metal chemistry there are the familiar examples of short M-M quadruple bonds constituted from one σ -, two π -, and one δ -bonds as in $\text{Re}_2\text{Cl}_8^{-2}$ of 2.240 Å.²

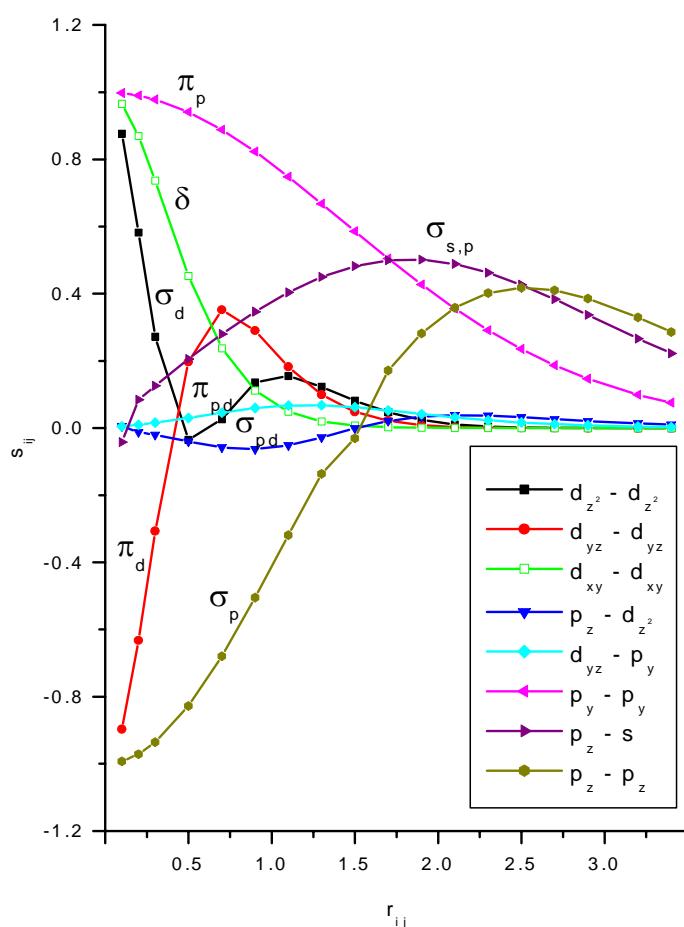


Figure 1: Variation of orbital overlap (s_{ij}) as a function of internuclear distance (r_{ij}) using contracted Gaussian orbitals corresponding to a minimal basis of Fe.

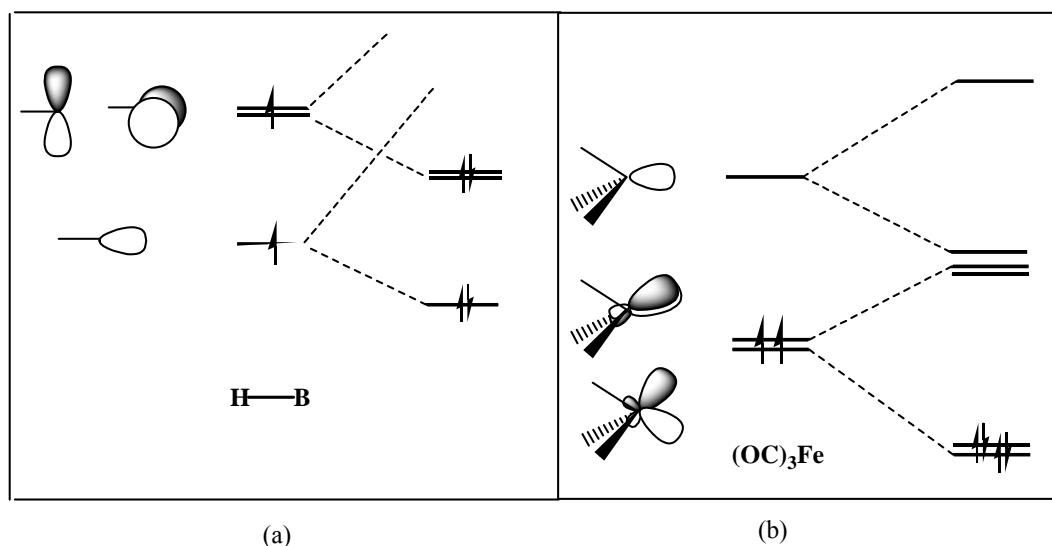
Very recently Roos *et al.*³ concluded that the maximum number of covalent chemical bonds between two shared atom will be six. To find the molecules with

the highest bond order, they theoretically studied the transition metal dimers of chromium (Cr_2), molybdenum (Mo_2) and tungsten (W_2), respectively. They predict the maximum number of chemical bonds will be six because the atoms of these transition metals have six outer, or ‘valence’ orbitals, all of which are available for bonding. In this perspective, Frenking *et al.* has reported^{4a} that six is the maximum limit for the covalent bonds between equal atoms but a measure of bond order between unequal atoms requires more developed model that includes electrostatic interaction. The calculated short M-M bond distances are 1.66, 1.95 and 2.01 Å for Cr_2 , Mo_2 and W_2 respectively. Power^{4b} has demonstrated that the multiple bonding between transition metals can be achieved by reducing the number of ligands, so that the number of valance orbitals and electrons available to form metal-metal bonds is optimized. It is always seen that the bond length decreases as the bond order increases. In these discussions the σ -bond is considered to be the strongest and the bond strength is thought to be inversely proportional to the bond length. However, the variation of orbital overlap as a function of internuclear distance (Figure 1) shows that maximum overlap occurs at shorter distances for π - and δ -bonds.

The shortness of bond length due to π -alone bonding has been in the literature for some time. In 1980, Bruna *et al.*⁵ theoretically reported the possible lowest lying states of the isovalent series of diatomics CN^+ , Si_2 , SiC , CP^+ , and SiN^+ . Comparisons with corresponding experimental data for C_2 , led to the conclusion that π^4 ($^1\Sigma^+$) configuration has uniformly shorter R_e than their $\pi^3\sigma^1$ ($^3\Pi$) counterparts by 0.07-0.10 Å. Corresponding bond lengths for the $\pi^2\sigma^2$ ($^1\Sigma^+$) species are seen to increase by an additional 0.1Å. The trend in relative bond lengths was explained on

the basis of stronger bonding character of the π -bonding MO than their corresponding σ species. In 2000, Sason Shaik *et al.*⁶ investigated whether Pauling's statement⁷ "the energy of an actual bond between unlike atoms is greater than (or equal to) the energy of a normal covalent bond between these atoms" is valid for π -bonds or not. They have calculated the π -bond energies in the inter- and intra-row double bonded species $H_mA=BH_n$ (where A, B= C, N, O Si, P and S) using VB theory. Their test reveals that Pauling's statement extends to π -bonds made from constituents belonging to the same row of the Periodic Table, but breaks down for comparisons involving inter-row π -bonds. This break down originates in the constraint applied by the σ frame which results in overstretched heteronuclear π bonds relative to homonuclear π bonds, thus disabling a comparison in the light of Pauling's statement. In a recent article Pyykkö *et al.* reported the triple-bond covalent radii for nearly all elements from Be to E112 (eka-mercury).⁸ Comparisons are made to fit with experimental data. There are many π -alone double bonded species which have comparable bond distances as those of triple bonded species. It is therefore logical to anticipate that π -bonds (unsupported by an underlying σ -bond) could be shorter than σ -bonds. But the difficulty in designing structures with π -alone-bonds is the following. The σ -levels (sp^x hybrid orbitals) of common main group fragments such as $-BH$, $-CH$ and $-CH_2$ are lower in energy than the p orbitals that form the π -bonds. As a result π -bonds always come with the underlying σ -bond (Scheme 2a) which largely dictates a "base line" distance. Transition metal fragments provide an opportunity to reverse this situation. For example the degenerate π -type frontier orbitals of the $Fe(CO)_3$ fragment are lower in energy than

the symmetric σ -orbital (Scheme 2b). It is therefore logical to anticipate shorter than usual M-M bond lengths in dimers of such fragments.



Scheme 2: Interaction diagram for the formation of (a) H₂B₂ and (b) Fe₂(CO)₆.

In this chapter, we have studied a list of inter- and intra-row main group (five, six, seven and eight valance electrons species) as well as few transition metal compounds. We attempted to explain their unusual shortness on the basis of their detailed electronic structures.

[5.2] Computational Details

The main group diatomic compounds are optimized at the CCSD(T) level⁹ using the GAUSSIAN 03 program.¹⁰ Frequency calculations confirmed the nature of the stationary points. The standard 6-311++G (p, d) basis set was employed for all atoms. In addition, for comparisons and calibration, we have done optimization as well as frequency calculation at the QCISD(T) level¹¹ using same basis set. The

transition metal complexes are studied using B3LYP/LANL2DZ¹² level of theory. Natural Bond Orbital (NBO)¹³ analysis are also done at the same level.

[5.3] Results and Discussion

[5.3.1] Short Bonds in Main Group Compounds

The influence of π -bonds in reducing bond lengths can be seen in many familiar examples. The C-C bond in cyclopropane is anticipated to be weak owing to strain. However, the C-C distance is shown to be shorter (1.510\AA)¹⁴ than is the case for regular C-C bonds (1.538\AA).^{1a} Optimum overlap for the orbitals, oriented in a sideways manner in the bent bonds [Scheme 1c], occurs at shorter distances than for a conventional σ -bond, explaining the short distance of a strained bond. The shorter distances necessary to obtain optimum overlap for these π -type MOs result in shorter than expected bond lengths. The fact that cyclopropane has several characteristic that are similar to olefins is in tune with this. If the shorter distances are a requirement for optimum overlap for π -MOs, these requirements must also exist in multiple bonds involving σ - and π -bonds. The π -bonds, however, are forced by the overwhelming σ -bonds to be at non-optimal overlapping distances.

First row diatomics provide examples where π -orbitals are filled before σ . The diatomic C_2 has a ground state $^1\Sigma_g^+$ with a double bond,¹⁵ both components of which are π -bonds (Scheme 3a). Relative to the standard triple bond in N_2 , the $3\sigma_g$ molecular orbital in C_2 is unoccupied. The bond distance in C_2 , of 1.240\AA , is shorter than any $\sigma+\pi$ carbon-carbon double bond by a large margin. Another example is B_2 .¹⁶ With two electrons less than C_2 , B_2 has two half π -bonds (Scheme

3d). The distance of 1.590 Å in B₂ is shorter than any B-B single σ-bond. Among the heavier main group elements with weak σ-bonds, there are examples of distorted structures with short π distances,¹⁷ arising from dative interactions.

The preference of π-bonds for short distances is further supported by the study of the excited states of C₂.^{15b} A triplet state obtained by shifting [Scheme 3b] one of the electrons from the π-bonding MO of C₂ to the vacant σ-bonding MO should increase the C-C distance. This is indeed found to be the case. Thus ³Π_u state of C₂ has a bond length of 1.313 Å. Another triplet state (³Σ_g⁺) obtained by shifting another electron from π to σ-level is calculated to have a bond length of 1.370 Å (Scheme 3c).

	¹ Σ _g ⁺	³ Π _u	³ Σ _g ⁺	³ Σ _g ⁻
3σ _g	—	↑↓	↑↓	—
1π _u	↑↓ ↑↓	↑↓ ↑	↑↓ ↑	↑↓ ↑
2σ _u [*]	↑↓	↑↓	↑↓	↑↓
2σ _g	↑↓	↑↓	↑↓	↑↓
Bond length	1.240 Å	1.313 Å	1.370 Å	1.590 Å
	(a) C ₂	(b) C ₂	(c) C ₂	(d) B ₂

Scheme 3: Experimental bond lengths of C₂ (a) ¹Σ_g⁺, (b) ³Π_u, (c) ³Σ_g⁺ and of B₂ (d) ³Σ_g⁻. Bond length of C₂ (c) ³Σ_g⁺ is obtained from calculations at B3LYP/6-311+G* method.

[5.3.1.1] Five Valance Electron Diatomic Species

Five valance electrons diatomic species can have a half π -alone bond (Scheme 4). The ground electronic state of five valance electron species AlBe,¹⁸ BeB,¹⁸ MgB¹⁸ and CaB¹⁸ is $^2\Pi$ ($1\sigma_g^2 1\sigma_u^2 1\pi^1$) calculated theoretically.¹⁸ To the best of our knowledge, there are no experimentally characterized ground state structure has been reported for these species. But the theoretical study predicts that these species may contain half π -alone bonds. The electronic ground state of the five valence cationic species B_2^+ , Al_2^+ , Ga_2^+ , BAI^+ , and $AlGa^+$, has been reported¹⁹ as $^2\Sigma_g^+$ ($1\sigma_g^2 1\sigma_u^2 2\sigma_g^1$) where the valance electrons are occupied in the σ -level. The anionic five valance electrons species Be_2^- has been studied theoretically²⁰ where the calculated ground electronic state changes with the method of calculation. The metastable state of Be_2^- has been characterized experimentally²¹ with a life time $> 180 \mu s$.

Table 1: The (E1-E2) bond lengths (\AA) of the $^2\Sigma_g^+$ ($1\sigma_g^2 1\sigma_u^2 2\sigma_g^1$) and $^2\Pi$ ($1\sigma_g^2 1\sigma_u^2 1\pi^1$) electronic state and their relative energies (R. E. in kcal/mol) calculated at CCSD(T)/6-311++G** level of theory (NC indicates not converged).

E1E2	State	E1-E2		E1E2	State	E1-E2	
		Cal.	R.E.			Cal.	R.E.
AlBe	$1\sigma_g^2 1\sigma_u^2 2\sigma_g^1$	2.626	2.09	BAI ⁺	$1\sigma_g^2 1\sigma_u^2 2\sigma_g^1$	2.724	0.00
	$1\sigma_g^2 1\sigma_u^2 1\pi^1$	2.430	0.00		$1\sigma_g^2 1\sigma_u^2 1\pi^1$	2.424	11.25
AlMg	$1\sigma_g^2 1\sigma_u^2 2\sigma_g^1$	3.302	3.33	BC ²⁺	$1\sigma_g^2 1\sigma_u^2 2\sigma_g^1$	NC	
	$1\sigma_g^2 1\sigma_u^2 1\pi^1$	2.900	0.00		$1\sigma_g^2 1\sigma_u^2 1\pi^1$	NC	
BeB	$1\sigma_g^2 1\sigma_u^2 2\sigma_g^1$	2.132	8.21	SiB ²⁺	$1\sigma_g^2 1\sigma_u^2 2\sigma_g^1$	NC	
	$1\sigma_g^2 1\sigma_u^2 1\pi^1$	1.946	0.00		$1\sigma_g^2 1\sigma_u^2 1\pi^1$	NC	
MgB	$1\sigma_g^2 1\sigma_u^2 2\sigma_g^1$	2.412	27.75	AlC ²⁺	$1\sigma_g^2 1\sigma_u^2 2\sigma_g^1$	NC	
	$1\sigma_g^2 1\sigma_u^2 1\pi^1$	2.152	0.00		$1\sigma_g^2 1\sigma_u^2 1\pi^1$	NC	
B_2^+	$1\sigma_g^2 1\sigma_u^2 2\sigma_g^1$	2.174	0.00	AlSi ²⁺	$1\sigma_g^2 1\sigma_u^2 2\sigma_g^1$	NC	
	$1\sigma_g^2 1\sigma_u^2 1\pi^1$	1.787	8.48		$1\sigma_g^2 1\sigma_u^2 1\pi^1$	NC	
Al_2^+	$1\sigma_g^2 1\sigma_u^2 2\sigma_g^1$	3.188	0.00	MgBe ⁻	$1\sigma_g^2 1\sigma_u^2 2\sigma_g^1$	2.805	0.75
	$1\sigma_g^2 1\sigma_u^2 1\pi^1$	2.796	14.58		$1\sigma_g^2 1\sigma_u^2 1\pi^1$	2.758	0.00

Our calculation on these five valance electron species shows that the bond length decreases considerably when the valance electron shifted from σ to the π -level (Table 1). The ${}^2\Pi$ ($1\sigma_g^2 1\sigma_u^2 1\pi^1$) electronic state is more stable state for the AlBe, AlMg, BeB and Al_2^+ species where as ${}^2\Sigma_g^+$ ($1\sigma_g^2 1\sigma_u^2 2\sigma_g^1$) is more stable for the rest.

[5.3.1.2] Six Valance Electron Diatomic Species

B_2 and its isovalent systems have been studied theoretically as well as experimentally. The diatomic B_2 has a ground state ${}^3\Sigma_g^-$ ($\sigma_g^2 \sigma_u^2 \pi_u^2$) with two half π -bonds.¹⁶ The distance 1.590 Å in B_2 is shorter than any B-B single (~ 1.706 Å)²² σ -bond. The calculated B-B bond lengths in B_2^+ (π^1), B_2 ($\pi^1 \pi^1$), B_2^- ($\pi^2 \pi^1$), and B_2^{2-} ($\pi^2 \pi^2$) are 1.790, 1.614, 1.586, and 1.587 Å (Scheme 2) respectively. So, the bond length decreases as their π -alone bond order increases. The B-B bond length in B_2 differs considerably while comparing with its other different electronic states. It has been found that the extra occupancy in π -levels lead to a much shorter bond than if it would have occupied a σ -level (Table 2). The neutral isovalent systems are Al_2 , AlB, MgSi, MgC, BeSi, and BeC (Table 2). The ground state of Al_2 is ${}^3\Pi_u$, characterized theoretically as well as experimentally. AlB,^{18b} MgSi,²³ BeSi,²³ and MgC²³ has ${}^3\Sigma^-$ ground state which has been calculated theoretically. The isovalent diatomic cations are BC^+ , AlSi^+ , AlC^+ , BSi^+ , SiC^{2+} , C_2^{2+} , and Si_2^{2+} . The theoretically calculated BC^+ has ${}^3\Sigma^-$ ground state.²⁴ We have studied three different electronic states by shifting the electrons from a π - to σ -level. The ${}^3\Sigma_g^-$ ($\pi_u^1 \pi_u^1$) state is the relatively most stable state for B_2 , AlB, MgB, MgC, BC^+ , AlC^+ , BBe^- , MgB^- , and

Table 2: The (E1-E2) bond lengths (Å) of the various electronic state and their relative energies (R. E. in kcal/mol) calculated at CCSD(T)/6-311++G** level of theory along with the experimental bond lengths wherever available.

E1E2	State	E1-E2			E1E2	State	E1-E2	
		Exp.	Cal.	R.E.			Cal	R.E.
B ₂	($\pi_u^1 \pi_u^1$)	1.590 ¹⁶	1.611	00.00	C ₂ ²⁺	($\pi_u^1 \pi_u^1$)	1.465	10.56
	($\sigma_g^1 \pi_u^1$)		1.770	08.33		($\sigma_g^1 \pi_u^1$)	1.473	00.00
	(σ_g^2)		1.917	25.70		(σ_g^2)	NC	NC
Al ₂	($\pi^1 \pi^1$)	2.701 ²⁰	2.480	01.48	Si ₂ ²⁺	($\pi_u^1 \pi_u^1$)	2.417,	23.05
	($\sigma_g^1 \pi_u^1$)		2.705	00.00		($\sigma_g^1 \pi_u^1$)	2.751,	00.00
	(σ_g^2)		2.956	08.52		(σ_g^2)	3.059,	-11.45
AlB	($\pi^1 \pi^1$)		2.044	00.00	CSi ²⁺	($\pi_u^1 \pi_u^1$)	1.954	20.75
	($\pi_u^1 \sigma_g^1$)		2.220	00.53		($\pi_u^1 \sigma_g^1$)	2.276,	00.00
	(σ_g^2)		2.425	14.17		(σ_g^2)	2.535	07.42
BeC	($\pi_u^1 \pi_u^1$)		1.520	38.580	BBe ⁻	($\pi_u^1 \pi_u^1$)	1.839	00.00
	($\pi_u^1 \sigma_g^1$)		1.678	0.00		($\pi_u^1 \sigma_g^1$)	1.984	07.92
	(σ_g^2)		NC	—		(σ_g^2)	2.070	23.67
SiBe	($\pi_u^1 \pi_u^1$)		2.135	05.29	MgB ⁻	($\pi_u^1 \pi_u^1$)	2.277	00.00
	($\sigma_g^1 \pi_u^1$)		2.287	00.00		($\pi_u^1 \sigma_g^1$)	2.484	01.73
	(σ_g^2)		NC	—		(σ_g^2)	NC	—
MgC	($\pi_u^1 \pi_u^1$)		2.102	00.00	AlBe ⁻	($\pi_u^1 \pi_u^1$)	2.308,	00.00
	($\pi_u^1 \sigma_g^1$)		2.392	27.39		($\sigma_g^1 \pi_u^1$)	2.470	04.89
	(σ_g^2)		2.117	33.88		(σ_g^2)	2.569	20.36
MgSi	($\pi_u^1 \pi_u^1$)		2.560	15.79	AlM ⁻	($\pi_u^1 \pi_u^1$)	2.741	00.00
	($\pi_u^1 \sigma_g^1$)		2.863	00.00		($\pi_u^1 \sigma_g^1$)	2.988	02.90
						(σ_g^2)	3.095	15.84
BC ⁺	($\pi_u^1 \pi_u^1$)		1.503	00.00	Be ₂ ²⁻	($\pi_u^1 \pi_u^1$)	2.014,	27.73
	($\sigma_g^1 \pi_u^1$)		1.733	13.08		($\sigma_g^1 \pi_u^1$)	2.291	00.00
	(σ_g^2)		2.093	42.86		(σ_g^2)	2.328	03.00
BSi ⁺	($\pi_u^1 \pi_u^1$)		1.935,	07.19	Mg ₂ ²⁻	($\pi_u^1 \pi_u^1$)	3.380,	02.61
	($\sigma_g^1 \pi_u^1$)		2.123,	00.00		($\sigma_g^1 \pi_u^1$)	3.424	00.00
	(σ_g^2)		2.462	13.50		(σ_g^2)	NC	
AlC ⁺	($\pi_u^1 \pi_u^1$)		1.964,	00.00	MgB ⁻	($\pi_u^1 \pi_u^1$)	2.794	03.13
	($\sigma_g^1 \pi_u^1$)		2.614,	02.84		($\sigma_g^1 \pi_u^1$)	2.799	00.00
	(σ_g^2)		2.727	32.14		(σ_g^2)	2.765	01.13
AlSi ⁺	($\pi_u^1 \pi_u^1$)		2.434,	03.98				
	($\sigma_g^1 \pi_u^1$)		2.826,	00.00				
	(σ_g^2)		3.026,	15.29				

AlMg⁻ where as $^3\Pi_u(\sigma_g^1 \pi_u^1)$ is for the other diatomic molecules (Table 2). So, it is the early intra or inter-row diatomic molecules which have more tendencies to form π -bonds rather than σ .²⁵ Here, we were searching for a molecule where $^3\Sigma_g^-$ and $^3\Pi_u$

states lie very close in energy because this can be a borderline molecule between the σ - and π -alone bonded species. The $^3\Sigma_g^-$ state of AlB is more stable by 0.53 kcal/mol than its $^3\Pi_u$ state where as the most stable $^3\Pi_u (\sigma_g^1 \pi_u^1)$ electronic state of Al₂ is stable by 1.48 kcal/mol. These are the two examples where the energy difference between those two states is very less. In AlB, π -level comes just below of σ where as in Al₂ σ -level comes below. These are the two examples where the σ - and π -levels just crosses to each other.

[5.3.1.3] Seven Valance Electron Diatomic Species

Here, we have studied four different electronic states [$^2\Pi (\pi_u^2 \pi_u^1)$, $^4\Sigma^- (\sigma_g^1 \pi_u^1 \pi_u^1)$, $^2\Pi (\sigma_g^2 \pi_u^1)$, and $^2\Sigma^- (\sigma_g^1 \pi_u^2)$] for each of the seven valance electrons species (Table 4). The ground electronic state of SiB,²⁶ BC,²⁷ SiAl,²⁶ AlC²⁷ is $^4\Sigma^- (\sigma^1 \pi^1 \pi^1)$ has been characterized experimentally as well as theoretically. The theoretical ground state of BN⁺ is $^4\Sigma^-$.²⁸ The $^4\Sigma^-$ electronic state is more stable state for all the seven valance electron species as some of these are characterized experimentally. The calculated bond lengths of $^4\Sigma^-$ electronic state of BC (1.518 Å) and AlC (1.974 Å) are very close to the experimental data available for BC (1.491 Å) and AlC (1.955 Å). For these diatomic species, the bond length increases considerably when the electrons are shifted from a π - to σ -level as seen in the previously discussed diatomic species even though energy decreases.

Table 4: The (E1-E2) bond lengths (Å) of the various electronic state and their relative energies (R. E. in kcal/mol) calculated at CCSD(T)/6-311++G** level of theory along with the experimental bond lengths wherever available.

E1E2	State	E1-E2			E1E2	State	E1-E2	
		Exp.	Cal.	R.E.			Cal.	R.E.
BC	$(\pi_u^2 \pi_u^1)$		1.427	0.00	CN ²⁺	$(\pi_u^2 \pi_u^1)$	1.320	0.00
	$(\sigma_g^1 \pi_u^2)$		1.517	19.26		$(\sigma_g^1 \pi_u^2)$	1.442	19.87
	$(\sigma_g^1 \pi_u^1 \pi_u^1)$	1.491	1.518	-11.95		$(\pi_u^1 \pi_u^1 \sigma_g^1)$	1.495	-23.28
	$(\sigma_g^2 \pi_u^1)$		1.639	29.45		$(\sigma_g^2 \pi_u^1)$	2.125	1.37
BSi	$(\pi_u^2 \pi_u^1)$		1.846	04.37	CP ²⁺	$(\pi_u^2 \pi_u^1)$	1.690	28.50
	$(\sigma_g^1 \pi_u^2)$		1.927	0.00		$(\sigma_g^1 \pi_u^2)$	1.765	0.00
	$(\sigma_g^1 \pi_u^1 \pi_u^1)^{22}$		1.926	-16.08		$(\sigma_g^1 \pi_u^1 \pi_u^1)$	1.772	-14.63
	$(\sigma_g^2 \pi_u^1)$		2.129	08.56		$(\sigma_g^2 \pi_u^1)$	2.114	13.47
AlC	$(\pi_u^2 \pi_u^1)$		1.873	06.29	SiN ²⁺	$(\pi_u^2 \pi_u^1)$	1.718	20.84
	$(\sigma_g^1 \pi_u^2)$		1.861	0.00		$(\sigma_g^1 \pi_u^2)$	1.716	17.06
	$(\pi_u^1 \pi_u^1 \sigma_g^1)$	1.955	1.974	-27.46		$(\pi_u^1 \pi_u^1 \sigma_g^1)$	2.152	-43.06
	$(\sigma_g^2 \pi_u^1)$		2.116	15.82		$(\sigma_g^2 \pi_u^1)$	2.324	0.00
AlSi	$(\pi_u^2 \pi_u^1)$		2.287	02.41	SiP ²⁺	$(\pi_u^2 \pi_u^1)$	2.493	28.50
	$(\sigma_g^1 \pi_u^2)$		2.429	01.33		$(\sigma_g^1 \pi_u^2)$	2.414	5.37
	$(\sigma_g^1 \pi_u^1 \pi_u^1)^{22}$		2.419	-22.01		$(\sigma_g^1 \pi_u^1 \pi_u^1)$	2.398	-7.22
	$(\sigma_g^2 \pi_u^1)$		2.620	0.00		$(\sigma_g^2 \pi_u^1)$	2.674	0.00
BN ⁺	$(\pi_u^2 \pi_u^1)$		1.363	0.00	B ₂ ⁻	$(\pi_u^2 \pi_u^1)$	1.582	0.00
	$(\sigma_g^1 \pi_u^2)$		1.444	22.35		$(\sigma_g^1 \pi_u^2)$	1.683	09.95
	$(\pi_u^1 \pi_u^1 \sigma_g^1)$		1.472	-19.30		$(\sigma_g^1 \pi_u^1 \pi_u^1)$	1.644	-13.95
	$(\sigma_g^2 \pi_u^1)$		2.046	51.96		$(\sigma_g^2 \pi_u^1)$	1.731	13.22
BP ⁺	$(\pi_u^2 \pi_u^1)$		1.762	00.00	Al ₂ ⁻	$(\pi_u^2 \pi_u^1)$	2.454	07.37
	$(\sigma_g^1 \pi_u^2)$		1.869	07.18		$(\sigma_g^1 \pi_u^2)$	2.570	0.00
	$(\sigma_g^1 \pi_u^1 \pi_u^1)$		1.884	-21.70		$(\sigma_g^1 \pi_u^1 \pi_u^1)$	2.549	10.51
	$(\sigma_g^2 \pi_u^1)$		2.304	20.68		$(\sigma_g^2 \pi_u^1)$	2.708	-07.59
AlN ⁺	$(\pi_u^2 \pi_u^1)$		1.767	0.00	AlB ⁻	$(\pi_u^2 \pi_u^1)$	2.017	0.00
	$(\sigma_g^1 \pi_u^2)$		NC	-----		$(\sigma_g^1 \pi_u^2)$	2.138	08.98
	$(\pi_u^1 \pi_u^1 \sigma_g^1)$		3.162	-36.45		$(\sigma_g^1 \pi_u^1 \pi_u^1)$	2.083	-15.96
	$(\sigma_g^2 \pi_u^1)$		1.952	24.62		$(\sigma_g^2 \pi_u^1)$	2.218	07.64
AlP ⁺	$(\pi_u^2 \pi_u^1)$		2.191	0.00	BBe ²⁻	$(\pi_u^2 \pi_u^1)$	1.839	06.91
	$(\sigma_g^1 \pi_u^2)$		2.430	19.56		$(\sigma_g^1 \pi_u^2)$	1.851	13.29
	$(\pi_u^1 \pi_u^1 \sigma_g^1)$		2.636	-32.35		$(\pi_u^1 \pi_u^1 \sigma_g^1)$	1.905	-08.12
	$(\sigma_g^2 \pi_u^1)$		2.899	26.67		$(\sigma_g^2 \pi_u^1)$	1.933	0.00
SiC ⁺	$(\pi_u^2 \pi_u^1)$		1.739	04.44	MgB ²⁻	$(\pi_u^2 \pi_u^1)$	2.320	02.14
	$(\sigma_g^1 \pi_u^2)$		1.867	02.46		$(\sigma_g^1 \pi_u^2)$	2.318	0.00
	$(\sigma_g^1 \pi_u^1 \pi_u^1)$		1.819	-32.97		$(\pi_u^1 \pi_u^1 \sigma_g^1)$	2.330	-6.51
	$(\sigma_g^2 \pi_u^1)$		1.999	0.00		$(\sigma_g^2 \pi_u^1)$	2.418	01.81
C ₂ ⁺	$(\pi_u^2 \pi_u^1)$		1.319	0.00	AlBe ²⁻	$(\pi_u^2 \pi_u^1)$	2.328	00.95
	$(\sigma_g^1 \pi_u^2)$		1.461	19.56		$(\sigma_g^1 \pi_u^2)$	2.407	02.65
	$(\sigma_g^1 \pi_u^1 \pi_u^1)$		1.419	-15.22		$(\sigma_g^1 \pi_u^1 \pi_u^1)$	2.379	-10.91
	$(\sigma_g^2 \pi_u^1)$		1.556	26.67		$(\sigma_g^2 \pi_u^1)$	2.428	0.00
Si ₂ ⁺	$(\pi_u^2 \pi_u^1)$		2.191	13.17	AlMg ²⁻	$(\pi_u^2 \pi_u^1)$	2.794	0.49
	$(\sigma_g^1 \pi_u^2)$		2.360	06.58		$(\sigma_g^1 \pi_u^2)$	2.895	10.00
	$(\sigma_g^1 \pi_u^1 \pi_u^1)$		2.277	-14.74		$(\sigma_g^1 \pi_u^1 \pi_u^1)$	2.827	-9.45
	$(\sigma_g^2 \pi_u^1)$		2.474	0.00		$(\sigma_g^2 \pi_u^1)$	2.886	00.00

[5.3.1.4] Eight Valance Electron Diatomic Species

The ground state of C_2 is $^1\Sigma_g^+$ where all the four valance electrons are in π -levels. The isovalent neutral diatomic species are Si_2 , BN , BP , AlN , and AlP . The experimentally^{16,25} characterized ground state and an excited states of Si_2 is $^3\Sigma_g^-$ ($\sigma_g^2 \pi_u^1 \pi_u^1$, Si-Si = 2.246 Å) and $^3\Pi_u$ ($\pi_u^3 \sigma_g^1$, Si-Si = 2.155 Å) respectively. So, in the $^3\Pi_u$ electronic state, the Si-Si bond length is shortened by 0.091 Å which is the result of an extra occupancy in the π -levels. Our calculations show that $^3\Pi_u$ is more stable by only 0.66 kcal/mol than the $^3\Sigma_g^-$ state. The previous theoretical studies show that these are the two lowest lying electronic states for Si_2 and $^3\Sigma_g^-$ is the ground state. Though the energy difference between these two states is very less (0.66 kcal/mol), the bond lengths differ considerably which is the resultant of an electron's occupancy in the σ - or π -level. The experimentally characterized ground state of BN and AlN is $^3\Pi_u$. The hetero-diatomics, BP and AlP , to date, has not been characterized experimentally. The theoretically calculated ground state of BP ²⁹ and AlP is $^3\Pi_u$. In all the eight valance electron diatomic species, the bond length decreases as the σ -bond order increases or π -bond order decreases. The available experimental data support these results. The calculated bond lengths (Table 5) of C_2 , Si_2 , BN , and CN^+ are very close to the experimental data available for them. The C-C experimental bond length in C_2 decreases by 0.069 Å (Table 5) close to the calculated value of 0.070 Å when one of the π -electron shifted to the σ -level. Similarly, the experimental bond length in Si_2 , BN , CN^+ , support our results that the element-element bond lengths increases considerably (Table 5) when one of the π -electron shifted to the σ -level.

Table 5: The (E1-E2) bond lengths (Å) of the various electronic state and their relative energies (R. E. in kcal/mol) calculated at CCSD(T)/6-311++G** level of theory along with the experimental bond lengths wherever available.

Species	State	E1-E2		R.E	Species	State	E1-E2	
		Exp.	Cal.				Cal.	R.E
C ₂	($\pi_u^2 \pi_u^2$)	1.243	1.259	00.00	CS ²⁺	($\pi_u^2 \pi_u^2$)	1.540	20.41
	($\pi_u^2 \sigma_g^1 \pi_u^1$)	1.312	1.329	01.84		($\pi_u^2 \sigma_g^1 \pi_u^1$)	1.617	00.00
	($\sigma_g^2 \pi_u^1 \pi_u^1$)		1.383	17.47		($\sigma_g^2 \pi_u^1 \pi_u^1$)	1.980	3.97
	($\pi_u^2 \sigma_g^2$)		1.397	36.95		($\pi_u^2 \sigma_g^2$)	1.916	35.86
Si ₂	($\pi_u^2 \pi_u^2$)		2.088	14.61	SiO ²⁺	($\pi_u^2 \pi_u^2$)	1.548	20.75
	($\pi_u^2 \sigma_g^1 \pi_u^1$)	2.155	2.173	00.00		($\pi_u^2 \sigma_g^1 \pi_u^1$)	1.872	00.00
	($\sigma_g^2 \pi_u^1 \pi_u^1$)	2.246	2.264	0.66		($\sigma_g^2 \pi_u^1 \pi_u^1$)	2.264	-21.85
	($\pi_u^2 \sigma_g^2$)		2.305	13.92		($\pi_u^2 \sigma_g^2$)	2.234	36.59
BN	($\pi_u^2 \pi_u^2$)	1.283	1.276	00.00	SiS ²⁺	($\pi_u^2 \pi_u^2$)	1.962	28.57
	($\pi_u^2 \sigma_g^1 \pi_u^1$)	1.329	1.338	00.20		($\pi_u^2 \sigma_g^1 \pi_u^1$)	2.166	00.00
	($\sigma_g^2 \pi_u^1 \pi_u^1$)		1.489	24.99		($\sigma_g^2 \pi_u^1 \pi_u^1$)	2.520	-26.23
	($\pi_u^2 \sigma_g^2$)		1.446	61.48		($\pi_u^2 \sigma_g^2$)	2.465	11.16
BP	($\pi_u^2 \pi_u^2$)		1.689	07.81	B ₂ ²⁻	($\pi_u^2 \pi_u^2$)	1.582	07.34
	($\pi_u^2 \sigma_g^1 \pi_u^1$)		1.757	00.00		($\pi_u^2 \sigma_g^1 \pi_u^1$)	1.634	00.00
	($\sigma_g^2 \pi_u^1 \pi_u^1$)		1.964	18.04		($\sigma_g^2 \pi_u^1 \pi_u^1$)	1.651	-2.62
	($\pi_u^2 \sigma_g^2$)		1.938	43.43		($\pi_u^2 \sigma_g^2$)	1.680	11.24
AlN	($\pi_u^2 \pi_u^2$)		NC	-----	Al ₂ ²⁻	($\pi_u^2 \pi_u^2$)	2.468	09.18
	($\pi_u^2 \sigma_g^1 \pi_u^1$)		1.662	7.23		($\pi_u^2 \sigma_g^1 \pi_u^1$)	2.557	00.00
	($\sigma_g^2 \pi_u^1 \pi_u^1$)		1.941	-38.98		($\sigma_g^2 \pi_u^1 \pi_u^1$)	2.610	0.34
	($\pi_u^2 \sigma_g^2$)		1.922	0.00		($\pi_u^2 \sigma_g^2$)	2.659	09.95
AlP	($\pi_u^2 \pi_u^2$)		2.097	12.55	AlB ²⁻	($\pi_u^2 \pi_u^2$)	2.025	21.45
	($\pi_u^2 \sigma_g^1 \pi_u^1$)		2.225	0.00		($\pi_u^2 \sigma_g^1 \pi_u^1$)	2.090	00.00
	($\sigma_g^2 \pi_u^1 \pi_u^1$)		2.421	-2.22		($\sigma_g^2 \pi_u^1 \pi_u^1$)	2.139	1.68
	($\pi_u^2 \sigma_g^2$)		2.403	29.20		($\pi_u^2 \sigma_g^2$)	2.175	11.77
CN ⁺	($\pi_u^2 \pi_u^2$)	1.173	1.172	00.00	BC ⁻	($\pi_u^2 \pi_u^2$)	1.396	02.13
	($\pi_u^2 \sigma_g^1 \pi_u^1$)	1.247	1.251	05.87		($\pi_u^2 \sigma_g^1 \pi_u^1$)	1.448	00.00
	($\sigma_g^2 \pi_u^1 \pi_u^1$)		1.369	26.32		($\sigma_g^2 \pi_u^1 \pi_u^1$)	1.504	6.23
	($\pi_u^2 \sigma_g^2$)		1.367	62.97		($\pi_u^2 \sigma_g^2$)	1.518	26.90
SiP ⁺	($\pi_u^2 \pi_u^2$)		2.000	19.55	BSi ⁻	($\pi_u^2 \pi_u^2$)	1.818	08.14
	($\pi_u^2 \sigma_g^1 \pi_u^1$)		2.094	00.00		($\pi_u^2 \sigma_g^1 \pi_u^1$)	1.878	00.30
	($\sigma_g^2 \pi_u^1 \pi_u^1$)		2.231	-7.84		($\sigma_g^2 \pi_u^1 \pi_u^1$)	1.982	8.54
	($\pi_u^2 \sigma_g^2$)		2.242	13.40		($\pi_u^2 \sigma_g^2$)	1.995	0.00
CP ⁺	($\pi_u^2 \pi_u^2$)		1.578	17.37	AlC ⁻	($\pi_u^2 \pi_u^2$)	1.816	11.94
	($\pi_u^2 \sigma_g^1 \pi_u^1$)		1.634	00.00		($\pi_u^2 \sigma_g^1 \pi_u^1$)	1.897	00.00
	($\sigma_g^2 \pi_u^1 \pi_u^1$)		1.769	15.15		($\sigma_g^2 \pi_u^1 \pi_u^1$)	1.954	4.98
	($\pi_u^2 \sigma_g^2$)		1.792	32.61		($\pi_u^2 \sigma_g^2$)	1.980	23.67
SiN ⁺	($\pi_u^2 \pi_u^2$)		1.578	18.81	AlSi ⁻	($\pi_u^2 \pi_u^2$)	2.242	10.42
	($\pi_u^2 \sigma_g^1 \pi_u^1$)		1.683	00.00		($\pi_u^2 \sigma_g^1 \pi_u^1$)	2.338	00.00
	($\sigma_g^2 \pi_u^1 \pi_u^1$)		1.797	-3.37		($\sigma_g^2 \pi_u^1 \pi_u^1$)	2.432	0.82
	($\pi_u^2 \sigma_g^2$)		1.788	32.33		($\pi_u^2 \sigma_g^2$)	2.456	15.99
N ₂ ²⁺	($\pi_u^2 \pi_u^2$)		1.139	00.00	CO ²⁺	($\pi_u^2 \pi_u^2$)	1.166	25.26
	($\pi_u^2 \sigma_g^1 \pi_u^1$)		1.248	04.57		($\pi_u^2 \sigma_g^1 \pi_u^1$)	1.254	00.00
	($\sigma_g^2 \pi_u^1 \pi_u^1$)		1.367	20.75		($\sigma_g^2 \pi_u^1 \pi_u^1$)	1.254	0.00
	($\pi_u^2 \sigma_g^2$)		1.421	38.12		($\pi_u^2 \sigma_g^2$)	1.735	60.55
P ₂ ²⁺	($\pi_u^2 \pi_u^2$)		2.457	15.28				
	($\pi_u^2 \sigma_g^1 \pi_u^1$)		2.055	00.30				
	($\sigma_g^2 \pi_u^1 \pi_u^1$)		2.168	-12.70				
	($\pi_u^2 \sigma_g^2$)		2.244	0.00				

[5.3.2] Short Bonds in Transition Metal Complexes

In the ML_3 (d^8) transition metal fragments, the degenerate π -type frontier orbitals are lower in energy than the symmetric σ -orbital (Scheme 2b). It is therefore logical to expect π -alone bonds in the transition metal complexes. The $Fe_2(CO)_6$ is calculated to be a minimum in its potential energy surface,³⁰ with relatively short predicted metal-metal distance of 2.002 Å [Figure 2]. Compared with experimentally known compounds such as $Mn_2(CO)_{10}$ (Mn–Mn = 2.904 Å) or $M_2(Cp)_2(CO)_6$ (M = Cr, Mo and W), which have only M–M single bonds in the range of 3.221–3.228 Å, the metal-metal bond length in $Fe_2(CO)_6$ is very short indeed.³¹⁻³³ The short bond length and a simple-minded application of the 18-electron rule would suggest an Fe-Fe quadruple bond. A detailed interaction diagram (Figure 2) provides an occupancy of $1a_1'$, $1e'$, $1e''$, $1a_2''$ and $2e'$ levels (counting from HOMO-7, as $1a_1'$) for the 16 valence electrons, corresponding to σ , π/δ , π^*/δ^* , σ^* , and two π levels. Thus the formal net M-M bonding is provided by two π -type molecular orbitals, [Scheme 1b]. At the long distances direct CO·····CO interactions in $(OC)_3Fe-Fe(CO)_3$ are minimal, so that the eclipsed conformation with better overlap is favored. This is to be contrasted with the rotational preferences of ethane.³⁴ Independent of the conformation, the bond multiplicity must be only two. If the shorter distances are a requirement for optimum overlap for π -MOs, these requirements must also exist in multiple bonds involving σ - and π -bonds. The π -bonds, however, are forced by the overwhelming σ -bonds to be at non-optimal overlapping distances. While there are many factors that contribute to the observed bond lengths in a binuclear transition metal complex, shorter distances would be mandated by π - and δ -MOs for optimum

overlap. The π -alone-bonding proposed for $\text{Fe}_2(\text{CO})_6$ allows π -bonds to attain their natural shorter distances. The overlap of orbitals in π -bonds in $\text{Fe}_2(\text{CO})_6$ [Scheme 1b] is similar to the bent bonds of cyclopropane [Scheme 1c].

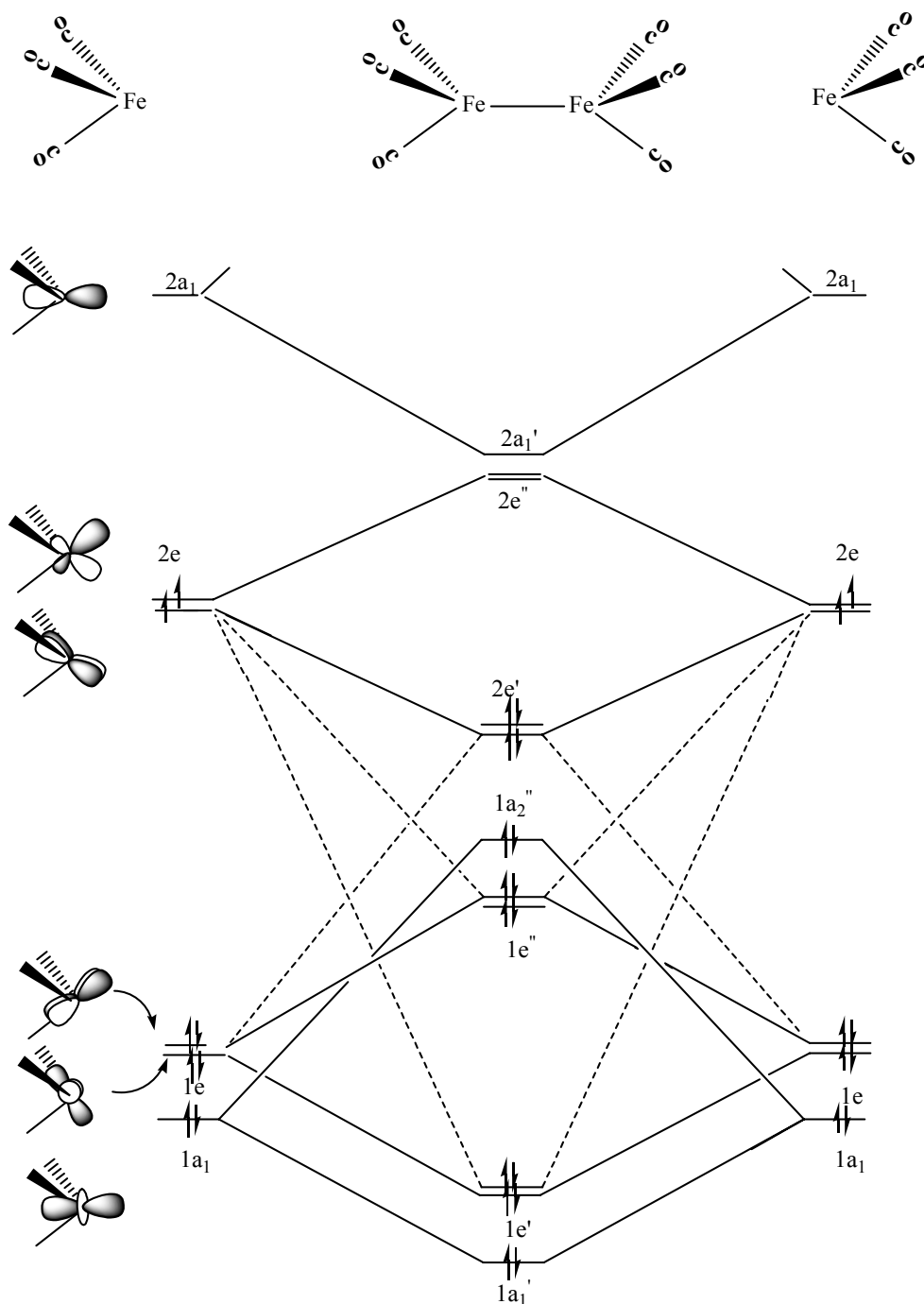


Figure 2: Interaction diagram between two $\text{Fe}(\text{CO})_3$ fragments to give $(\text{OC})_3\text{Fe}-\text{Fe}(\text{CO})_3$

The influence of σ -bonds in bond lengthening is seen in L_3M-ML_3 complexes with six valence electrons. According to the ordering of MO energy levels (Figure 2), such compounds should be triply bonded with one σ -bond and two π -bonds ($1a_1'$, $1e'$). The bond is expected to be longer due to its σ -component. There are four examples from literature, namely $Mo_2(CH_2Ph)_2(NMe_2)_4$ 2.20Å, $Mo_2(O^iPr)_2(SC_6H_2Me_3)_4$ 2.23Å, $Mo_2(OC(CF_3)_2CH_3)_6$ 2.23Å, $W_2Br_2(NEt_2)_4$ 2.30Å.³⁵ While these distances are not directly comparable, the M-M bond distances are much longer than that calculated for $Fe_2(CO)_6$.

The bonding in $Co_2(CO)_5$ presents a similar situation.³⁶ It's structure is best analyzed by bringing a $Co_2(CO)_4$ and a CO in a bridging arrangement. The C_{2v} geometry of $Co_2(CO)_5$ provides (Figure 3) an occupancy of $5a_1$, $7b_1$, $10a_1$, $7b_2$, $6a_2$, $8b_2$, $9b_2$, $11a_1$ and $8b_1$ levels for the 18d electrons, corresponding to σ , σ^* , π , π^* , δ , δ^* , and π levels. Thus the net M-M bonding is provided by one π - type molecular orbital. So the electronic structure of the d^9-d^9 $Co_2(CO)_4$ is predicted to have a π -bond. The interaction with the bridging carbonyl decreases the antibonding character of the σ^* to some extent. The Mullikan population, an indication of bond strength, remain the same before and after the interaction. Thus despite the short distance only a formal single bond (π -bond) may be assigned to the Co-Co interaction in $Co_2(CO)_5$. While it is tempting to assume exact cancellation of a bond when both the bonding and the corresponding antibonding orbitals are occupied, this is never the case. We have analyzed the nature and the extent of bonding in some of these molecules by overlap populations and electron density analysis. Any method of estimating the bond strength based on overlap population has limitations.

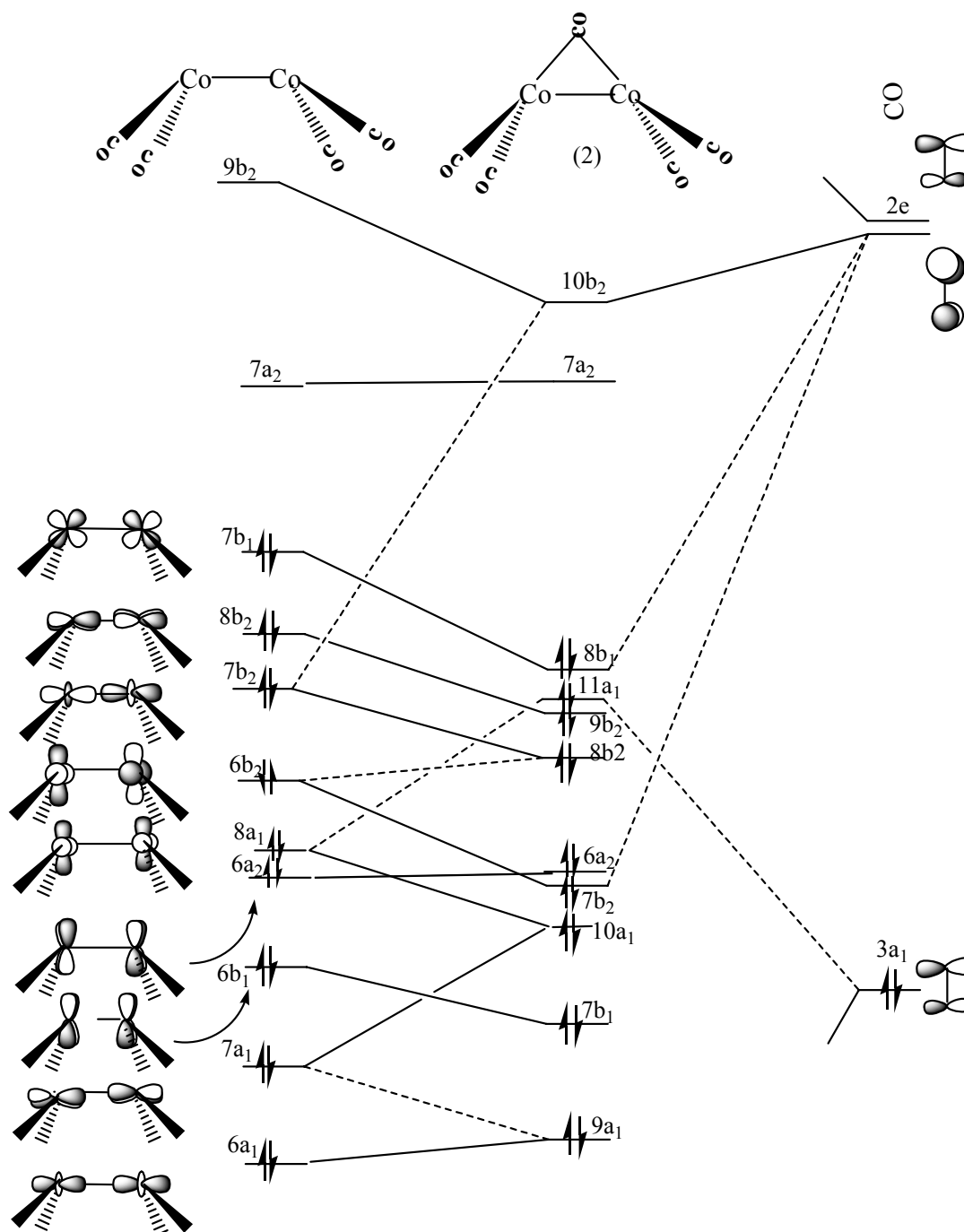


Figure 3: Interaction diagram between $(OC)_2Co-Co(CO)_2$ and CO fragments to give $Co_2(CO)_5$

Similarly quantitative comparisons of bond order indices of different pairs of atom are also difficult. Despite these limitations, we have found it profitable to compare

the Mulliken overlap populations and NBO atom-atom overlap weighted NAO bond order calculated at B3LYP/LANL2DZ for all molecules. The overlap population and the bond orders calculated for C_2 (0.728, 2.104) are between those of C_2H_4 (0.596, 1.288) and C_2H_2 , (1.007, 2.640). Comparisons of overlap populations are even more difficult in the transition metal complexes. We have calculated the NBO bond order for the binuclear complexes $[M_2(Cp)_2(CO)_6]$ which are known to have single σ bonds. These are 0.044 (M=Cr), 0.141 (M=Mo) and 0.170 (M=W). This is to be compared with the bond order of 0.951 calculated for $Re_2Cl_8^{-2}$ which is known to have a Re-Re quadruple bond. The bond order for $Fe_2(CO)_6$ (0.353) and $Co_2(CO)_5$ (0.218) is much lower than those for the quadruple bonded $Re_2Cl_8^{-2}$, justifying the bond order analysis. Similar conclusions can be obtained by taking any other method of estimating bond orders and overlap populations. The variation of the electron density³⁷ at the center of the C–C bond in C_2 , C_2H_2 , C_2H_4 and C_2H_6 (0.2690, 0.3741, 0.3064 and 0.2198 a.u. respectively) indicates that in the absence of a full fledged sigma bond the electron density in the middle of C_2 is lower as anticipated.

[5.4] Conclusions

The detailed electronic structures of (five, six, seven and eight valance electrons) inter- and intra-row main-group diatomic species shows that the element-element bond length decreases considerably when their π -levels are filled up instead of σ . The unusual shortness in the main group diatomic species is explained on the basis of their π -alone bonding. This is found in the transition metal complexes $[Fe_2(CO)_6, Co_2(CO)_5]$ as the frontier orbitals are reversed (Scheme 2b) in comparison to the

main-group fragments (Scheme 2a) where the σ -levels (sp^x hybrid orbitals of common main group fragments such as -BH, -CH and -CH₂) are lower in energy than the p orbitals that form the π -bonds.

Our work suggests that it may be profitable to leave out σ bonds while designing molecules with unusually short bond length!

[5.6] References

1. (a) Vannes, G. J. H.; Vos A. *Acta Cryst.* **1978**, *B34*, 1947. (b) Vannes, G. J. H.; Vos, A. *Acta Cryst.* **1979**, *B35*, 2593. (c) McMullan, R. K.; Kvik, A. *Acta Cryst.* **1992**, *B48*, 726.
2. Cotton, F. A, Harris, C. B. *Inorg. Chem.* **1965**, *4*, 330.
3. Roos, B.O; Borin, A. C.; Gagliardi, L.; *Angew. Chem. Int. Ed.* **2007**, *46*, 1469.
4. (a) Frenking, G.; Tonner, R. *Nature* **2007**, *446*, 276. (b) Nguyen, T.; Sutton, A. D.; Brynda, M.; Fetting, J. C.; Long, G. J.; Power, P. P. *Science* **2005**, *310*, 844.
5. Bruna, P. J.; Peyerimhoff, S. D.; Buenker, R. J. *J. Chem. Phys.* **1980**, *72*, 5437-5445.
6. Galbraith, J. M.; Blank, E.; Shaik, S.; Hiberty, P. C. *Chem. Eur. J.* **2000**, *6*, 2425-2434.
7. Pauling, L. *The Nature of the Chemical Bond*, 2nd ed., Cornell University Press, Ithaca, NY, **1945**.
8. Pyykkö, P.; Riedel, S.; Patzschke, M. *Chem. Eur. J.* **2005**, *11*, 3511-3520.
9. (a) Raghavachari, K.; Trucks, G. W.; Pople, J. A.; Head-Gordon, M. *Chem. Phys. Lett.* **1989**, *157*, 479. (b) Bartlett, R. J.; Watts, J. D.; Kucharski, S. A.; Noga, J. *Chem. Phys. Lett.* **1990**, *165*, 513. (c) Scuseria, G. E. *Chem. Phys. Lett.* **1991**, *176*, 27.
10. Gaussian 03, Revision C.02, Frisch, M. J.; Trucks, G. W.; Schlegel, H. B.; Scuseria, G. E.; Robb, M. A.; Cheeseman, J. R.; Montgomery, Jr., J. A.; Vreven, T.; Kudin, K. N.; Burant, J. C.; Millam, J. M.; Iyengar, S. S.; Tomasi, J.; Barone, V.; Mennucci, B.; Cossi, M.; Scalmani, G.; Rega, N.; Petersson, G. A.;

- Nakatsuji, H.; Hada, M.; Ehara, M.; Toyota, K.; Fukuda, R.; Hasegawa, J.; Ishida, M.; Nakajima, T.; Honda, Y.; Kitao, O.; Nakai, H.; Klene, M.; Li, X.; Knox, J. E.; Hratchian, H. P.; Cross, J. B.; Bakken, V.; Adamo, C.; Jaramillo, J.; Gomperts, R.; Stratmann, R. E.; Yazyev, O.; Austin, A. J.; Cammi, R.; Pomelli, C.; Ochterski, J. W.; Ayala, P. Y.; Morokuma, K.; Voth, G. A.; Salvador, P.; Dannenberg, J. J.; Zakrzewski, V. G.; Dapprich, S.; Daniels, A. D.; Strain, M. C.; Farkas, O.; Malick, D. K.; Rabuck, A. D.; Raghavachari, K.; Foresman, J. B.; Ortiz, J. V.; Cui, Q.; Baboul, A. G.; Clifford, S.; Cioslowski, J.; Stefanov, B. B.; Liu, G.; Liashenko, A.; Piskorz, P.; Komaromi, I.; Martin, R. L.; Fox, D. J.; Keith, T.; Al-Laham, M. A.; Peng, C. Y.; Nanayakkara, A.; Challacombe, M.; Gill, P. M. W.; Johnson, B.; Chen, W.; Wong, M. W.; Gonzalez, C.; and Pople, J. A.; Gaussian, Inc., Wallingford CT, 2004.
11. Pople, J. A.; Head-Gordon, M.; Raghavachari, K. *J. Chem. Phys.* **1987**, 87, 5968.
12. (a) Becke, A. D. *J. Chem. Phys.* **1993**, 98, 5648. (b) Becke, A. D. *Phys. Rev. A* **1988**, 38, 2398. (c) Lee, C.; Yang, W.; Parr, R. G. *Phys. Rev. B* **1988**, 37, 785.
13. Reed, A. E.; Curtiss, L. A.; Weinhold, F. *Chem. Rev.* **1988**, 88, 899.
14. Rademacher, P.; *Chem. Rev.* **2003**, 103, 933.
15. (a) Fox, J. G.; Hertzberg, G.; *Phys. Rev* **1937**, 52, 638. (b) Mulliken, R. S.; *Phys. Rev.* **1939**, 56, 778. (c) Ballik, E. A.; Ramsay, D. A.; *J. Chem. Phys.* **1959**, 31, 1128.
16. (a) Huber, K. P.; Herzberg, G. In *Molecular Spectra and Molecular Structure. IV. Constants of Diatomic Molecules*; Van Nostrand-

- Reinhold Co.: New York, **1979**. (b) Knight, L. B.; *J. Am. Chem. Soc.* **1987**, *109*, 3521.
17. Power, P. P.; *Chem. Rev.* **1999**, *99*, 3463.
18. (a) Gutsev, G. L.; Jena, P.; Bartlett, R. J. *J. Chem. Phys.* **1999**, *110*, 2928-2935.
(b) Pelegrini, M.; Roberto-Neto, O.; Machado, F. B. C. *Int. J. Quantum Chem.* **2003**, *95*, 205-212.
19. Bruna, P. J.; Grein, F. *J. Chem. Phys.* **2002**, *117*, 2103-2111.
20. (a) Bruna, P. J.; Labio, G. A. D.; Wright, J. S. *J. Phys. Chem.* **1992**, *96*, 6269-6278. (b) Kaplan, L. G.; Dolgounitchewa, O.; Watts, J. D.; Ortiz, J. V. *J. Phys. Chem.* **2002**, *117*, 3687-3693.
21. Middleton, R.; Klein, J. *Phys. Rev. A* **1999**, *60*, 3786.
22. (a) Power, P. P. *Chem. Rev.* **1999**, *99*, 3463-3503. (b) Moezzi, A.; Olmstead, M. M.; Bartlett, R. A.; Power, P. P. *Organometallics* **1992**, *11*, 2383-2388. (c) Moezzi, A.; Olmstead, M. M.; Power, P. P. *J. Chem. Soc., Dalton Trans.* **1992**, 2429.
23. Kalcher, J.; Sax, A. F. *J. Mol. Struct.: THEOCHEM*, **2000**, *498*, 77-85.
24. Midda, S.; Das, A.K. *J. of Mol. Spectroscopy*, **2004**, *224*, 1-6.
25. Windus, T. L.; Gordon, M. S. *J. Am. Chem. Soc.* **1992**, *114*, 9559-9568.
26. Knight, L. B.; Mckinley, A. J.; Babb, M. R.; Morse, M. D.; Arrington, C. A. *J. Chem. Phys.* **1993**, *98*, 6749-6757.
27. Tzeli, D.; Mavridis, A. *J. Phys. Chem. A* **2001**, *105*, 1175-1184.
28. Karna, S. P.; Grein, F. *Chem. Phys. Lett.* **1988**, *144*, 149-152.
29. Miguel, B.; Omar, S.; Mori-Sanchez P.; Vega J. M. G. *Chem. Phys. Lett.* **2003**, *381*, 720-724.

30. Y. Xie, H.F.Schaefer, R. B.King, *J. Am. Chem. Soc.* **2000**, *122*, 8746-8761.
31. Binachi, R.; Gervasio, G.; Marabello, *Inorg. Chem.* **2000**, *39*, 2360.
32. Adams, R. D.; Collins, D. M.; Cotton, F. A. *J. Am. Chem. Soc.* **1974**, *96*, 749.
33. Adams, R. D.; Collins, D. M.; Cotton, F. A. *Inorg. Chem.* **1974**, *13*, 1086.
34. (a) Pophristic, V.; Goodman, L. *Nature* **2001**, *411*, 565. (b) Bickelhaupt, F. M.; Baerends, E. J. *Angew. Chem. Int. Edn. Engl.* **2003**, *42*, 4183. (c) Weinhold, F. *Angew. Chem. Int. Edn. Engl.* **2003**, *42*, 4188-4194.
35. (a) Chetcuti, M. J.; Chisholm, M. H.; Folting, K.; Huffman, J. C.; Janos, J.; *J. Am. Chem. Soc.* **1982**, *104*, 4684. (b) Chisholm, M. H.; Corning, J. F.; Huffman, J. C.; *Inorg. Chem.*; **1984**, *23*, 754. (c) Gilbert, T. M.; Landes, A. M.; Rogers, R. D.; *Inorg. Chem.*; **1992**, *31*, 3438. (d) Chisholm, M. H.; Cotton, F. A.; Extine, M. W.; Millar, M.; Stults, B. R. *Inorg. Chem.*; **1977**, *16*, 320.
36. Kenny, J. P.; King, R. B.; Schaefer III, H. F. *Inorg. Chem.* **2001**, *40*, 900.
37. Bader, R. F. W. *Atoms in Molecules: A quantum Theory*; Clarendon Press; Oxford, **1994**.

Synopsis

Submitted for the thesis entitled

Theoretical Studies on Polyhedral Boranes, Main Group and Transition Metal Compounds

By

Biswarup Pathak

School of Chemistry
University of Hyderabad
Hyderabad 500 046
INDIA

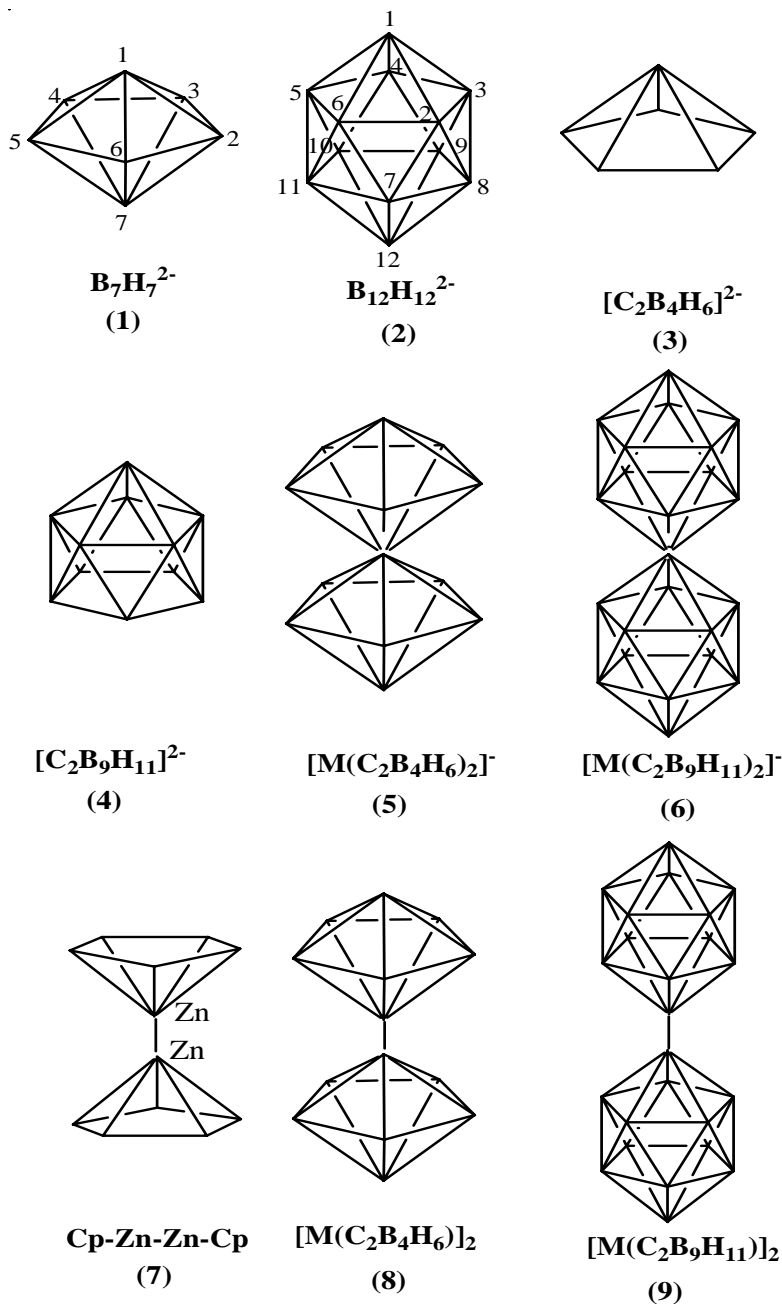
May 2007

The thesis consists of five chapters. The first chapter explains the theoretical methods employed in the computational study and a brief overview of the work done. Second chapter discusses the structure, bonding and relative stabilities of the group 13 incorporated icosahedral and pentagonal-bipyramidal boranes. Further their condensation through single atom sharing and binuclear metallocenes is presented. The condensed single atom sharing polyhedral boranes discussed in the second chapter is extended to the four atom sharing condensed system in the third chapter. Here, we explain the structure and bonding of the condensed four atom sharing ($B_{20}H_{16}$) of the two icosahedral ($B_{12}H_{12}^{2-}$) units and comparisons are made vis-à-vis with the edge sharing ($C_{10}H_8$) of the two benzene units. The electronic requirements of these condensed structures are well understood by *mno* Rule. The metallaboranes studied in the second chapter and benzene, naphthalene as a part of the third chapter lead us to study the C-H bond activation process in presence of transition metal complexes in the fourth chapter. In the fifth chapter we explain the unusual shortness of the bond length in several main group and transition metal compounds on the basis of their π -alone bonding.

Chapter 2: Reversal of Stability on Metalation of Pentagonal-Bipyramidal ($1\text{-MB}_6\text{H}_7^{2-}$, $1\text{-M-2-CB}_5\text{H}_7^{1-}$ and $1\text{-M-2,4-C}_2\text{B}_4\text{H}_7$) and Icosahedral ($1\text{-MB}_{11}\text{H}_{12}^{2-}$, $1\text{-M-2-CB}_{10}\text{H}_{12}^{1-}$ and $1\text{-M-2,4-C}_2\text{B}_9\text{H}_{12}$) Boranes (M=Al, Ga, In and Tl): Energetics of Condensation and Relationship to Binuclear Metallocenes

The pentagonal-bipyramid (**1**) and the icosahedron (**2**) are the two related polyhedra that dominate the chemistry of polyhedral boranes. The icosahedral boranes are usually considered to be the most stable among the polyhedral boranes. The pentagonal-bipyramidal *closo*-borane $\text{B}_7\text{H}_7^{2-}$ (**1**), in contrast, is highly reactive. However this difference in reactivity appears to be altered with the substitution of one of the vertices by a heavier group 13 metal.

We show here that the usual assumption of the extra stability of icosahedral boranes (**2**) over pentagonal-bipyramidal boranes (**1**) is reversed by substitution of a boron vertex by a group 13 metal. This preference is a result of the geometrical requirements for optimum overlap between the five membered face of the ligand and the metal fragment as they all obey the *mno* Rule. Isodesmic equations calculated at the B3LYP/LANL2DZ level indicate that the extra stability of $1\text{-M-2,4-C}_2\text{B}_4\text{H}_7$ (**1**) varies from 14.44 kcal/mol (M = Al) to 15.30 kcal/mol (M = Tl). Similarly, $\text{M}(\text{2,4-C}_2\text{B}_4\text{H}_6)_2^{1-}$ (**5**) is more stable than $\text{M}(\text{2,4-C}_2\text{B}_9\text{H}_{11})_2^{1-}$ (**6**) by 9.26 kcal/mol (M = Al) and by 6.75 kcal/mol (M = Tl). The preference for $(\text{MC}_2\text{B}_4\text{H}_6)_2$ (**8**) over $(\text{MC}_2\text{B}_9\text{H}_{11})_2$ (**9**) at the same level is 30.54 kcal/mol (M = Al), 33.16 kcal/mol (M = Ga) and 37.77 kcal/mol (M = In). The metal-metal bonding here is



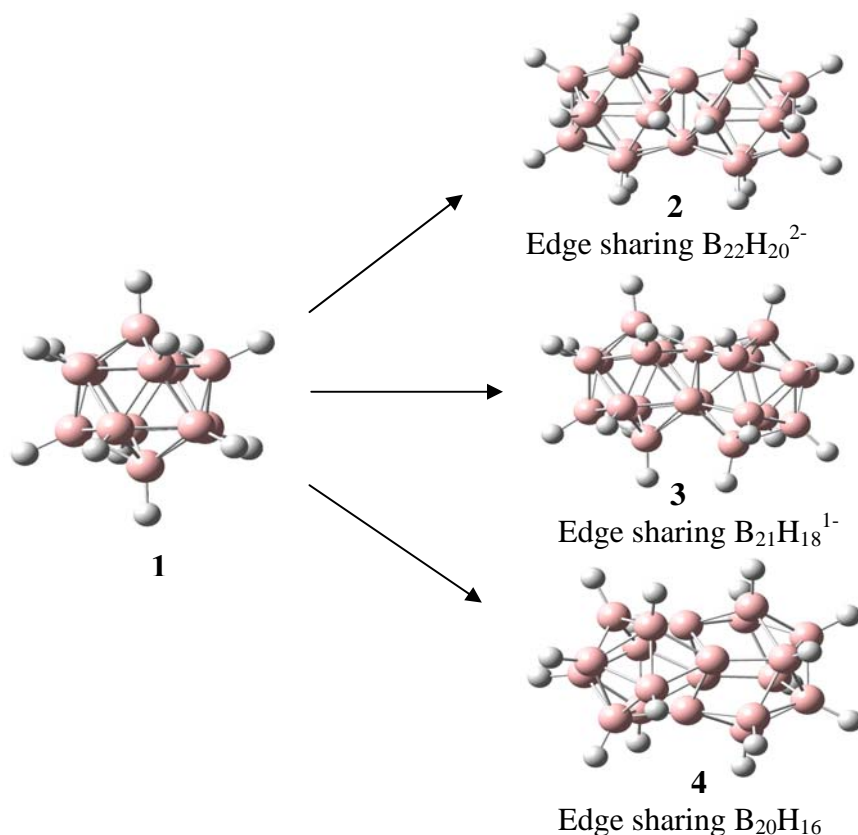
comparable to those in CpZn-ZnCp (**7**) and $\text{H}_2\text{M-MH}_2$ ($\text{M} = \text{Al}, \text{Ga}, \text{and In}$). The trend that group 13 metals prefer pentagonal-bipyramidal skeleton, rather than an icosahedron, is well explained by the orientation of the π -orbitals of the ring in both cases. In $\text{B}_7\text{H}_7^{2-}$, the π MOs of the B_5H_5 ring will span too large an area to have optimum overlap with the

MOs of the two BH fragments. A B_4H_4 ring or caps with more diffuse orbitals would have been better suited for such interaction. Thus, the B-H bonds of the B_5H_5 ring would bend out of the B_5 plane, rehybridizing the orbitals so that the larger lobe is directed toward the group with more diffuse orbitals. The overlap of fragment MOs in $B_{11}H_{11}^{2-}$ requires rehybridization for better overlap with the metal atom. This leads to the distortion of *exo*-polyhedral B-H bonds farther away from the metal so that there is a better orbital match. The overlap between ring π -orbitals and the cap orbitals is improved by the out-of-plane bending of ring hydrogens. The five-membered ring of a pentagonal-bipyramid makes better overlap with the diffuse orbital of metals more effectively than that of an icosahedron. Five-membered faces of the $C_2B_4H_6$ ring can be more easily brought together to form a sandwich because the B-H and the C-H bonds of the five-membered rings are bent away from the central metal atom. This explains the relative stability of the single-atom sharing complexes involving $C_2B_4H_6$ over their icosahedral analogues.

Chapter 3: Condensed 2- and 3-Dimensional Aromatic Systems: A Theoretical Study on the Relative Stabilities of Isomers of $CB_{19}H_{16}^+$, $B_{20}H_{15}Cl$ and $B_{20}H_{14}Cl_2$ and Comparison to $B_{12}H_{10}Cl_2^{2-}$, $C_6H_4Cl_2$, $C_{10}H_7Cl$ and $C_{10}H_6Cl_2$

Benzene and $B_{12}H_{12}^{2-}$ are important prototypes of two- and three-dimensional aromatic compounds in the carbon and boron families. Condensation of two benzenes sharing an edge gives naphthalene, which has a well-developed chemistry of its own. The properties

of benzene and naphthalene are contrasted frequently in the early days of aromaticity. The variation of aromaticity and reactivity has been especially noted. In contrast, the chemistry of condensed polyhedral borane is only being developed. Among the possible condensation products of $B_{12}H_{12}^{2-}$ (**1**), such as the edge sharing $B_{22}H_{20}^{2-}$ (**2**), face sharing $B_{21}H_{18}^{-}$ (**3**) and four-atom sharing $B_{20}H_{16}$ (**4**) (Scheme 1), the latter is synthesized and



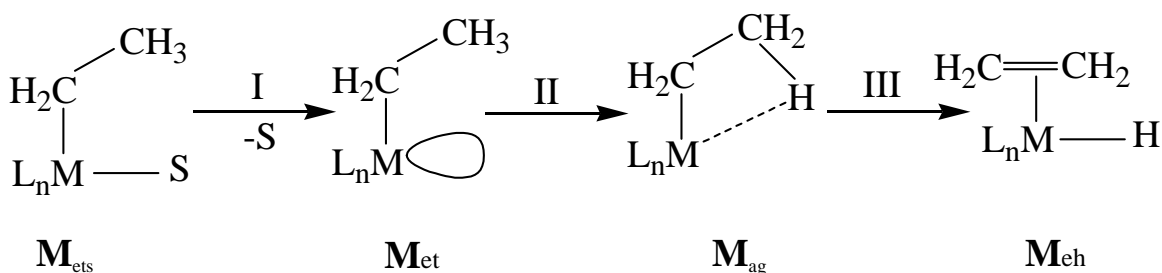
characterized. Though $B_{20}H_{16}$ is one of the borane equivalent of naphthalene, there is limited information available on $B_{20}H_{16}$. A major part of the development in the chemistry of polyhedral boranes came from the study of carboranes. While borane cations are not common, we compare here the isomers of $C_2B_{10}H_{12}$ and $CB_{19}H_{16}^{+}$. We find that such cross comparisons between two and three dimensional structures are useful for understanding their chemistry.

We also study here the structure and stability of the chloroderivatives of $B_{12}H_{12}^{2-}$ and of the condensed product $B_{20}H_{16}$ and compare them to their benzenoid counterparts.

Our DFT studies (B3LYP/6-31G*) on mono- and dichloroderivatives of benzene, naphthalene, $B_{12}H_{12}^{2-}$, four atom sharing condensed systems $B_{20}H_{16}$, and mono-carborane isomers of $B_{20}H_{16}$, are used to compare the variation of relative stability and aromaticity between condensed aromatics. The trends in the variation of the relative energies and aromaticity in these 2- and 3-Dimensional systems are similar. Aromaticity, estimated by NICS values, does not change considerably with condensation or substitution. The minor variation in the relative energies of the isomers of chloro derivatives are explained by the topological charge stabilization rule of Gimarc. The compatibility of cap and ring orbitals decides the relative stability of $CB_{19}H_{16}^+$.

Chapter 4: The Intra-molecular Activation of C_β -H Bond by Transition Metal Complexes

The activation of inert C-H bonds by a transition metal is of fundamental interest for stoichiometric and catalytic reactions particularly for functionalization of hydrocarbons. The development of catalytic variants of these high barrier reactions allows for efficient syntheses of many types of organic molecules. Binding a transition metal to the C-H bond is the first step in the activation of C-H bonds which leads to the formation of agostic complexes. This is considered to be important especially for α - and β -hydride elimination reactions.



Scheme 1

In this chapter, we attempt to find factors that distinguish the process of C-H bond activation as a function of the transition metal. In addition, we compare agostic complex formation and β -hydride addition reactions catalyzed by transition metal complexes along the groups and across the row of a periodic table. We predict based on their relative stabilities whether a given metal complex will be suitable for a polymerization reactions or β -hydride elimination reactions.

The $\text{C}_\beta\text{-H}$ bond activation process is studied in greater detail using two model set of complexes. The neutral first row complexes are modeled by $\text{Sc}(\text{Cp})_2\text{Et}$, $\text{TiCpEt}(\text{PH}_3)_2$, $\text{VCpEt}(\text{NO})$, $\text{Cr}(\text{PH}_3)_2\text{CpEt}$, $\text{MnEt}(\text{PH}_3)_4$, $\text{FeEt}(\text{PH}_3)_2\text{NO}$, $\text{CoC}_6\text{H}_6\text{Et}$, and $\text{Ni}(\text{Cp})\text{Et}$ and the cationic first row complexes by $[\text{ScCp}(\text{C}_6\text{H}_6)\text{Et}]^+$, $[\text{TiCpEt}(\text{NO})]^+$, $[\text{V}(\text{Cp})\text{Et}(\text{PH}_3)_2]^+$, $[\text{Cr}(\text{Cp})_2\text{Et}]^+$, $[\text{MnEt}(\text{PH}_3)_2\text{NO}]^+$, $[\text{FeEt}(\text{PH}_3)_4]^+$, $[\text{CoCpEt}(\text{PH}_3)]^+$, and $[\text{Ni}(\text{C}_6\text{H}_6)\text{Et}]^+$. The combination of ligands used around the metal centre is from the group Cp, C_6H_6 , $-\text{PH}_3$, and $-\text{NO}$ ligands. Same model complexes are studied for their corresponding group metals. The three possible species involved in the bond activation reaction are Metal-ethyl (M_{et}), Metal-agostic (M_{ag}) and Metal-ethylene-hydride (M_{eh}) (Scheme 1).

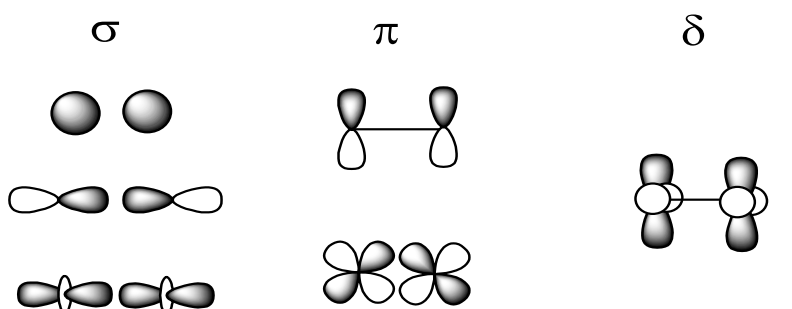
It has been noticed that as we move from left to right across the periodic table, the metal atomic energy levels increase but proper combination of ligands prevents the usual trend.

As a result the LUMO of the unsaturated metal-ethyl complex comes within the range of interaction for C-H σ -bonding MO and this complex gets stabilized by forming an agostic metal complex. It is possible to fine tune ligands in transition metal complexes so that metal LUMO energy is brought down to interact with the C-H σ -bonding MO. We conclude that any transition metal could be capable of activating the C-H bond if the proper combinations of ligands are provided.

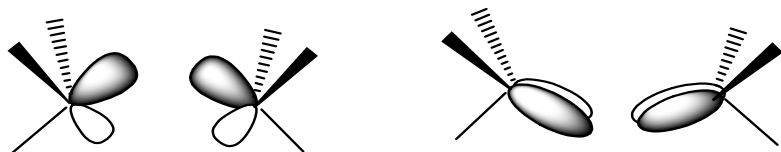
Chapter 5: Bond Length and Bond Multiplicity: σ Bond Prevents Short π Bonds

The concept of σ -, π - and δ -bonds is ingrained into the thought process of chemists. The cylindrically symmetrical σ -bond is traditionally estimated to be stronger than the π -bond, which in turn is stronger than the δ -bond. The linear overlap of orbitals in the σ -bond is supposed to be more effective than the sideways overlap available in the π - and δ -bonds [Scheme 1a]. Closely related to the discussion of σ -, π - and δ -bonds and their bond strengths is the issue of bond length. The decrease of bond length in going from a single σ -bond to multiple bonds involving σ and π components are exemplified by $\text{H}_3\text{C}-\text{CH}_3$, $\text{H}_2\text{C}=\text{CH}_2$, and $\text{HC}\equiv\text{CH}$ with C-C bond length of 1.538Å, 1.338Å and 1.203Å, respectively. In transition metal chemistry there are the familiar examples of short M-M quadruple bonds constituted from one σ -, two π -, and one δ -bonds as in $\text{Re}_2\text{Cl}_8^{-2}$ of 2.240 Å. Very recently (*Angew. Chem. Int. Ed.* Volume 46, Page No 1469-72) Roos et. al concludes that the maximum number of covalent chemical bonds between two shared

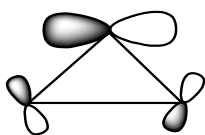
atoms will be six. To find the molecules with the highest bond order, they theoretically studied the transition metal dimers of chromium (Cr_2), molybdenum (Mo_2) and tungsten (W_2) respectively. They predict the maximum number of chemical bonds will be six because the atoms of these transition metals have six outer, or ‘valence’ orbitals, all of which are available for bonding. The Corresponding short M-M bond distances are 1.66 1.95 and 2.01 Å for Cr_2 , Mo_2 and W_2 respectively. So, the bond length decreases as their bond order increases.



Overlap of orbitals corresponding to σ , π and δ MOs



(b) π -MOs of $\text{Fe}_2(\text{CO})_6$



(c) Bent bonding in cyclopropane

However the variation of orbital overlap as a function of internuclear distance (Figure 1) shows that maximum overlap occurs at shorter distances for π - and δ -bonds. It is therefore logical to anticipate that π -bonds (unsupported by an underlying σ -bond) could be shorter than σ -bonds. We present here several such examples and conclude that σ -

bonds prevent π -bonds from getting to their natural, shorter interatomic distances. Here, we have used DFT theory for analyzing main group and transition metal compounds in greater detail. First row diatomics provide examples where π -orbitals are filled before σ . The diatomic C_2 (1.240 Å, Scheme 1a) has a ground state $^1\Sigma_g^+$ with a double bond,

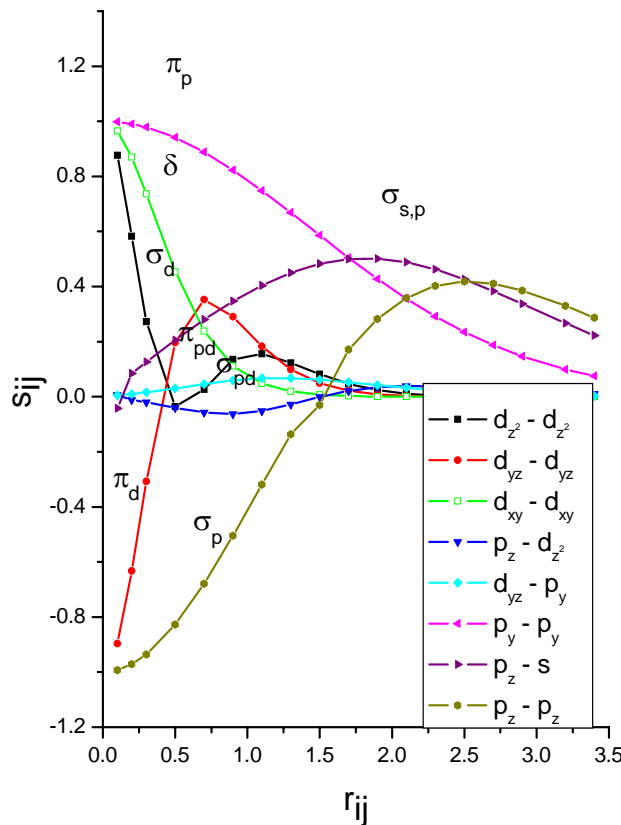


Figure 1: Variation of orbital overlap (s_{ij}) as a function of internuclear distance (r_{ij}) using contracted gaussian orbitals corresponding to a minimal basis of Fe.

both components of which are π -bonds. A triplet state obtained by shifting [Scheme 1b] one of the electrons from the π -bonding MO of C_2 to the vacant σ -bonding MO should increase the C-C distance ($^3\Pi_u$, 1.313 Å, Scheme 1b). Another triplet state ($^3\Sigma_g^+$) obtained by shifting another electron from π to σ -level elongates the bond to 1.370 Å (Scheme 1c).

This led to the conclusion that π^4 ($^1\Sigma^+$) configuration has uniformly shorter R_e than their $\pi^3\sigma^1$ ($^3\Pi$) counterparts by 0.073 Å. Corresponding bond lengths for the $\pi^2\sigma^2$ ($^3\Sigma_g^+$) species are seen to increase by an additional 0.13Å. Similarly, the diatomic B_2 (Scheme 1d) has a ground state $^3\Sigma_g^-$ ($\sigma_g^2\sigma_u^2\pi_u^2$) with two half π -bonds. The B-B distance (Scheme 1d, 1.590 Å) in B_2 is shorter than any B-B single (~ 1.706 Å) σ - bond.

	$^1\Sigma_g^+$	$^3\Pi_u$	$^3\Sigma_g^+$	$^3\Sigma_g^-$
$3\sigma_g$	—	↑↓	↑↓	—
$1\pi_u$	↑↓ ↑↓	↑↓ ↑↓	↑↓ ↑↓	↑↓ ↑↓
$2\sigma_u^*$	↑↓	↑↓	↑↓	↑↓
$2\sigma_g$	↑↓	↑↓	↑↓	↑↓
Bond length	1.240 Å	1.313 Å	1.370 Å	1.590 Å
	(a)	(b)	(c)	(d)

Scheme 1: Experimental bond lengths of C_2 (a) $^1\Sigma_g^+$, (b) $^3\Pi_u$, and of B_2 (d) $^3\Sigma_g^-$. Bond length of C_2 (c) $^3\Sigma_g^+$ is obtained from calculations at B3LYP/6-311+G* method.

We have found similar examples in the transition metal complexes too. Our detailed electronic structure calculation on the transition metal compound, $Fe_2(CO)_6$, explains the unusual shortness of Fe-Fe bond (Fe-Fe=2.002 Å) on the basis of their π -alone bonding. Our detailed study on the second and third row diatomics and transition metal complexes shows that π -bonds left to themselves are shorter than σ -bonds; in many ways σ -bonds prevent π -bonds from adopting their optimal shorter distances.

The results of some of these chapters have been published

1. Condensed Two- and Three-Dimensional Aromatic Systems: A Theoretical Study on the Relative Stabilities of Isomers of $\text{CB}_{19}\text{H}_{16}^{+}$, $\text{B}_{20}\text{H}_{15}\text{Cl}$, and $\text{B}_{20}\text{H}_{14}\text{Cl}_2$ and Comparison to $\text{B}_{12}\text{H}_{10}\text{Cl}_2^{2-}$, $\text{C}_6\text{H}_4\text{Cl}_2$, $\text{C}_{10}\text{H}_7\text{Cl}$, and $\text{C}_{10}\text{H}_6\text{Cl}_2$, Jemmis, E. D.; Pathak, B.; P.; Anoop, A. *Inorg. Chem.* **2005**, *44*, 7184.
2. Bond Length and Bond Multiplicity: σ Bond Prevents Short π Bonds, Jemmis, E. D.; Pathak, B.; King, R. B.; Schaefer III, H. F. *Chem. Comm.* **2006**, 2164.
3. Reversal of Stability on Metalation of Pentagonal-Bipyramidal ($1\text{-MB}_6\text{H}_7^{2-}$, $1\text{-M-2-CB}_5\text{H}_7^{1-}$ and $1\text{-M-2,4-C}_2\text{B}_4\text{H}_7$) and Icosahedral ($1\text{-MB}_{11}\text{H}_{12}^{2-}$, $1\text{-M-2-CB}_{10}\text{H}_{12}^{1-}$ and $1\text{-M-2,4-C}_2\text{B}_9\text{H}_{12}$) Boranes (M=Al, Ga, In and Tl) : Energetics of Condensation and Relationship to Binuclear Metallocenes, Pathak, B.; Pandian, S.; Hosmane, N.; Jemmis, E. D. *J. Am. Chem. Soc.* **2006**, *128*, 10915.

The results of some of these chapters yet to be published

1. σ -bond Prevents Short π -bonds: A Detailed Theoretical Study on the Main Group and Transition metal compounds
2. The Intramolecular Activation of $\text{C}_\beta\text{-H}$ Bond by Transition Metal Complexes